



A pulsar, a highly magnetized rotating neutron star, is shown at the center of the image. It emits a powerful beam of particles and energy, depicted as bright blue and white streaks against a dark background. The pulsar's surface is visible as a glowing blue sphere.

TIM LINDEN

• THE RISE OF THE LEPTONS PULSAR EMISSION DOMINATES THE TEV GAMMA-RAY SKY

Astronomy Colloquium
The Ohio State University
November 8, 2018



THE OHIO STATE UNIVERSITY
CENTER FOR COSMOLOGY AND
ASTROPARTICLE PHYSICS

TEV HALOS



Moon (To Scale)

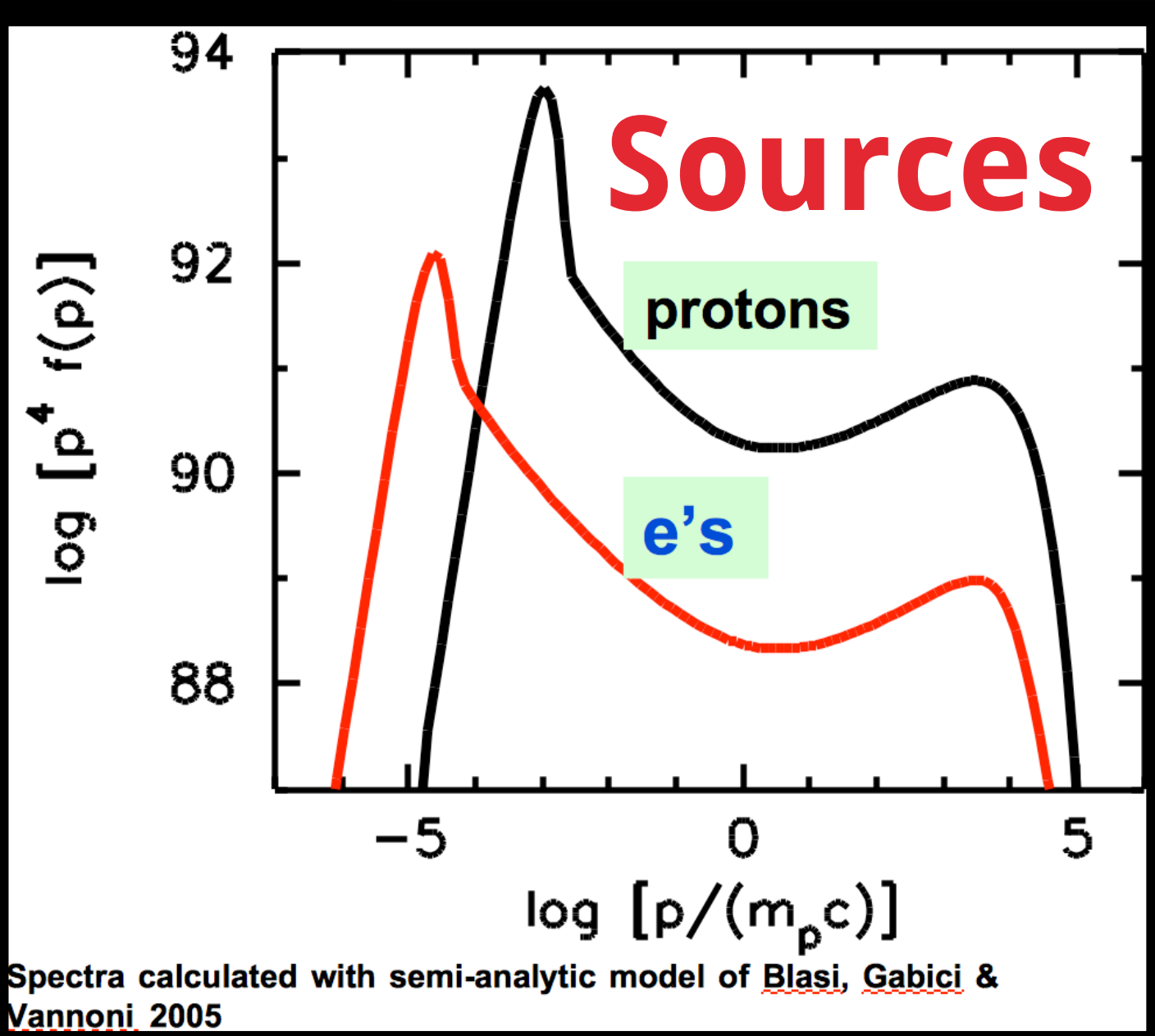
Geminga

PSR B0656+14
(Monogem)

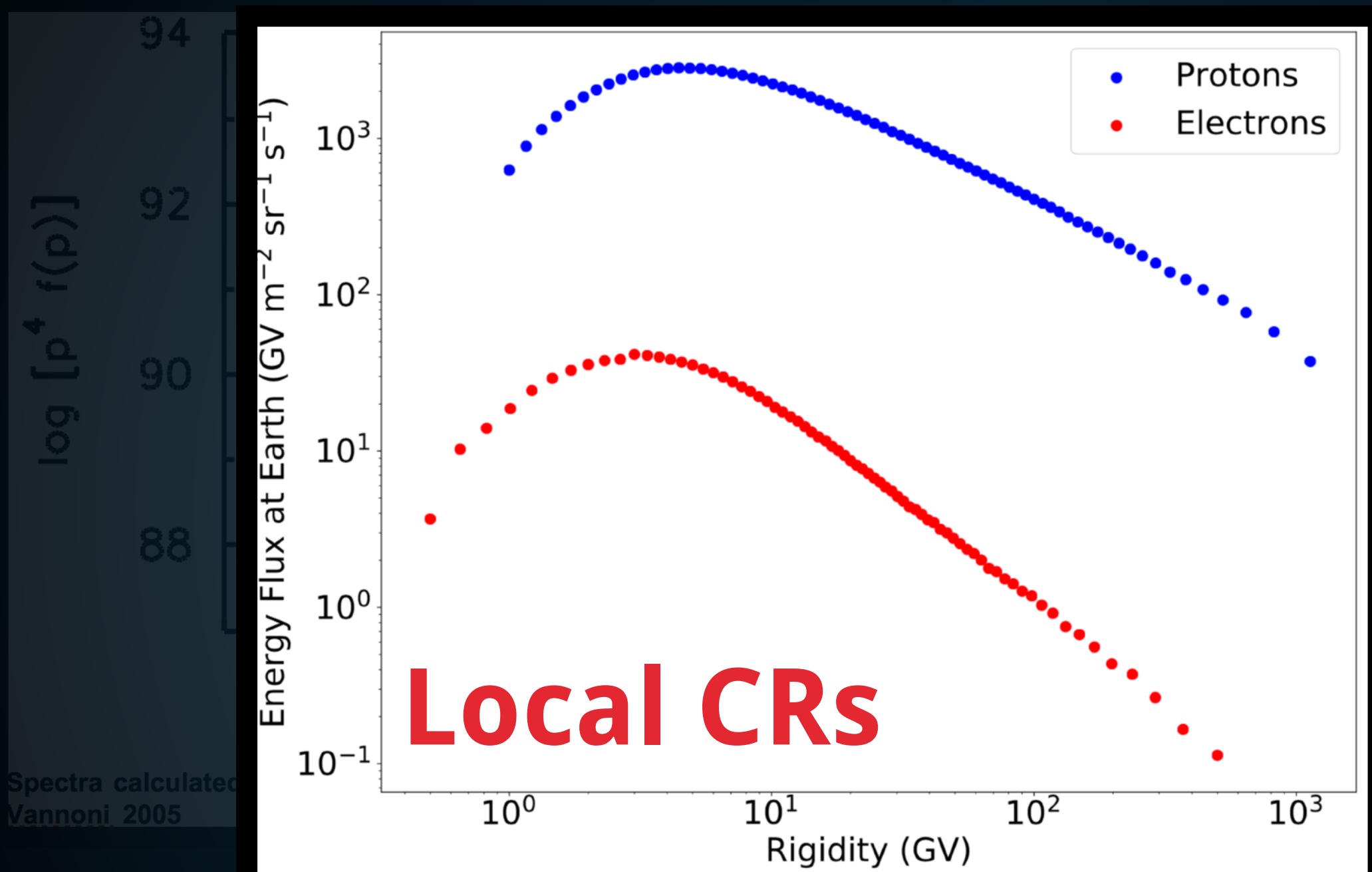


The Hadronic Fairy Tale

A UNIVERSE DOMINATED BY PROTONS

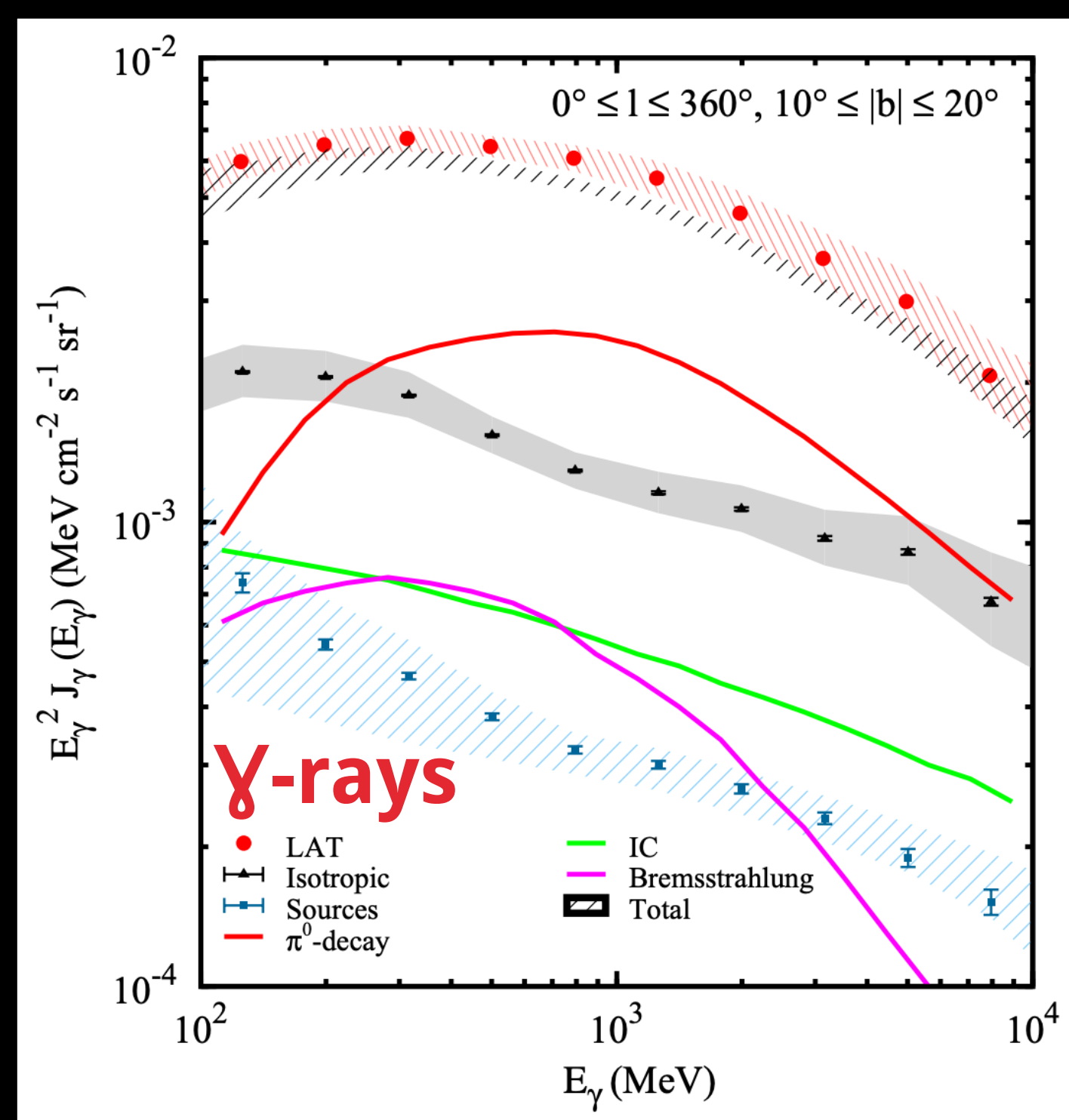
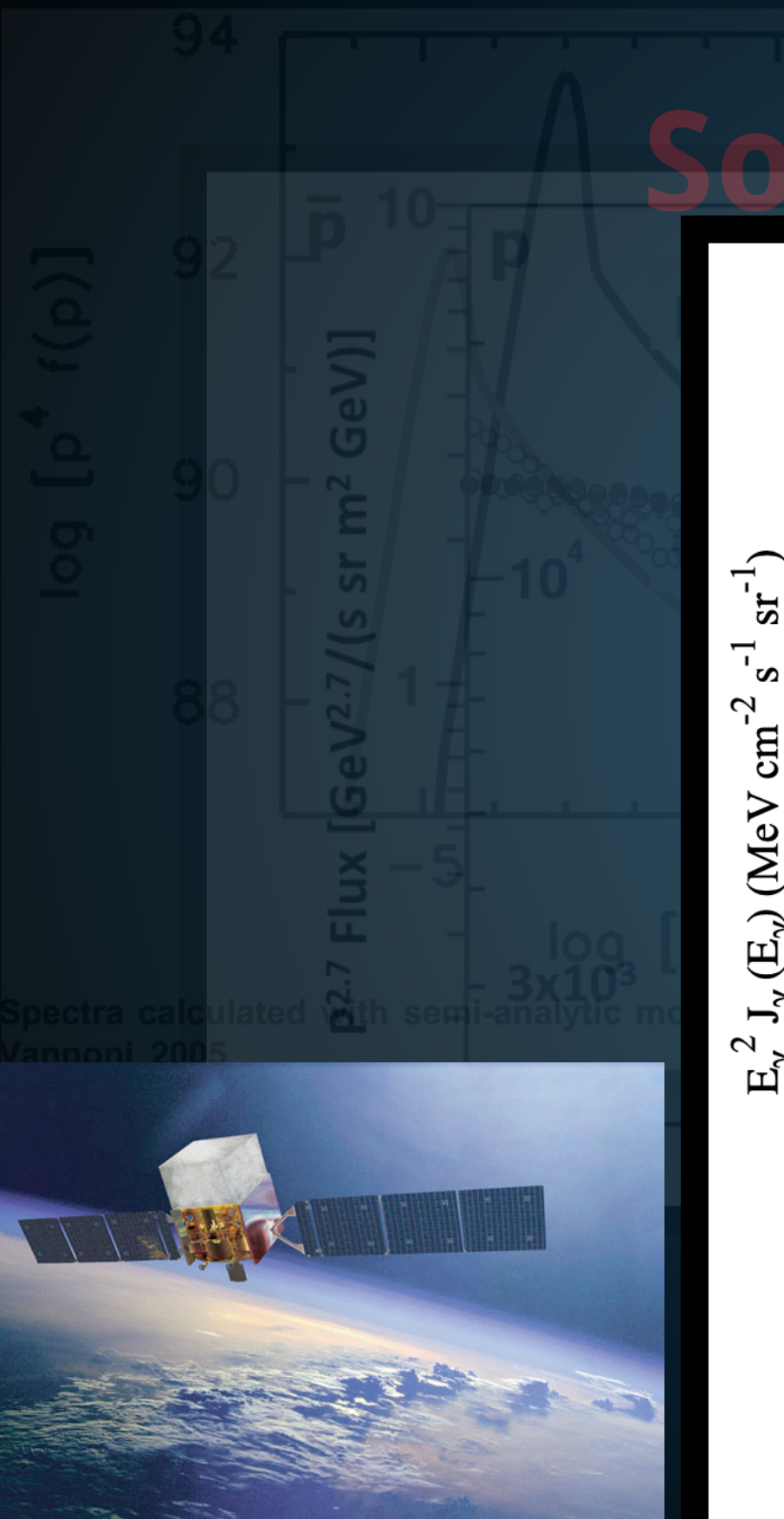


A UNIVERSE DOMINATED BY PROTONS



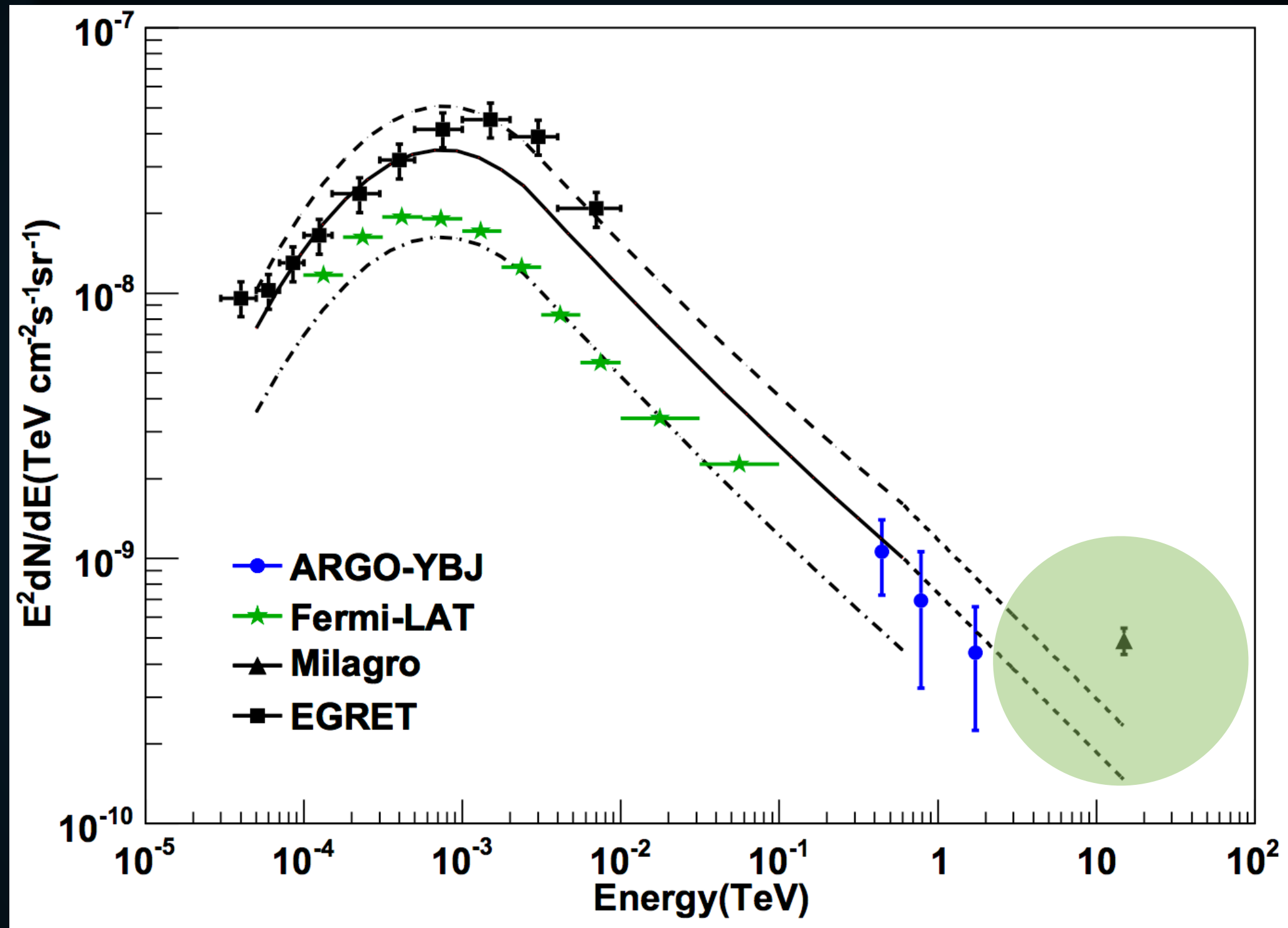
A UNIVERSE DOMINATED BY PROTONS

Sources



Cracks in the story...

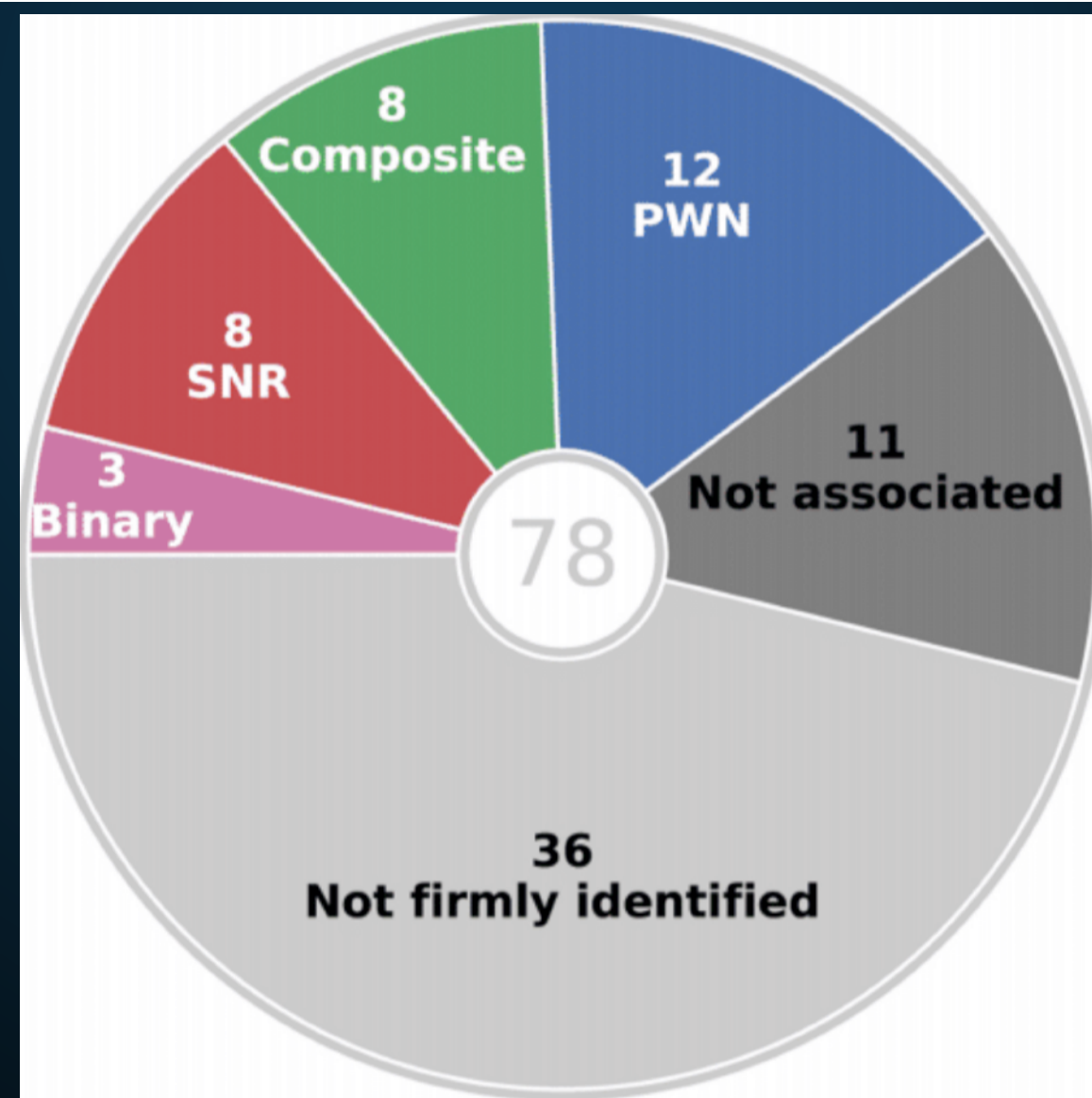
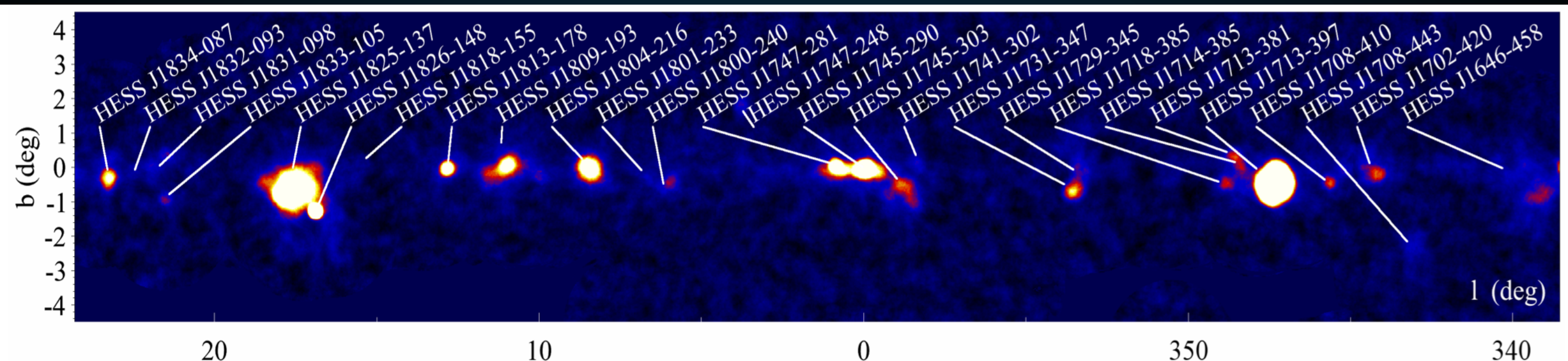
CRACKS IN THE STORY



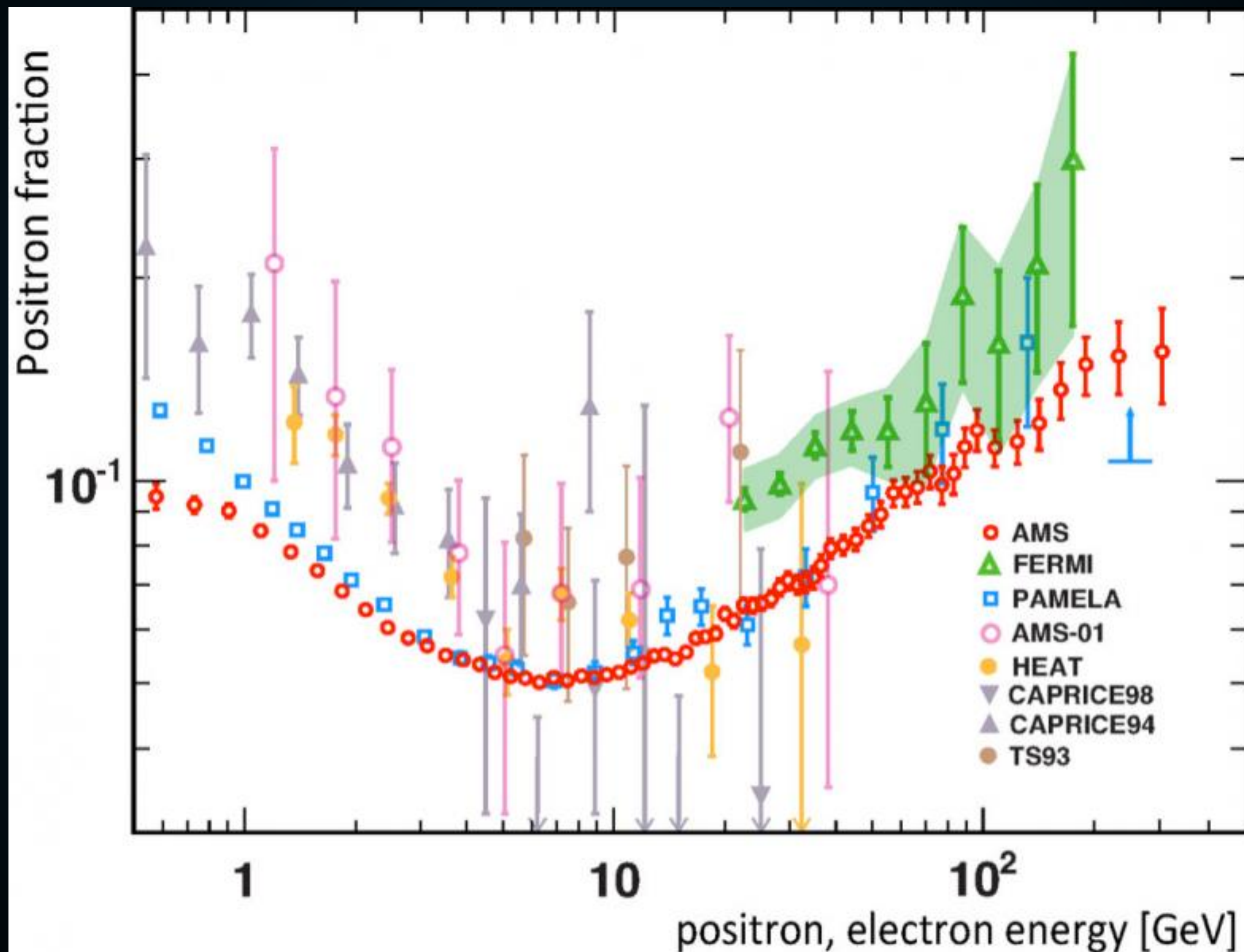
- Milagro observations found an excess in TeV gamma-ray emission along the Galactic plane.

CRACKS IN THE STORY

HESS Collaboration 2018



CRACKS IN THE STORY

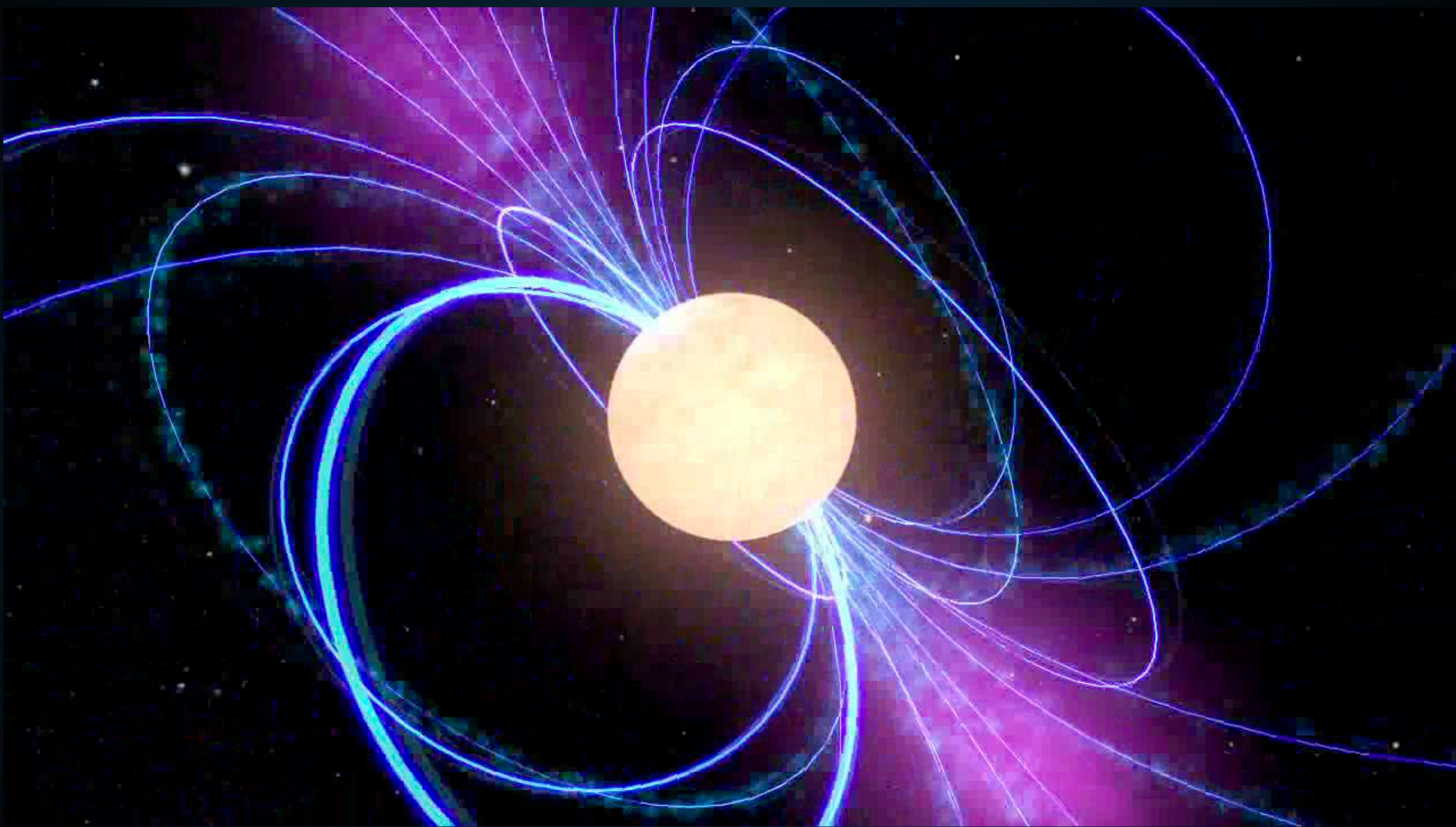


A NEW PICTURE

- In this talk, I will argue that electrons and positrons dominate the Milky Way's energetics at TeV energies:
- 1.) Pulsars dominate the diffuse TeV gamma-ray emission.
- 2.) Pulsars produce the majority of the bright TeV sources.
- 3.) Pulsars are responsible for the rising positron fraction.

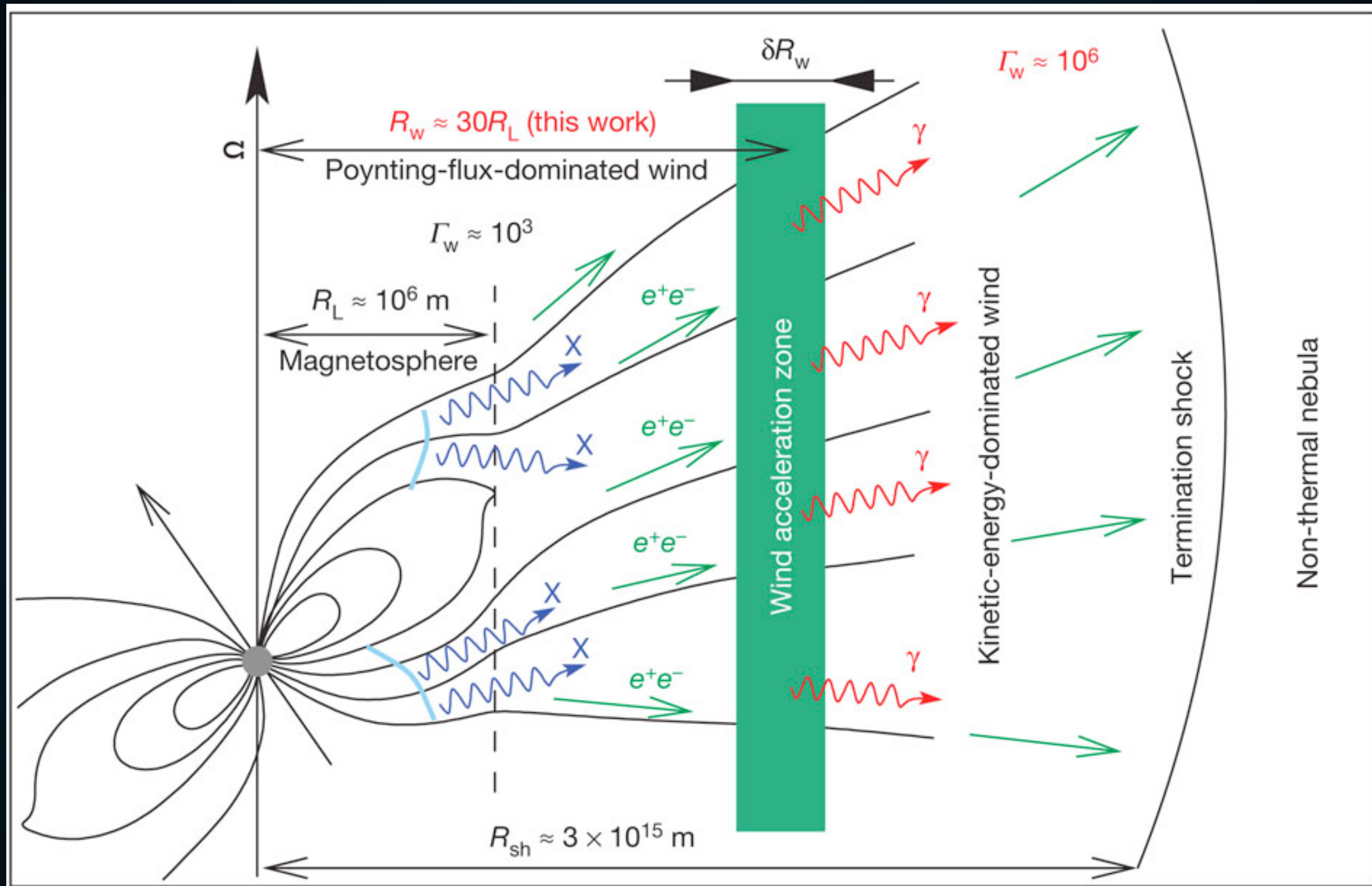
What do we know about pulsars?

PULSARS AS ASTROPHYSICAL ACCELERATORS



- Rotational Kinetic Energy of the neutron star is the ultimate power source of all emission in this problem.

PRODUCTION OF ELECTRON AND POSITRON PAIRS



- Electrons boiled off of the pulsar surface produce e^+e^- pairs.
- Final e^+e^- Spectrum is model dependent.

REACCELERATION IN THE PULSAR WIND NEBULA



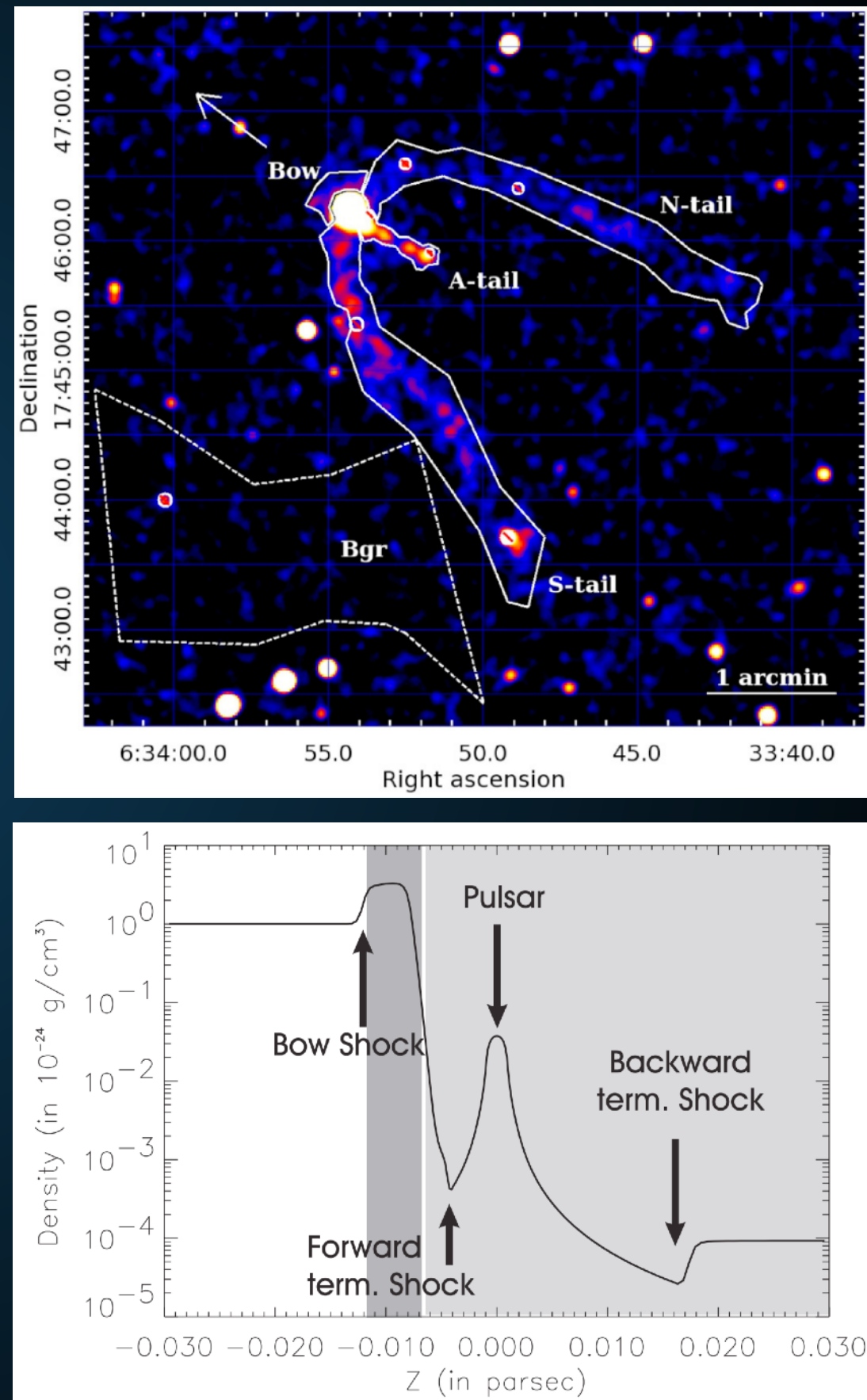
Blandford & Ostriker (1978)
Hoshino et al. (1992)
Coroniti (1990)
Sironi & Spitkovsky (2011)

- **PWN termination shock:**
 - **Voltage Drop > 30 PV**
 - **e^+e^- energy > 1 PeV
(known from synchrotron)**
- **Resets e^+e^- spectrum.**
- **Many Possible Models:**
 - **1st Order Fermi-Acceleration**
 - **Magnetic Reconnection**
 - **Shock-Driven Reconnection**

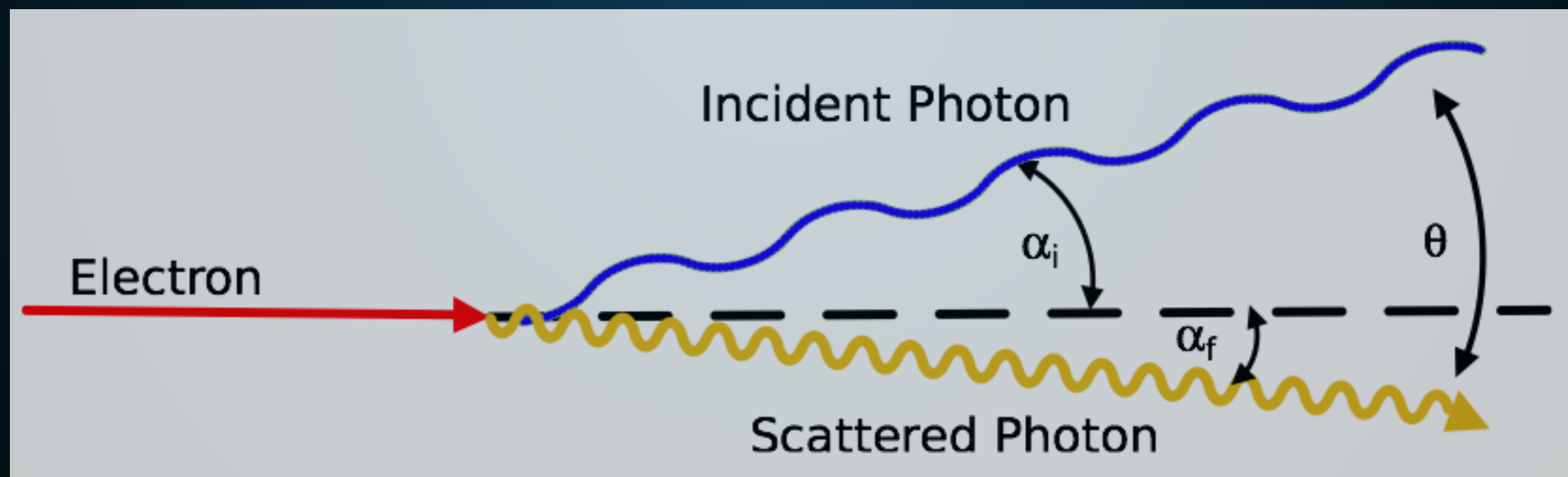
- Extent of radio and X-Ray PWN is approximately 1 pc.
- Termination shock produced when ISM energy density stops the relativistic pulsar wind.

$$R_{\text{PWN}} \simeq 1.5 \left(\frac{\dot{E}}{10^{35} \text{ erg/s}} \right)^{1/2} \times \left(\frac{n_{\text{gas}}}{1 \text{ cm}^{-3}} \right)^{-1/2} \left(\frac{v}{100 \text{ km/s}} \right)^{-3/2} \text{ pc}$$

- NOTE: The radial extent of PWN is explained by a known physical mechanism.



High energy electrons should also make gamma-rays.



New Observations!



HAWC OBSERVATIONS OF GEMINGA AND MONOGEM

Moon (To Scale)

PSR B0656+14

Geminga



- **Geminga**
 - $4.9 \times 10^{-14} \text{ TeV}^{-1} \text{ cm}^{-2} \text{ s}^{-1}$ (7 TeV)
 - $1.4 \times 10^{31} \text{ TeV s}^{-1}$ (7 TeV)
 - **25 pc extension**
 - **300 kyr**

HAWC OBSERVATIONS OF GEMINGA AND MONOGEM

Moon (To Scale)

PSR B0656+14

Geminga

- **Monogem**
 - $2.3 \times 10^{-14} \text{ TeV}^{-1} \text{ cm}^{-2} \text{ s}^{-1}$ (7 TeV)
 - $1.1 \times 10^{31} \text{ TeV s}^{-1}$ (7 TeV)
 - **25 pc extension**
 - **110 kyr !**

HAWC OBSERVATIONS OF GEMINGA AND MONOGEM

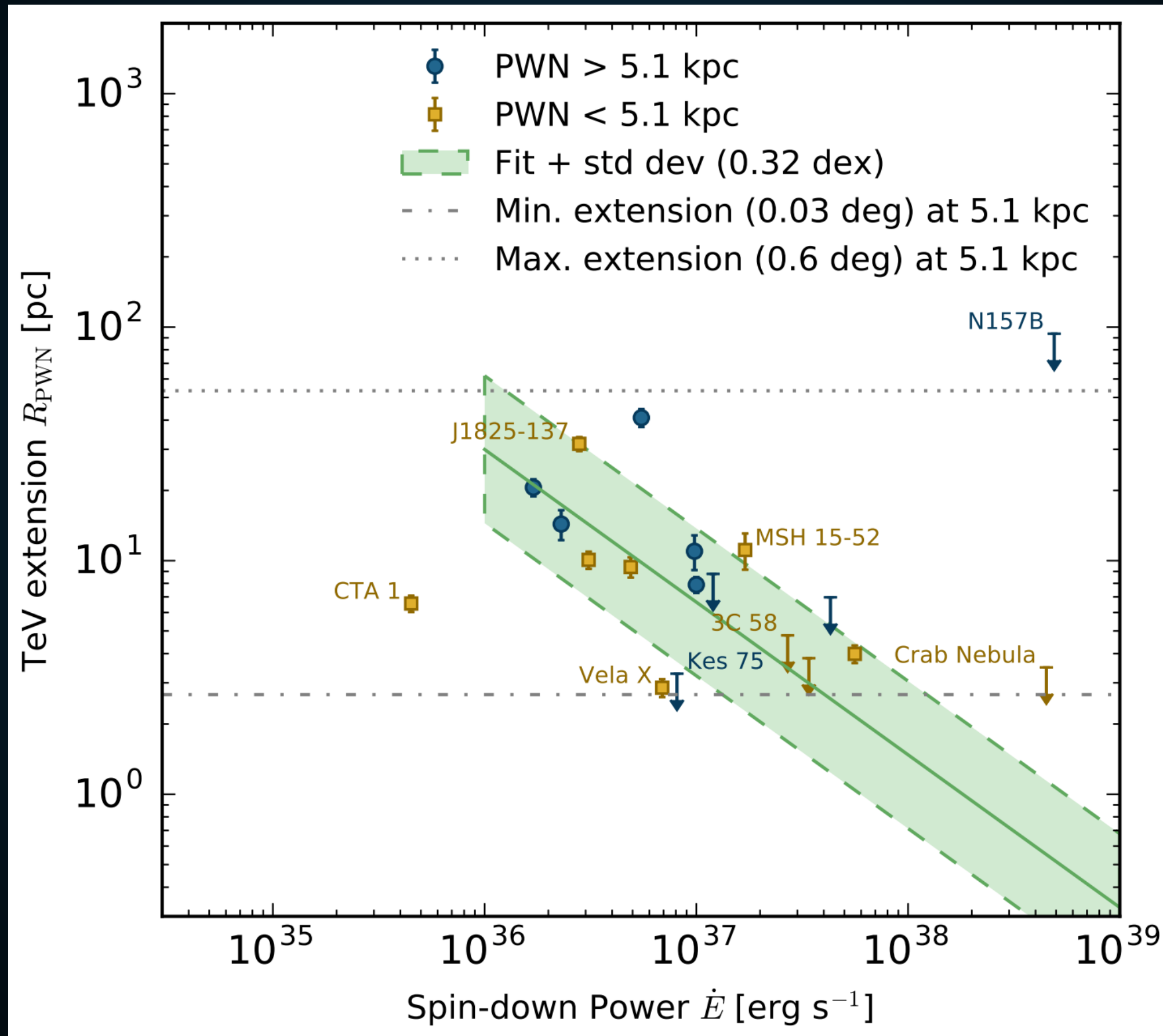
Moon (To Scale)

PSR B0656+14

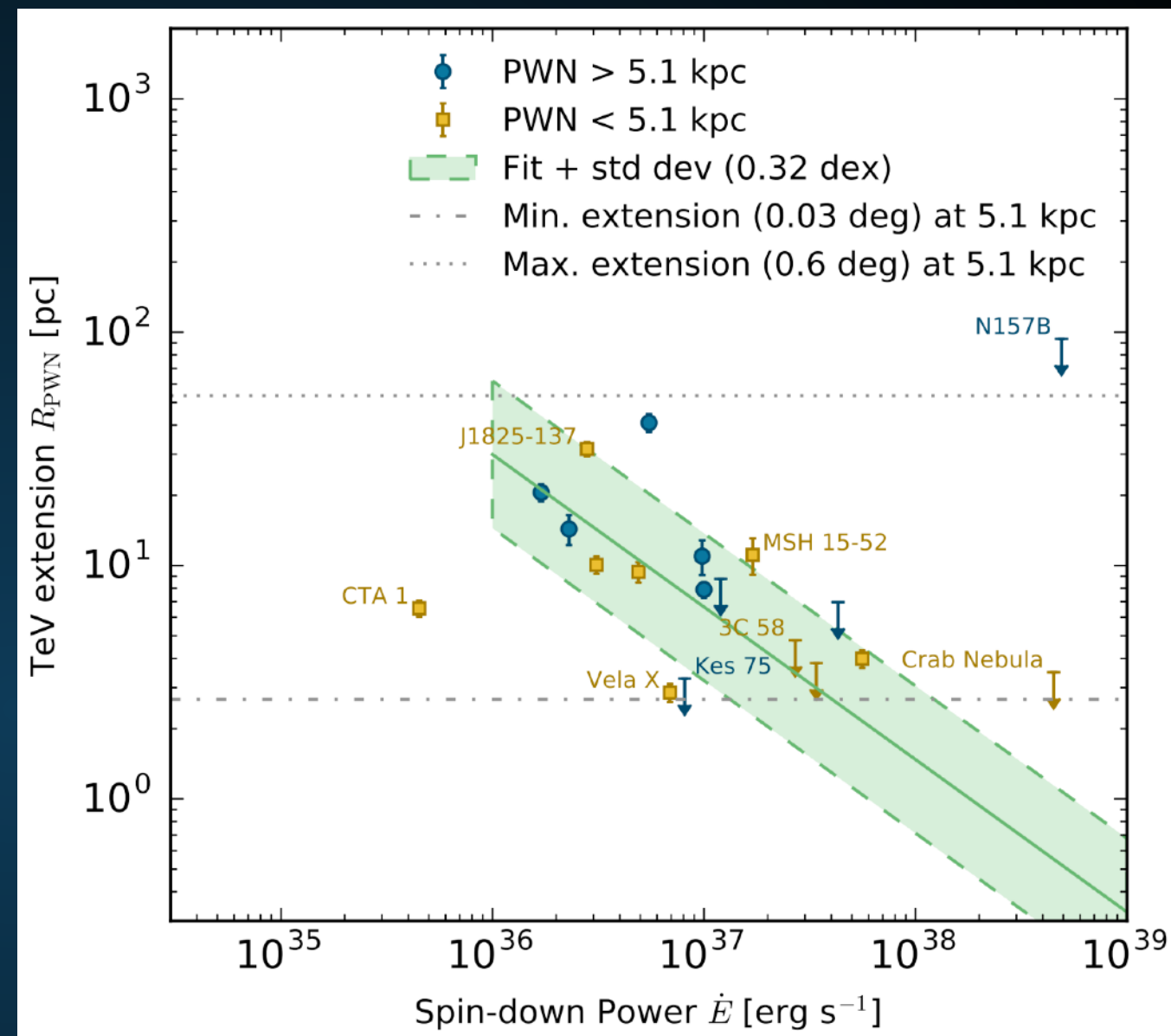
Geminga

- Emission is:
 - Very hard spectrum
 - Does not trace gas
 - Almost certainly leptonic.





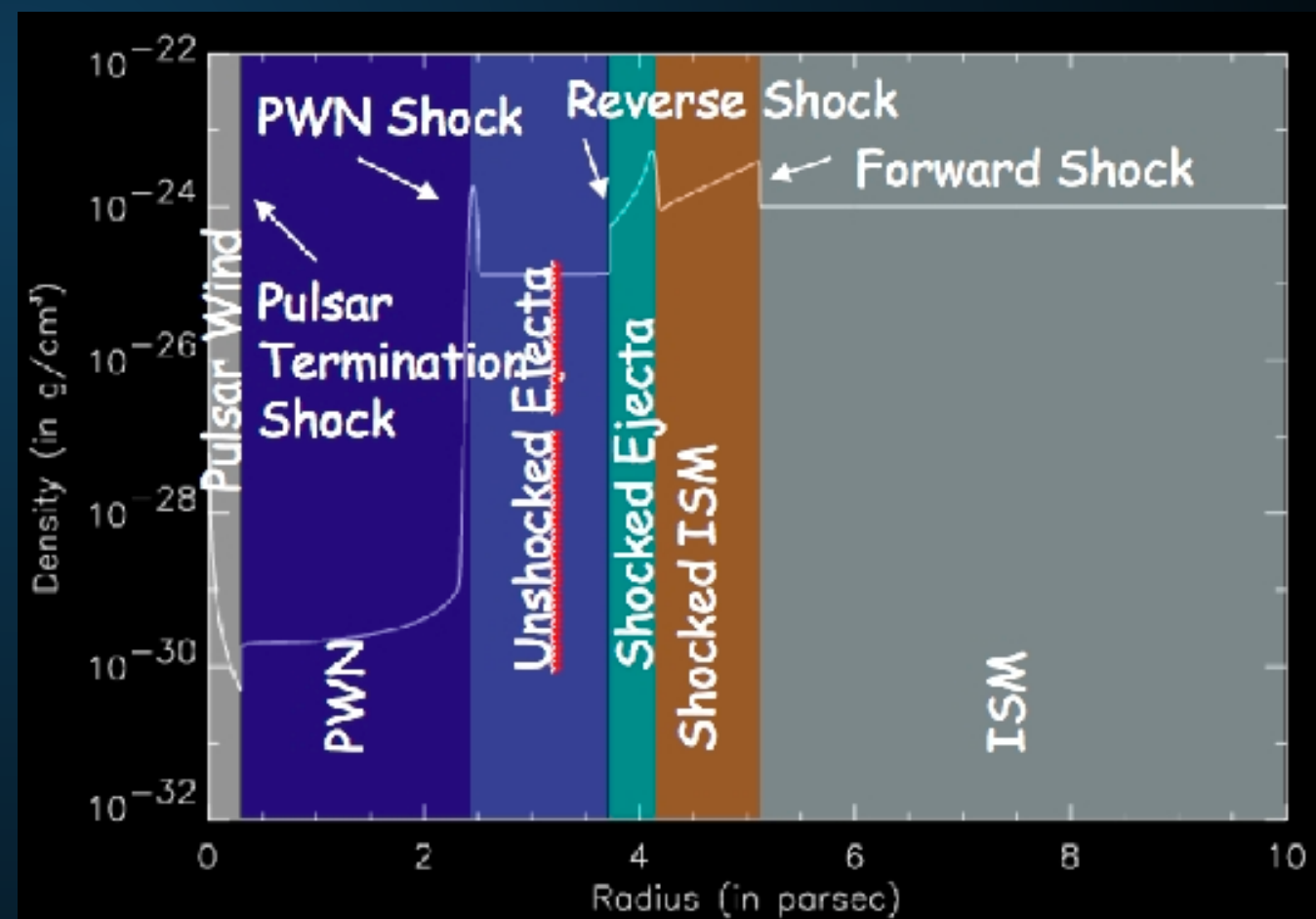
- They are much larger than the PWN.
- Especially at low-energies.



NOTE: This has the opposite energy dependence as the X-Ray PWN.

$$R_{\text{PWN}} \simeq 1.5 \left(\frac{\dot{E}}{10^{35} \text{ erg/s}} \right)^{1/2} \times \left(\frac{n_{\text{gas}}}{1 \text{ cm}^{-3}} \right)^{-1/2} \left(\frac{v}{100 \text{ km/s}} \right)^{-3/2} \text{ pc}$$

- TeV halos are a new feature
 - 3 orders of magnitude larger than PWN in volume
 - Opposite energy dependence
- PWN are morphologically connected to the physics of the termination shock
- TeV halos need a similar morphological description.



We'll go back to the model later...

What do TeV observations tell us about pulsars?

TEV HALOS - AN EMPIRICAL MODEL

$$\phi_{\text{TeV halo}} = \left(\frac{\dot{E}_{\text{psr}}}{\dot{E}_{\text{Geminga}}} \right) \left(\frac{d_{\text{Geminga}}^2}{d_{\text{psr}}^2} \right) \phi_{\text{Geminga}}$$

$$\theta_{\text{TeV halo}} = \left(\frac{d_{\text{Geminga}}}{d_{\text{psr}}} \right) \theta_{\text{Geminga}}$$

Name	Tested radius [°]	Index	$F_7 \times 10^{15}$ [TeV $^{-1}$ cm $^{-2}$ s $^{-1}$]	TeVCat
2HWC J0631+169	-	-2.57 \pm 0.15	6.7 \pm 1.5	Geminga
"	2.0	-2.23 \pm 0.08	48.7 \pm 6.9	Geminga
2HWC J0635+180	-	-2.56 \pm 0.16	6.5 \pm 1.5	Geminga

- Assume that every pulsar converts an equivalent fraction of its spin down power into gamma-rays, with the same spectrum as Geminga.

Note: Using Monogem would increase fluxes by nearly a factor of 2.

- **Assumption: Geminga (and Monogem) are typical pulsars.**
- **This statement is well supported:**
 - Observed because they are the two closest sources.
 - Many similar HESS Sources

ASSUMPTION: PULSAR POPULATION MODELS

- Use a generic model for pulsar luminosities
- $B_0 = 10^{12.5} \text{ G } (+/- 10^{0.3} \text{ G})$
- $P_0 = 0.3 \text{ s } (+/- 0.15 \text{ s})$
- Spindown Timescale of $\sim 10^4 \text{ yr}$ (depends on B_0)
- Galprop model for supernova distances

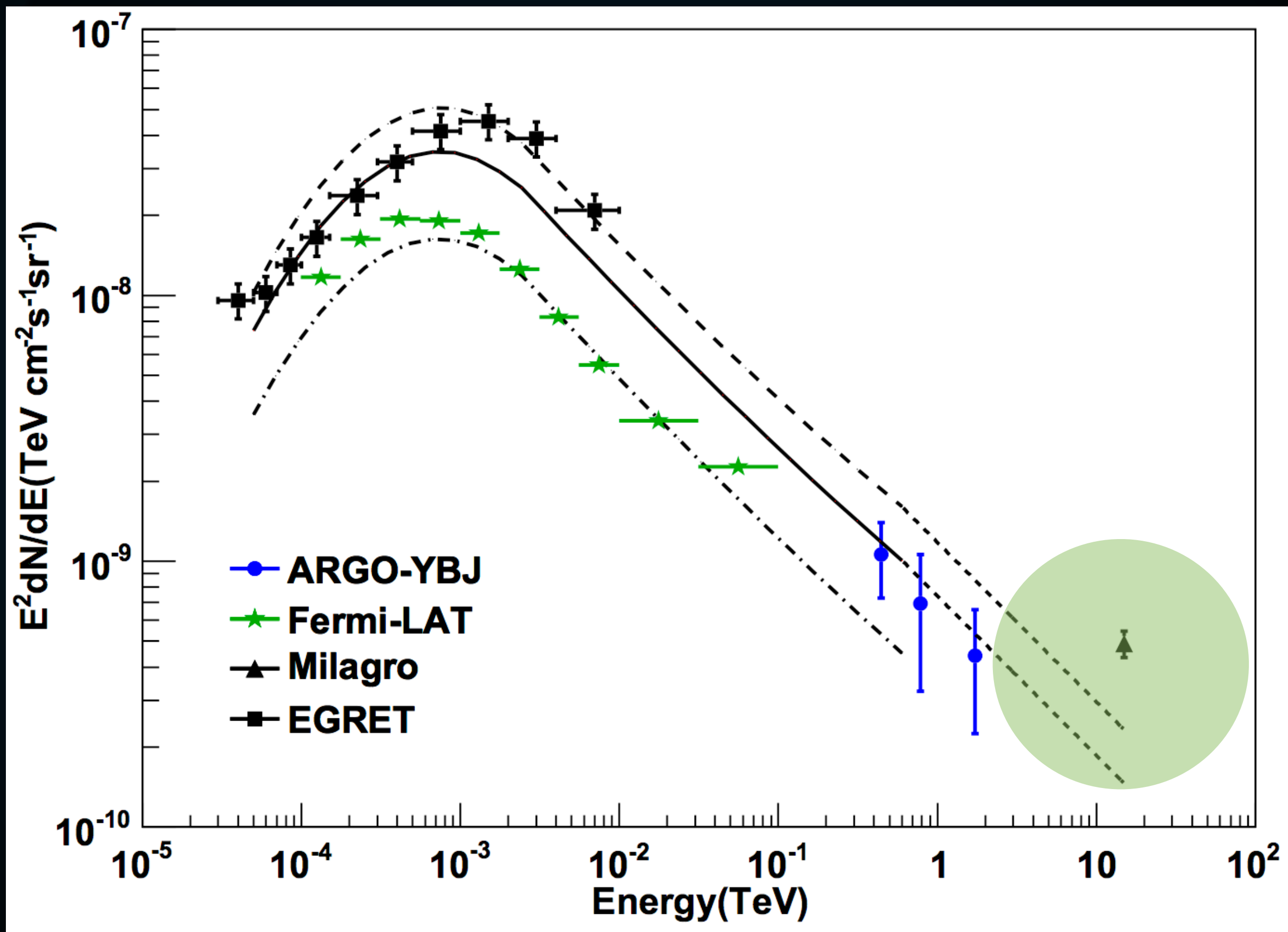
PsrPopPy: An open-source package for pulsar population simulations

D. Bates^{1,2}, D. R. Lorimer^{1,3}, A. Rane¹ and J. Swiggum¹
¹Department of Physics and Astronomy, West Virginia University, Morgantown, WV, 26506 USA
²Centre for Astrophysics, School of Physics and Astronomy, The University of Manchester, Manchester M13 9PL, UK
³Green Bank Observatory, PO Box 2, Green Bank, WV 24944, USA

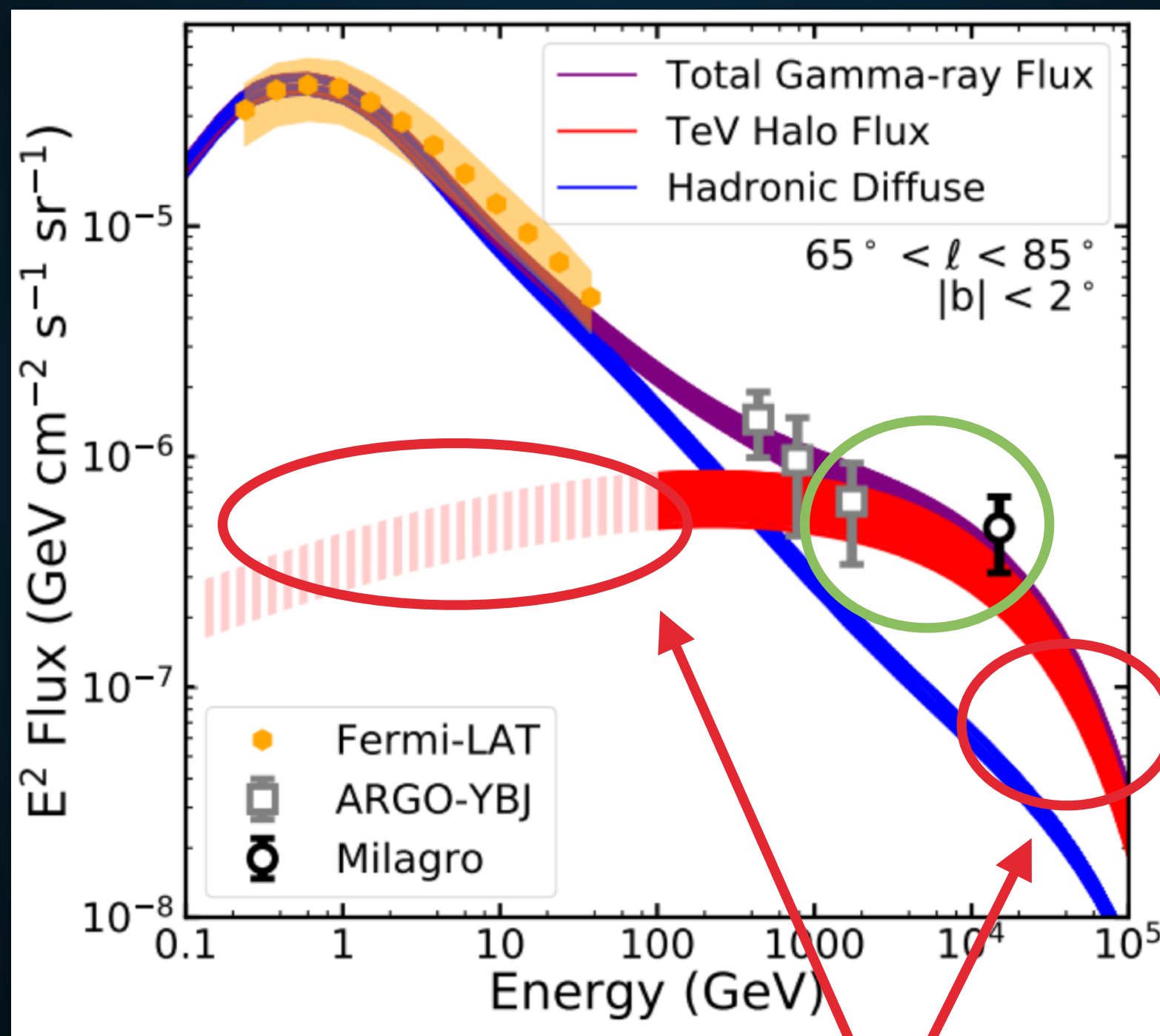
Implication II:

Most TeV emission is produced by TeV halos

IMPLICATION I: THE TEV EXCESS



- TeV halos naturally explain the TeV excess!



spectral assumption!

Implication II:

Most TeV gamma-ray sources are TeV halos.

TEV HALO NUMEROLOGY

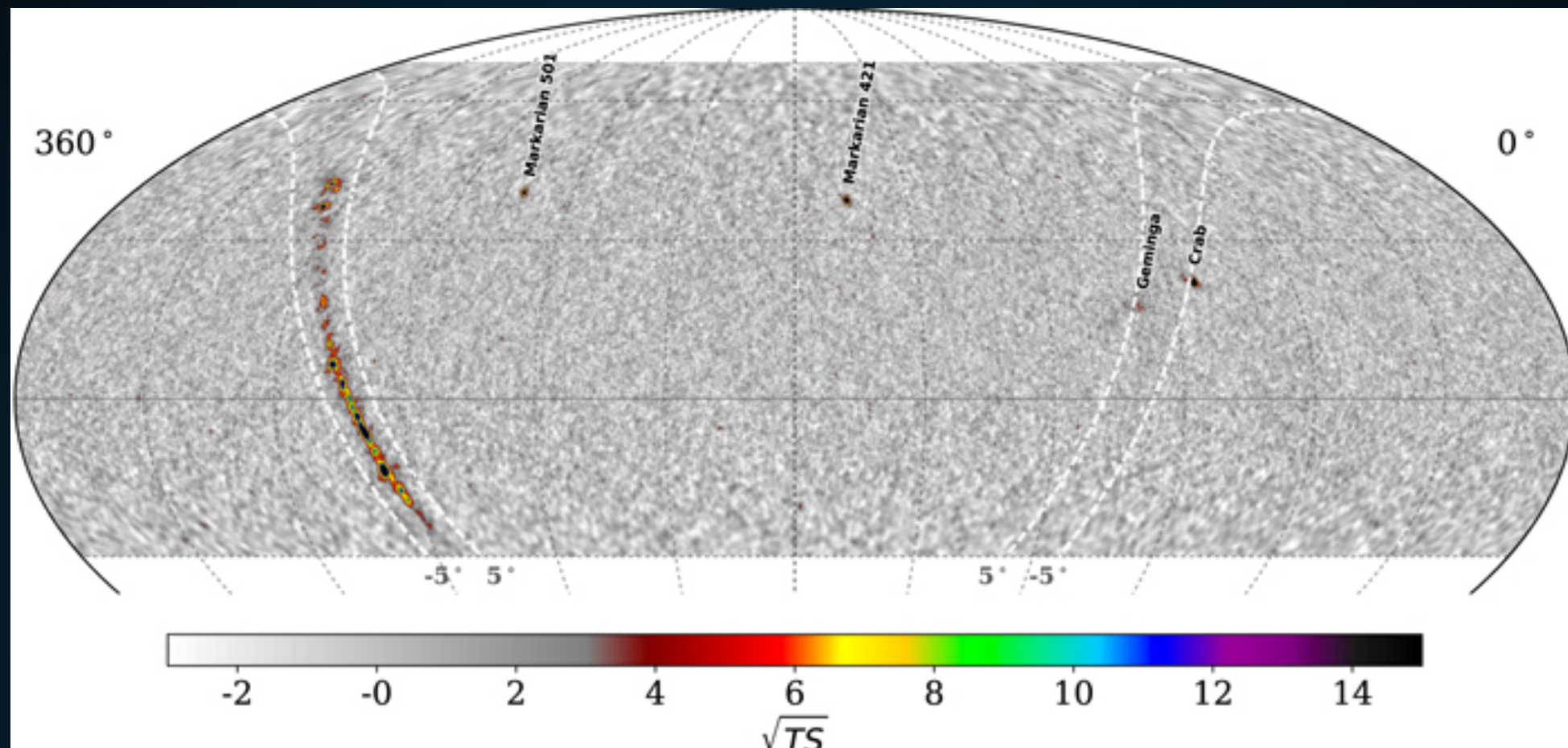
- HAWC has observed 39 sources.
- 5 are coincident with old (>100 kyr) pulsars

2HWC Name	ATNF Name	Distance (kpc)	Angular Separation	Projected Separation	Expected Flux ($\times 10^{-15}$)	Actual Flux ($\times 10^{-15}$)	Flux Ratio	Expected Extension	Actual Extension	Age (kyr)	Chance Overlap
J0700+143	B0656+14	0.29	0.18°	0.91 pc	43.0	23.0	1.87	2.0°	1.73°	111	0.0
J0631+169	J0633+1746	0.25	0.89°	3.88 pc	48.7	48.7	1.0	2.0°	2.0°	342	0.0
J1912+099	J1913+1011	4.61	0.34°	27.36 pc	13.0	36.6	0.36	0.11°	0.7°	169	0.30
J2031+415	J2032+4127	1.70	0.11°	3.26 pc	5.59	61.6	0.091	0.29°	0.7°	181	0.002
J1831-098	J1831-0952	3.68	0.04°	2.57 pc	7.70	95.8	0.080	0.14°	0.9°	128	0.006

- 12 others coincident with young (<100 kyr) pulsars
 - TeV emission may be contaminated by SNR

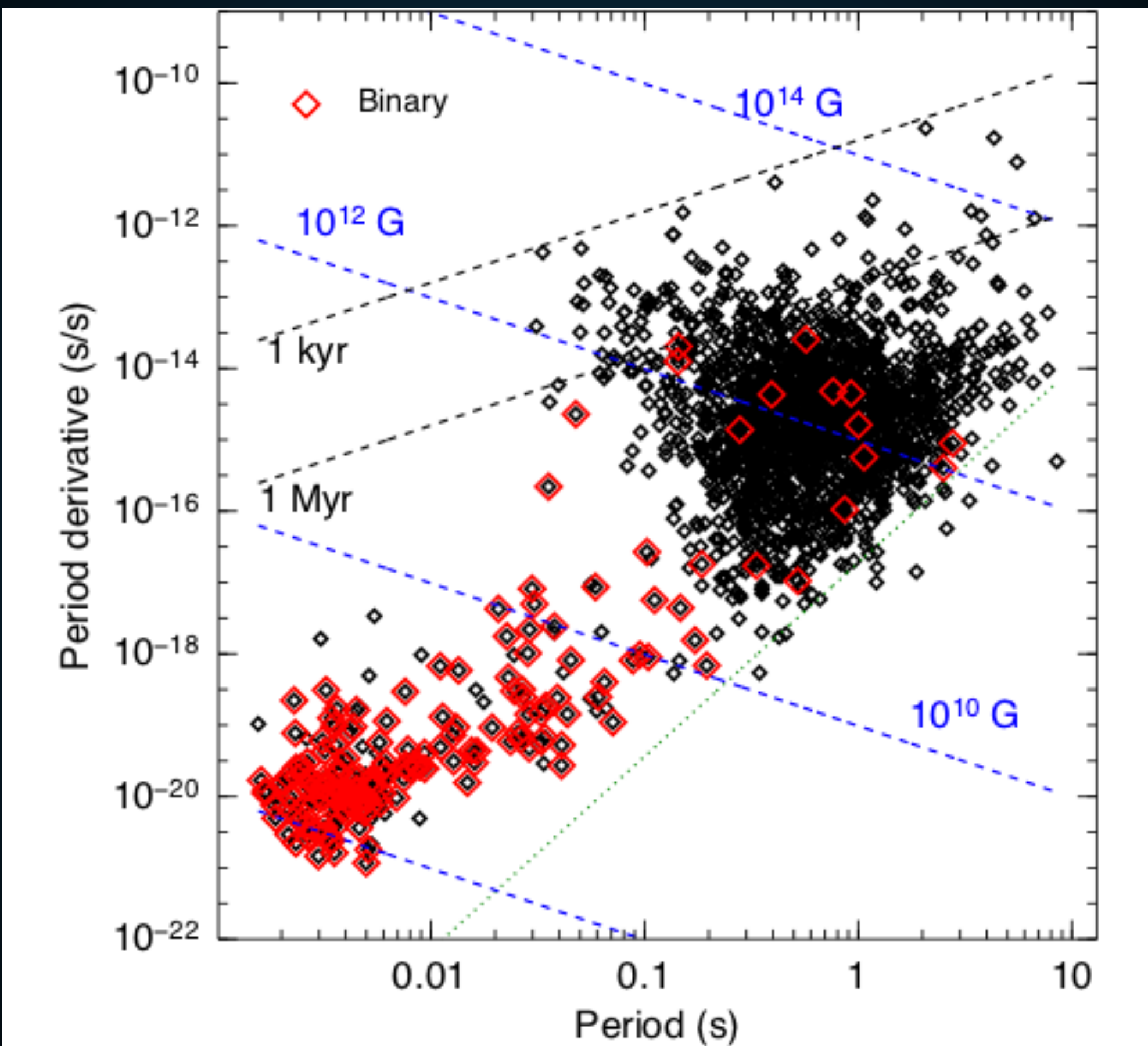
2HWC Name	ATNF Name	Distance (kpc)	Angular Separation	Projected Separation	Expected Flux ($\times 10^{-15}$)	Actual Flux ($\times 10^{-15}$)	Flux Ratio	Expected Extension	Actual Extension	Age (kyr)	Chance Overlap
J1930+188	J1930+1852	7.0	0.03°	3.67 pc	23.2	9.8	2.37	0.07°	0.0°	2.89	0.002
J1814-173	J1813-1749	4.7	0.54°	44.30 pc	243	152	1.60	0.11°	1.0°	5.6	0.61
J2019+367	J2021+3651	1.8	0.27°	8.48 pc	99.8	58.2	1.71	0.28°	0.7°	17.2	0.04
J1928+177	J1928+1746	4.34	0.03°	2.27 pc	8.08	10.0	0.81	0.11°	0.0°	82.6	0.002
J1908+063	J1907+0602	2.58	0.36°	16.21 pc	40.0	85.0	0.47	0.2°	0.8°	19.5	0.26
J2020+403	J2021+4026	2.15	0.18°	6.75 pc	2.48	18.5	0.134	0.23°	0.0°	77	0.01
J1857+027	J1856+0245	6.32	0.12°	13.24 pc	11.0	97.0	0.11	0.08°	0.9°	20.6	0.06
J1825-134	J1826-1334	3.61	0.20°	12.66 pc	20.5	249	0.082	0.14°	0.9°	21.4	0.14
J1837-065	J1838-0655	6.60	0.38°	43.77 pc	12.0	341	0.035	0.08°	2.0°	22.7	0.48
J1837-065	J1837-0604	4.78	0.50°	41.71 pc	8.3	341	0.024	0.10°	2.0°	33.8	0.68
J2006+341	J2004+3429	10.8	0.42°	80.07 pc	0.48	24.5	0.019	0.04°	0.9°	18.5	0.08

TEV HALO NUMEROLOGY



ATNF Name	Dec. ($^{\circ}$)	Distance (kpc)	Age (kyr)	Spindown Lum. (erg s^{-1})	Spindown Flux ($\text{erg s}^{-1} \text{kpc}^{-2}$)	2HWC
J0633+1746	17.77	0.25	342	3.2e34	4.1e34	2HWC J0631+169
B0656+14	14.23	0.29	111	3.8e34	3.6e34	2HWC J0700+143
B1951+32	32.87	3.00	107	3.7e36	3.3e34	—
J1740+1000	10.00	1.23	114	2.3e35	1.2e34	—
J1913+1011	10.18	4.61	169	2.9e36	1.1e34	2HWC J1912+099
J1831-0952	-9.86	3.68	128	1.1e36	6.4e33	2HWC J1831-098
J2032+4127	41.45	1.70	181	1.7e35	4.7e33	2HWC J2031+415
B1822-09	-9.58	0.30	232	4.6e33	4.1e33	—
B1830-08	-8.45	4.50	147	5.8e35	2.3e33	—
J1913+0904	9.07	3.00	147	1.6e35	1.4e33	—
B0540+23	23.48	1.56	253	4.1e34	1.4e33	—

WHY DO WE CARE?



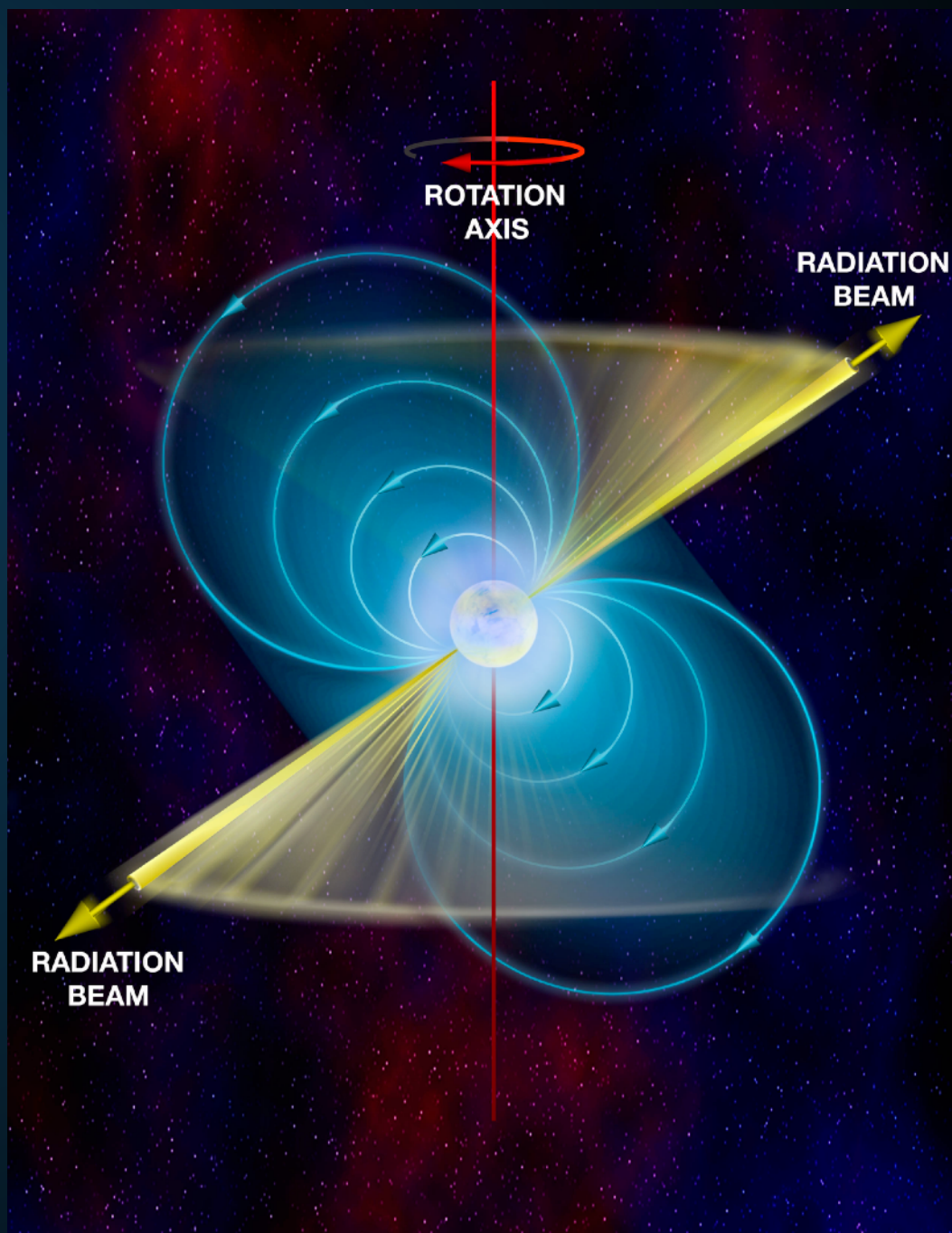
- Radio pulsars are beamed!

- Beaming fraction is small

$$f = \left[1.1 \left(\log_{10} \left(\frac{\tau}{100 \text{ Myr}} \right) \right)^2 + 15 \right] \%$$

- This varies between 15-30%.

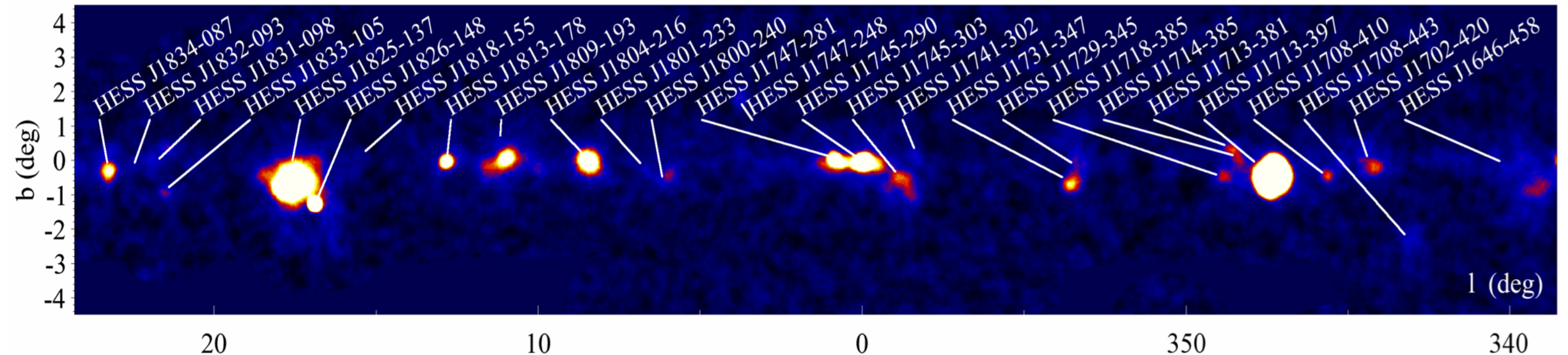
- Most pulsars are unseen in radio!



2HWC Name	ATNF Name	Distance (kpc)	Angular Separation	Projected Separation	Expected Flux ($\times 10^{-15}$)	Actual Flux ($\times 10^{-15}$)	Flux Ratio	Expected Extension	Actual Extension	Age (kyr)	Chance Overlap
J0700+143	B0656+14	0.29	0.18°	0.91 pc	43.0	23.0	1.87	2.0°	1.73°	111	0.0
J0631+169	J0633+1746	0.25	0.89°	3.88 pc	48.7	48.7	1.0	2.0°	2.0°	342	0.0
J1912+099	J1913+1011	4.61	0.34°	27.36 pc	13.0	36.6	0.36	0.11°	0.7°	169	0.30
J2031+415	J2032+4127	1.70	0.11°	3.26 pc	5.59	61.6	0.091	0.29°	0.7°	181	0.002
J1831-098	J1831-0952	3.68	0.04°	2.57 pc	7.70	95.8	0.080	0.14°	0.9°	128	0.006

2HWC Name	ATNF Name	Distance (kpc)	Angular Separation	Projected Separation	Expected Flux ($\times 10^{-15}$)	Actual Flux ($\times 10^{-15}$)	Flux Ratio	Expected Extension	Actual Extension	Age (kyr)	Chance Overlap
J1930+188	J1930+1852	7.0	0.03°	3.67 pc	23.2	9.8	2.37	0.07°	0.0°	2.89	0.002
J1814-173	J1813-1749	4.7	0.54°	44.30 pc	243	152	1.60	0.11°	1.0°	5.6	0.61
J2019+367	J2021+3651	1.8	0.27°	8.48 pc	99.8	58.2	1.71	0.28°	0.7°	17.2	0.04
J1928+177	J1928+1746	4.34	0.03°	2.27 pc	8.08	10.0	0.81	0.11°	0.0°	82.6	0.002
J1908+063	J1907+0602	2.58	0.36°	16.21 pc	40.0	85.0	0.47	0.2°	0.8°	19.5	0.26
J2020+403	J2021+4026	2.15	0.18°	6.75 pc	2.48	18.5	0.134	0.23°	0.0°	77	0.01
J1857+027	J1856+0245	6.32	0.12°	13.24 pc	11.0	97.0	0.11	0.08°	0.9°	20.6	0.06
J1825-134	J1826-1334	3.61	0.20°	12.66 pc	20.5	249	0.082	0.14°	0.9°	21.4	0.14
J1837-065	J1838-0655	6.60	0.38°	43.77 pc	12.0	341	0.035	0.08°	2.0°	22.7	0.48
J1837-065	J1837-0604	4.78	0.50°	41.71 pc	8.3	341	0.024	0.10°	2.0°	33.8	0.68
J2006+341	J2004+3429	10.8	0.42°	80.07 pc	0.48	24.5	0.019	0.04°	0.9°	18.5	0.08

- **Correcting for the beaming fraction implies that 56^{+15}_{-11} TeV halos are currently observed by HAWC.**
- **However, only 39 total HAWC sources.**



The H.E.S.S. Galactic plane survey

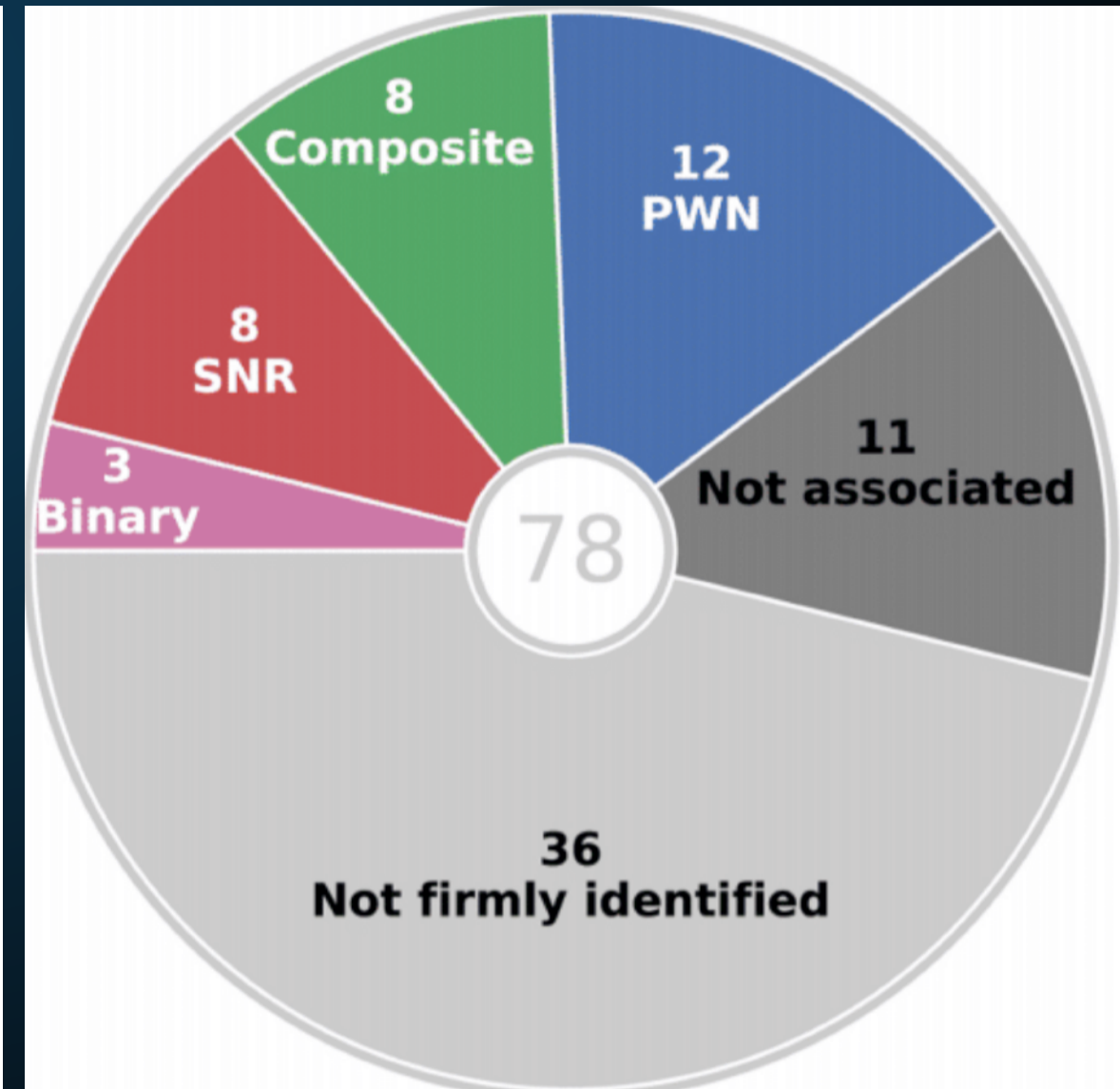
H.E.S.S. Collaboration, H. Abdalla¹, A. Abramowski², F. Aharonian^{3,4,5}, F. Ait Benkhali³, E.O. Angüner²¹, M. Arakawa⁴³, M. Arrieta¹⁵, P. Aubert²⁴, M. Backes⁸, A. Balzer⁹, M. Barnard¹, Y. Becherini¹⁰, J. Becker Tjus¹¹, D. Berge¹², S. Bernhard¹³, K. Bernlöhr¹, R. Blackwell¹⁴, M. Böttcher¹, C. Boisson¹⁵, J. Bolmont¹⁶, S. Bonnefoy³⁷, P. Bordas³, J. Bregeon¹⁷, F. Brun^{*26}, P. Brun¹⁸, M. Bryan⁹, M. Büchele³⁶, T. Bulik¹⁹, M. Capasso²⁹, S. Carrigan^{3,48}, S. Caroff³⁰, A. Carosi²⁴, S. Casanova^{21,3}, M. Cerruti¹⁶, N. Chakraborty³, R.C.G. Chaves^{*17,22}, A. Chen²³, J. Chevalier²⁴, S. Colafrancesco²³, B. Condon²⁶, J. Conrad^{27,28}, I.D. Davids⁸, J. Decock¹⁸, C. Deil^{*3}, J. Devin¹⁷, P. deWilt¹⁴, L. Dirson², A. Djannati-Atai³¹, W. Domankos³, A. Donath^{*3}, L.O'C. Drury⁴, K. Dutson³³, J. Dyks³⁴, T. Edwards³, K. Egberts³⁵, P. Eger³, G. Emery¹⁶, J.-P. Ernenwein²⁰, S. Eschbach³⁶, C. Farnier^{27,10}, S. Fegan³⁰, M.V. Fernandes², A. Fiasson²⁴, G. Fontaine³⁰, A. Förster³, S. Funk³⁶, M. Füßling³⁷, S. Gabici³¹, Y.A. Gallant¹⁷, T. Garrigoux¹, H. Gast^{3,49}, F. Gate²⁴, G. Giavitto³⁷, B. Giebel³⁰, D. Glawion²⁵, J.F. Glicenstein¹⁸, D. Gottschall²⁹, M.-H. Grondin²⁶, J. Hahn³, M. Haupt³⁷, J. Hawkes¹⁴, G. Heinzelmann², G. Henri³², G. Hermann³, J.A. Hinton³, W. Hofmann³, C. Hoischen³⁵, T. L. Holch⁷, M. Holler¹³, D. Horns², A. Ivascenko¹, H. Iwasaki⁴³, A. Jacholkowska¹⁶, M. Jamrozy³⁸, D. Jankowsky³⁶, F. Jankowsky²⁵, M. Jingó²³, L. Jouvin³¹, I. Jung-Richardt³⁶, M.A. Kastendieck², K. Katarzyński³⁹, M. Katsuragawa⁴⁴, U. Katz³⁶, D. Kerszberg¹⁶, D. Khangulyan⁴³, B. Khéifis³¹, J. King³, S. Klepser³⁷, D. Klochkov²⁹, W. Kluzniak³⁴, Nu. Komin²³, K. Kosack¹⁸, S. Krakau¹¹, M. Kraus³⁶, P.P. Krüger¹, H. Laffon²⁶, G. Lamanna²⁴, J. Lau¹⁴, J.-P. Lees²⁴, J. Lefaucheur¹⁵, A. Lemoine-Goumard²⁶, J.-P. Lenain¹⁶, E. Leser³⁵, T. Lohse⁷, M. Lorentz¹⁸, R. Liu³, R. López-Coto³, I. Lytova³⁷, V. Marandon^{*3}, D. Malyshev²⁹, A. Marcowith¹⁷, C. Mariaud³⁰, R. Marx³, G. Maurin²⁴, N. Maxted^{14,45}, M. Mayer⁷, P.J. Meintjes⁴⁰, M. Meyer²⁷, A.M.W. Mitchell³, R. Moderski³⁴, M. Mohamed²⁵, L. Mohrmann³⁶, K. Mora²⁷, E. Moulin¹⁸, T. Murach³⁷, S. Nakashima⁴⁴, M. de Naurois³⁰, H. Ndiyavala¹, F. Niederwanger¹³, J. Niemiec²¹, L. Oakes⁷, P. O'Brien³³, H. Odaka⁴⁴, S. Ohm³⁷, M. Ostrowski³⁸, I. Oya³⁷, M. Padovani¹⁷, M. Panter³, R.D. Parsons³, M. Paz Arribas¹, N.W. Pekeur¹, G. Pelletier³², C. Perennes¹⁶, P.-O. Petrucci³², B. Peyaud¹⁸, Q. Piel²⁴, S. Pita³¹, V. Poireau²⁴, H. Poon³, D. Prokhorov¹⁰, H. Prokoph¹², G. Pühlhofer²⁹, M. Punch^{31,10}, A. Quirrenbach²⁵, S. Raab³⁶, R. Rauth¹³, A. Reimer¹³, O. Reimer¹³, M. Renaud¹⁷, R. de los Reyes³, F. Rieger^{3,41}, L. Rinchiuso¹⁸, C. Romoli⁴, G. Rowell¹⁴, B. Rudak³⁴, C.B. Rulten¹⁵, S. Safi-Harb⁵⁰, V. Sahakian^{6,5}, S. Saito⁴³, D.A. Sanchez²⁴, A. Santangelo²⁹, M. Sasaki³⁶, M. Schandri³⁶, R. Schlickeiser¹¹, F. Schüssler¹⁸, A. Schulz³⁷, U. Schwanke⁷, S. Schwemmer²⁵, M. Seglar-Arroyo¹⁸, M. Settimio¹⁶, A.S. Seyffert¹, N. Shafi²³, I. Shilon³⁶, K. Shiningayamwe⁸, R. Simoni⁹, H. Sol¹⁵, F. Spanier¹, M. Spir-Jacob³¹, L. Stawarz³⁸, R. Steenkamp⁸, C. Stegmann^{35,37}, I. Sushch¹, T. Takahashi⁴⁴, J.-P. Tavernet¹⁶, T. Tavernier³¹, A.M. Taylor³⁷, R. Terrier³¹, L. Tibaldo³, D. Tiziani³⁶, M. Tluczykont², C. Trichard²⁰, M. Tsirou¹⁷, N. Tsuji⁴³, R. Tuffs³, Y. Uchiyama⁴³, D.J. van der Walt¹, C. van Eldik³⁶, C. van Rensburg¹, B. van Soelen⁴⁰, G. Vasileiadis¹⁷, J. Veh³⁶, C. Venter¹, A. Viana^{3,46}, P. Vincent¹⁶, J. Vink⁹, F. Voisin¹⁴, H.J. Völk³, T. Vuillaume²⁴, Z. Wadiasingh¹, S.J. Wagner²⁵, P. Wagner⁷, R.M. Wagner²⁷, R. White³, A. Wierzcholska²¹, P. Willmann³⁶, A. Wörlein³⁶, D. Wouters¹⁸, R. Yang³, D. Zaborov³⁰, M. Zacharias¹, R. Zanin³, A.A. Zdziarski³⁴, A. Zech¹⁵, F. Zefi³⁰, A. Ziegler³⁶, J. Zorn³, and N. Źywucka³⁸

(Affiliations can be found after the references)

April 10, 2018

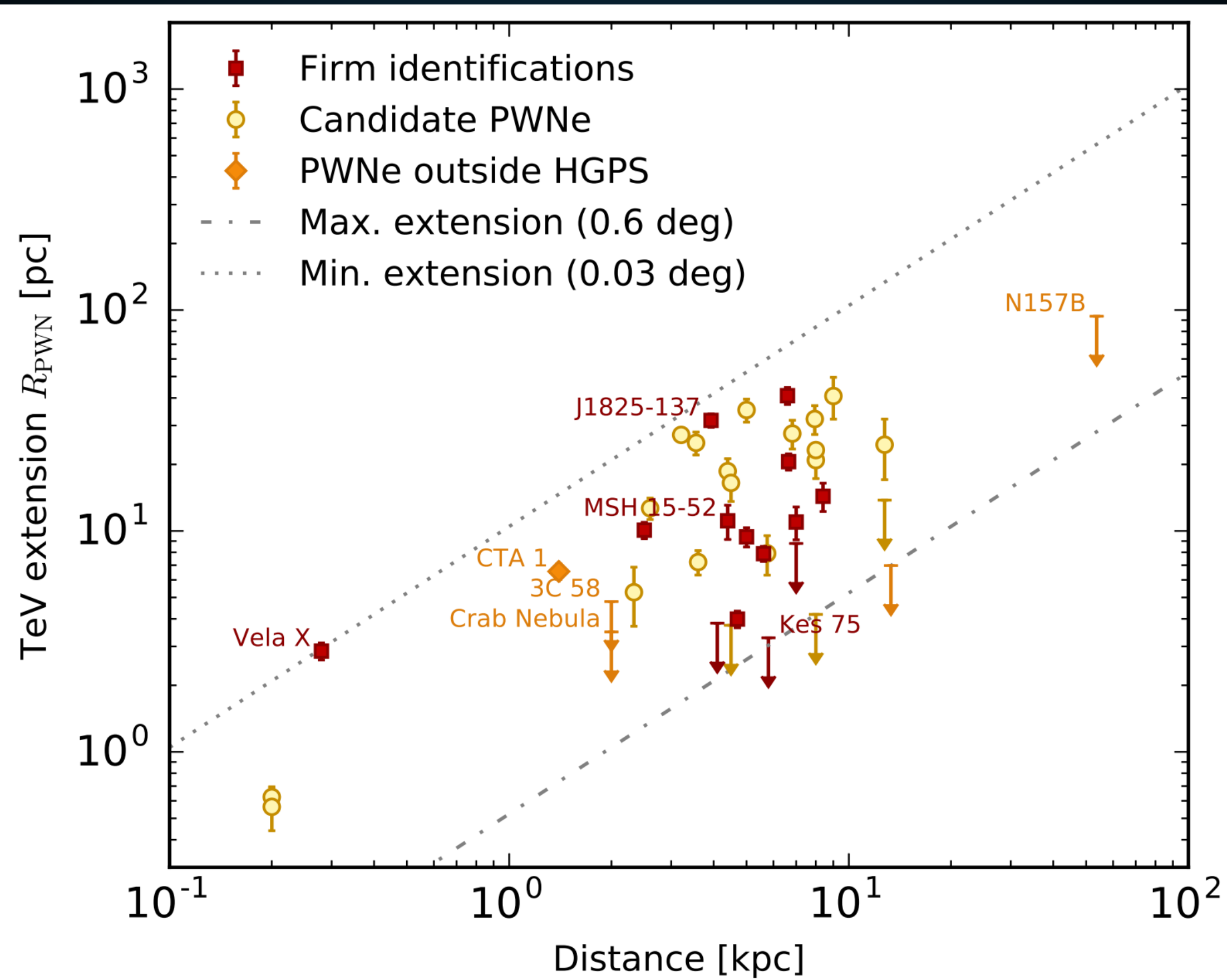
ABSTRACT

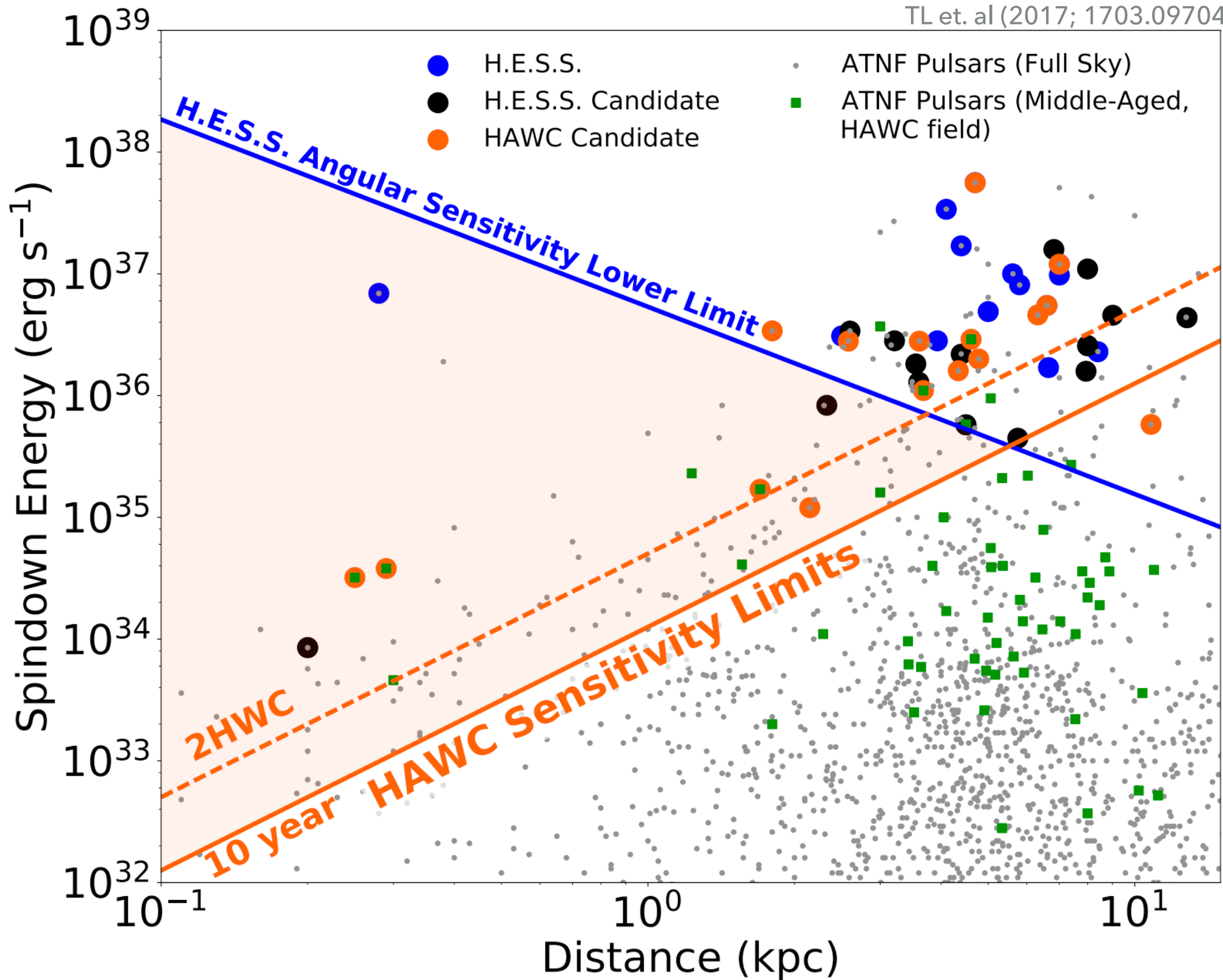
We present the results of the most comprehensive survey of the Galactic plane in very high-energy (VHE) γ -rays, including a public release of Galactic sky maps, a catalog of VHE sources, and the discovery of 16 new sources of VHE γ -rays. The High Energy Spectroscopic System (H.E.S.S.) Galactic plane survey (HGPS) was a decade-long observation program carried out by the H.E.S.S. I array of Cherenkov telescopes in Namibia from 2004 to 2013. The observations amount to nearly 2700 h of quality-selected data, covering the Galactic plane at longitudes from $\ell = 250^\circ$ to 65° and latitudes $|b| \leq 3^\circ$. In addition to the unprecedented spatial coverage, the HGPS also features a relatively high angular resolution ($0.08^\circ \approx 5$ arcmin mean point spread function 68% containment radius), sensitivity ($\lesssim 1.5\%$ Crab flux for point-like sources), and energy range (0.2 to 100 TeV). We constructed a catalog of VHE γ -ray sources from the HGPS data set with a systematic procedure for both source detection and characterization of morphology and spectrum. We present this likelihood-based method in detail, including the introduction of a model component to account for unresolved, large-scale emission along the Galactic plane. In total, the resulting HGPS catalog contains 78 VHE sources, of which 14 are not reanalyzed here, for example, due to their complex morphology, namely shell-like sources and the Galactic center region. Where possible, we provide a firm identification of the VHE source or plausible associations with sources in other astronomical catalogs. We also studied



WHY IS HAWC IMPORTANT

HESS Collaboration 2017 (1702.08280)





FIRST DETECTIONS!

[Previous | Next | [ADS](#)]

HAWC detection of TeV emission near PSR B0540+23

ATel #10941; *Colas Riviere (University of Maryland), Henrike Fleischhack (Michigan Technological University), Andres Sandoval (Universidad Nacional Autonoma de Mexico) on behalf of the HAWC collaboration*

on 9 Nov 2017; 23:11 UT

Credential Certification: Colas Riviere (riviere@umd.edu)

Subjects: Gamma Ray, TeV, VHE, Pulsar

[Tweet](#) [Recommend 5](#)

The High Altitude Water Cherenkov (HAWC) collaboration reports the discovery of a new TeV gamma-ray source HAWC J0543+233. It was discovered in a search for extended sources of radius 0.5° in a dataset of 911 days (ranging from November 2014 to August 2017) with a test statistic value of 36 (6σ pre-trials), following the method presented in Abeysekara et al. 2017, ApJ, 843, 40. The measured J2000.0 equatorial position is RA= 85.78° , Dec= 23.40° with a statistical uncertainty of 0.2° . HAWC J0543+233 was close to passing the selection criteria of the 2HWC catalog (Abeysekara et al. 2017, ApJ, 843, 40, see [HAWC J0543+233 in 2HWC map](#)), which it now fulfills with the additional data.

HAWC J0543+233 is positionally coincident with the pulsar PSR B0540+23 (Edot = 4.1×10^{34} erg s $^{-1}$, dist = 1.56 kpc, age = 253 kyr). It is the third low Edot, middle-aged pulsar announced to be detected with a TeV halo, along with Geminga and B0656+14. It was predicted to be one of the next such detection by HAWC by Linden et al., 2017, arXiv:1703.09704.

Using a simple source model consisting of a disk of radius 0.5° , the measured spectral index is -2.3 ± 0.2 and the differential flux at 7 TeV is $(7.9 \pm 2.3) \times 10^{-15}$ TeV $^{-1}$ cm $^{-2}$ s $^{-1}$. The errors are statistical only. Further morphological and spectral analysis as well as studies of the systematic uncertainty are ongoing.

[Previous | Next | [ADS](#)]

HAWC detection of TeV source HAWC J0635+070

ATel #12013; *Chad Brisbois (Michigan Technological University), Colas Riviere (University of Maryland), Henrike Fleischhack (Michigan Technological University), Andrew Smith (University of Maryland) on behalf of the HAWC collaboration*

on 6 Sep 2018; 14:47 UT

Credential Certification: Colas Riviere (riviere@umd.edu)

Subjects: Gamma Ray, TeV, VHE, Pulsar

[Tweet](#) [Recommend 2](#)

The High Altitude Water Cherenkov (HAWC) collaboration reports the discovery of a new TeV gamma-ray source HAWC J0635+070. It was discovered in a search for extended sources covering 1128 days of HAWC observations with a test statistic value of 27 ($>5\sigma$ pre-trials), following the method presented in [Abeysekara et al. 2017, ApJ, 843, 40]. Its significance in the 2HWC data set excluded it from being included in the catalog ($\sim 3.5\sigma$ pre-trials), but with the addition of ~ 600 more days of data it now satisfies that criterion. The best-fit J2000.0 equatorial position is RA= $98.71 \pm 0.20^\circ$, Dec= $7.00 \pm 0.22^\circ$, with a Gaussian 1-sigma extent of $0.65^\circ \pm 0.18^\circ$.

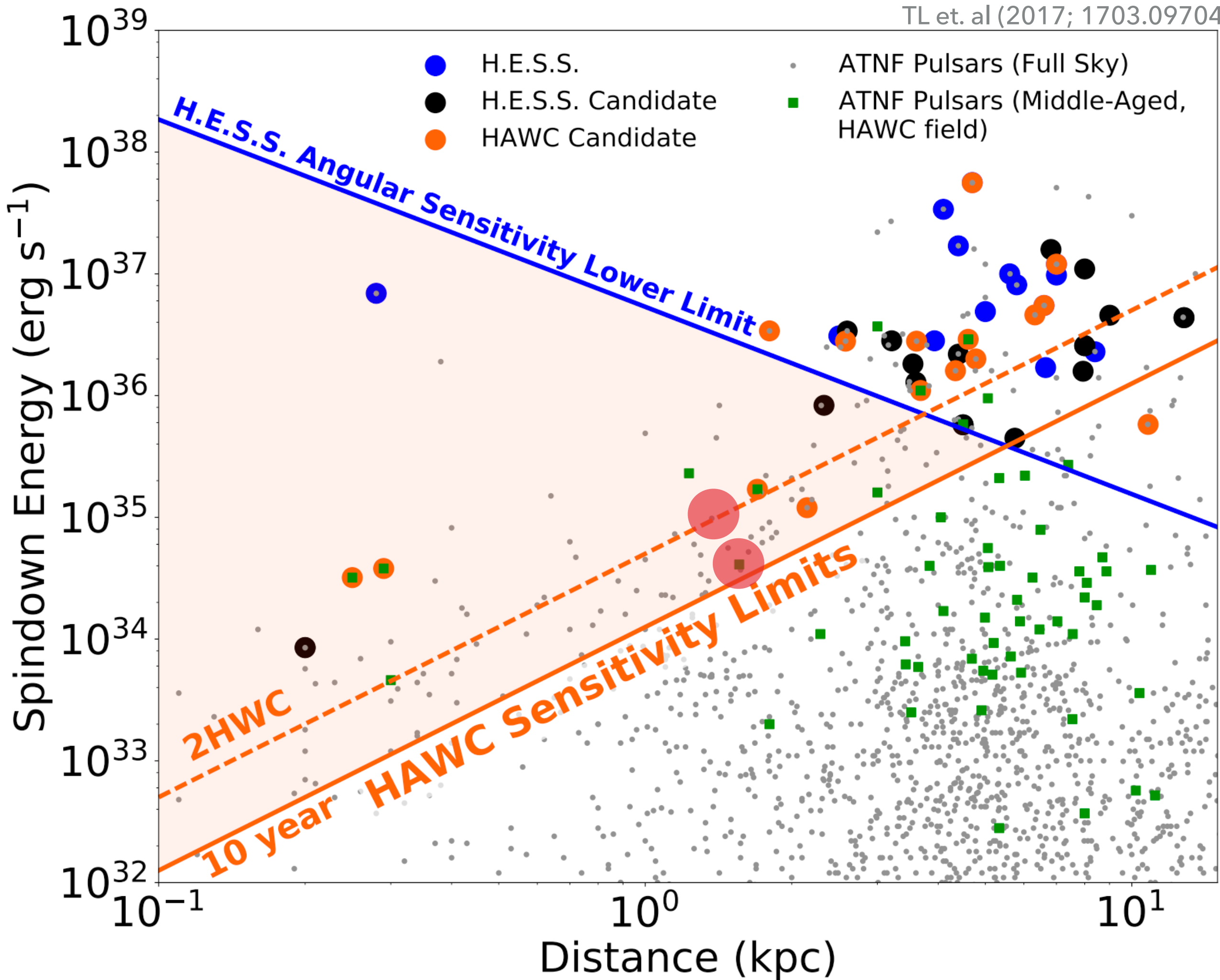
The spectral energy distribution is well-fit by a power law with spectral index -2.15 ± 0.17 . The differential flux at 10 TeV is $(8.6 \pm 3.2) \times 10^{-15}$ TeV $^{-1}$ cm $^{-2}$ s $^{-1}$. All errors are statistical only; further morphological and spectral analysis as well as studies of the systematic uncertainty are ongoing.

Given its spectrum and morphology, we believe HAWC J0635+070 may be the TeV halo of the pulsar PSR J0633+0632 (Edot = 1.2×10^{35} erg s $^{-1}$, dist = 1.35 kpc, age = 59 kyr, unknown proper motion [Manchester et al., 2005, AJ, 129]). The gamma-ray spectrum and morphology is compatible with a "Geminga-like" TeV Halo [Abeysekara et al. 2017, Science, 358, 911; Linden et al., 2017, PRD, 96, 103016]. We encourage follow-up observations at other wavelengths.

- **HAWC has detected two additional TeV halos**

- **Total Count:**

- **Middle-Aged: 6**
- **Younger: 13**



Implication III: The positron excess is due to pulsar activity

Positron fraction

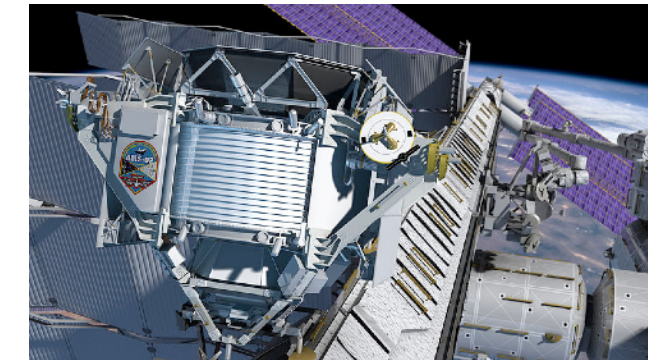
10^{-1}

1

10

10^2

positron, electron energy [GeV]



- AMS
- FERMI
- PAMELA
- AMS-01
- HEAT
- CAPRICE98
- CAPRICE94
- TS93

PULSARS PRODUCE THE POSITRON EXCESS

- **What were the uncertainties in pulsar models?**

- **I: The e^+e^- production efficiency?**

Profumo (0812.4457); Malyshev et al. (0903.1310)

%. A quantitative discussion of plausible values for f_{e^\pm} was recently given in Ref. [38]. We shall not review their discussion here, but Ref. [38] argues (see in particular their very informative App. B and C) that in the context of a standard model for the pulsar wind nebulae, a reasonable range for f_{e^\pm} falls between 1% and 30%.

- **II: The e^+e^- spectrum.**
 - **III: The propagation of e^+e^- to Earth.**

PULSARS PRODUCE THE POSITRON EXCESS

- **What were the uncertainties in pulsar models?**

- I: The e^+e^- production efficiency?

- II: The e^+e^- spectrum.

Hooper et al. (0810.1527)

part of their energy adiabatically because of the expansion of the wind. The energy spectrum injected by a single pulsar depends on the environmental parameters of the pulsar, but some attempts to calculate the average spectrum injected by a population of mature pulsars suggest that the spectrum may be relatively hard, having a slope of $\sim 1.5\text{-}1.6$ [18]. This spectrum, however, results from a complex interplay of individual pulsar spectra, of the spatial and age distributions of pulsars in the Galaxy, and on the assumption that the chief channel for pulsar spin down is magnetic dipole radiation. Due to the related uncertainties, variations from this injection spectra cannot be ruled out. Typically, one concentrates the attention on pulsars of age $\sim 10^5$ years because younger pulsars are likely to still

- III: The propagation of e^+e^- to Earth.

TEV HALOS ANSWER THE KEY QUESTIONS!

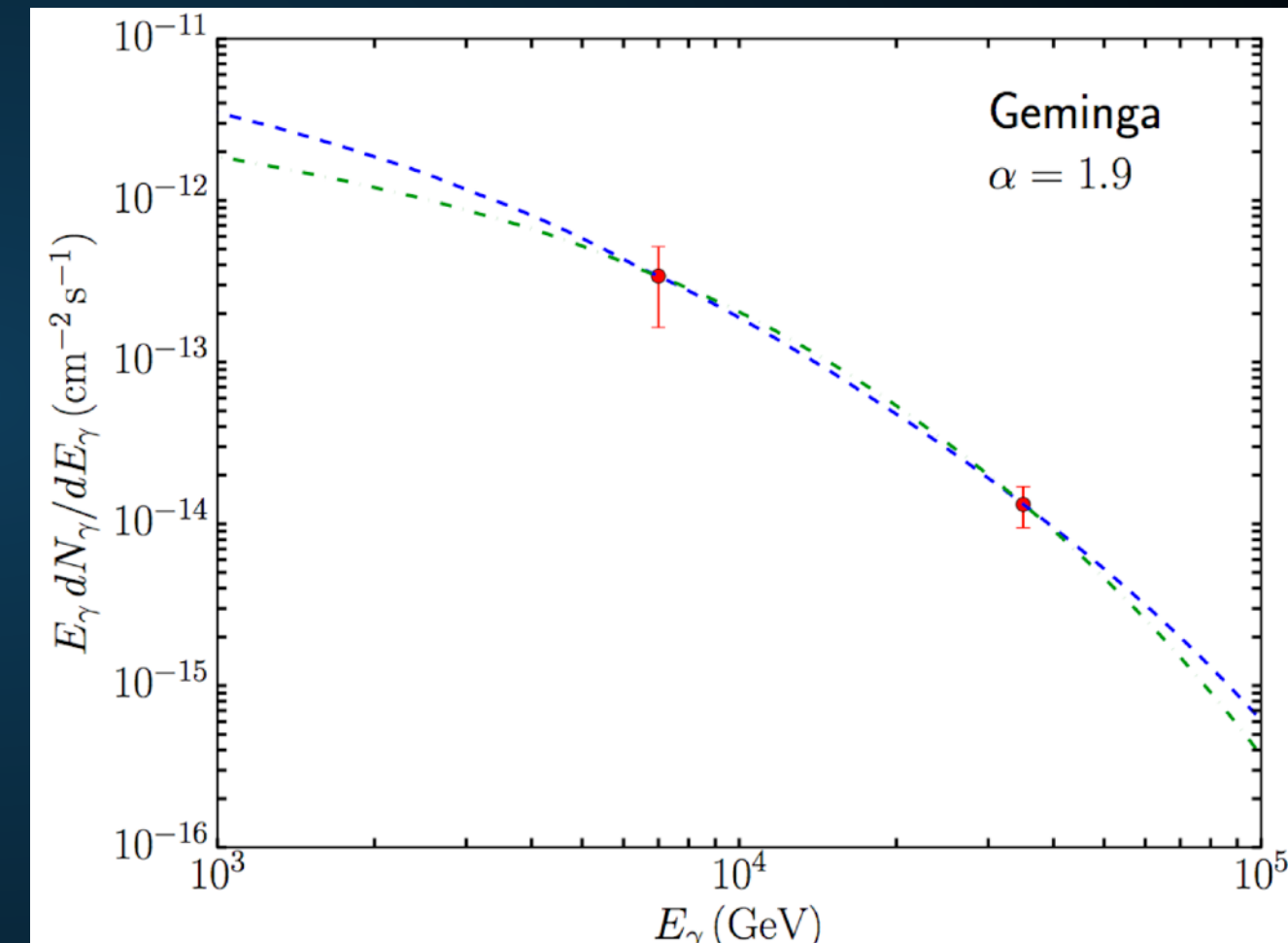
Name	Tested radius [°]	Index	$F_7 \times 10^{15}$ [TeV $^{-1}$ cm $^{-2}$ s $^{-1}$]	TeVCat
2HWC J0631+169	-	-2.57 ± 0.15	6.7 ± 1.5	Geminga
"	2.0	-2.23 ± 0.08	48.7 ± 6.9	Geminga
2HWC J0635+180	-	-2.56 ± 0.16	6.5 ± 1.5	Geminga

- **We assume a power-law electron injection spectrum with an exponential cutoff**

- Best Fit:

$$-1.9 < \alpha < -1.5$$

$$E_{\text{cut}} \approx 50 \text{ TeV}$$



$\sim 3-9 \times 10^{33} \text{ erg s}^{-1}$!

9-27% of the total pulsar spin-down power!

PULSARS PRODUCE THE POSITRON EXCESS

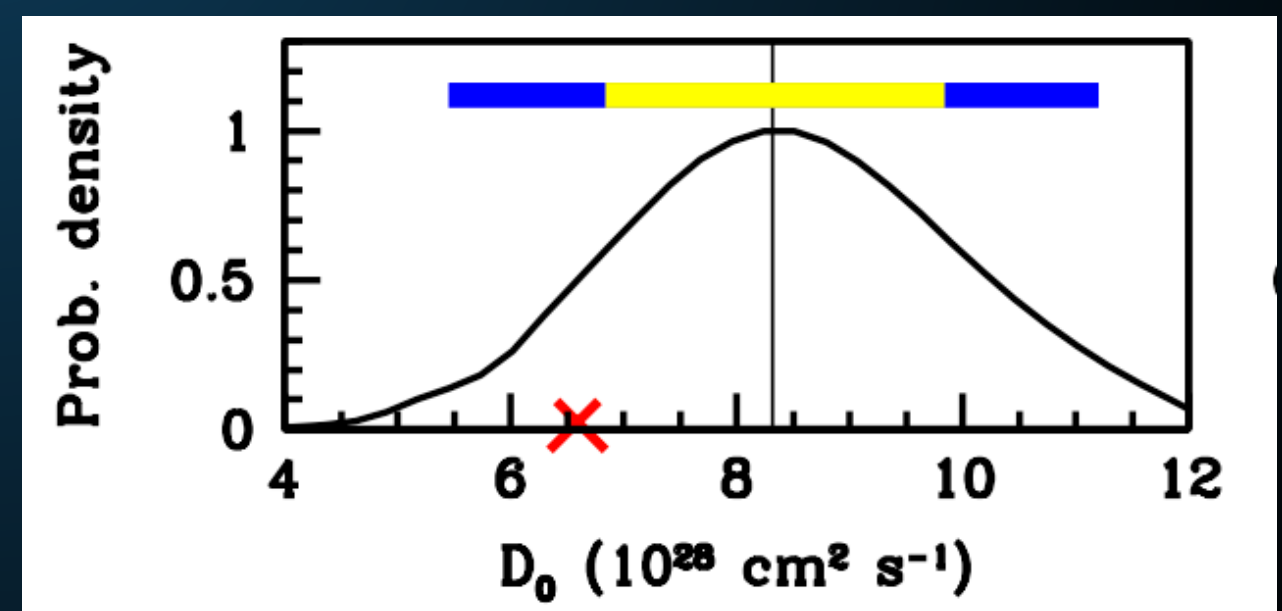
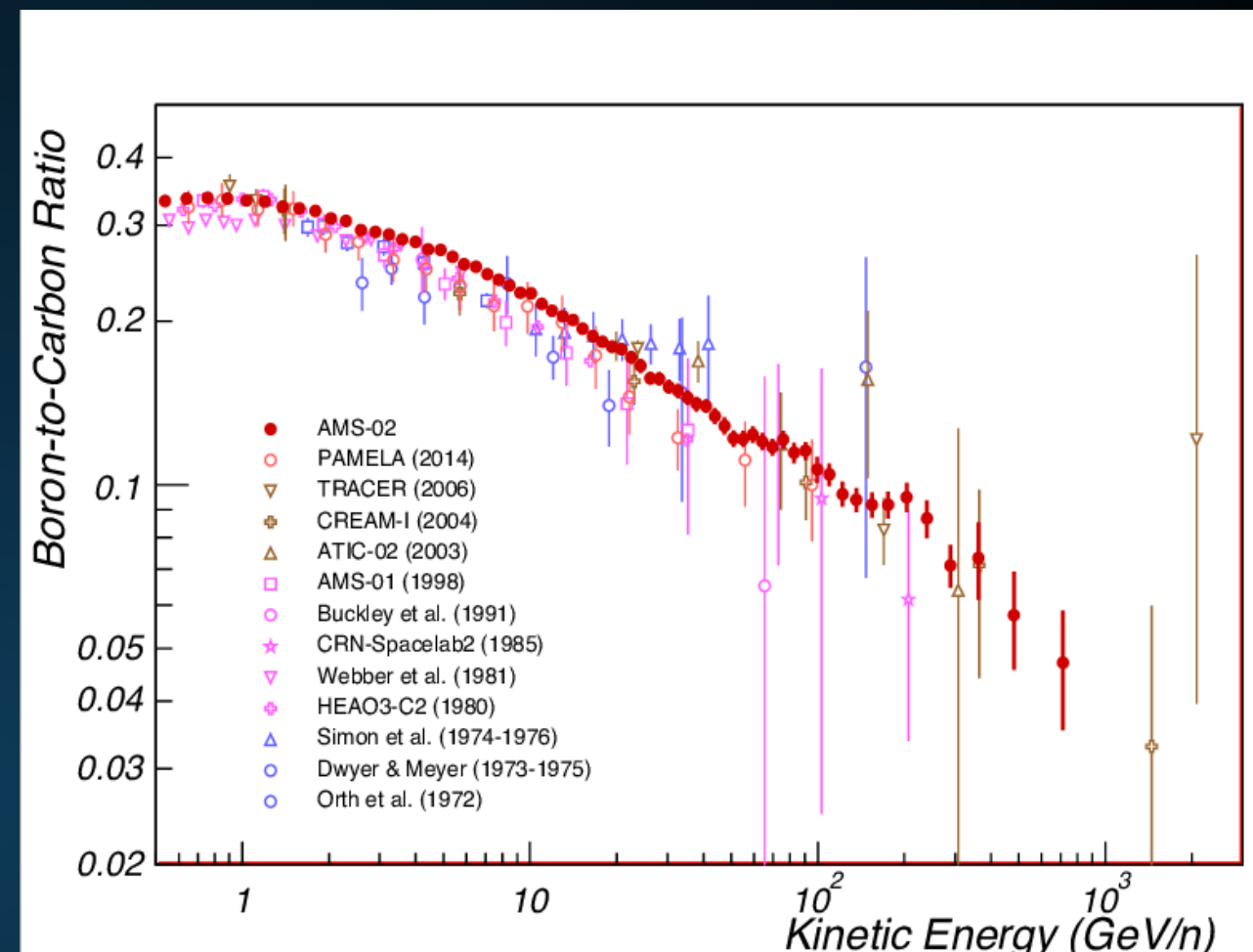
- **What were the uncertainties in pulsar models?**
 - I: The e^+e^- production efficiency?
 - II: The e^+e^- spectrum.
 - III: The propagation of e^+e^- to Earth.

Malyshev et al. (0903.1310)

The observed spectrum on Earth of electrons and positrons injected by pulsars is also strongly dependent on propagation effects. In particular, the observed cutoff in the flux of electrons from a pulsar can be much smaller than the injection cutoff due to energy losses (“cooling”) during propagation. We define the cooling break, $E_{\text{br}}(t)$, as the maximal energy electrons can have after propagating for time t . Since – as stated above – the typical

Cosmic-ray propagation is the last key.

- Cosmic-Ray primary to secondary ratios tell us about:
 - The average grammage encountered by cosmic-rays before they escape the galaxy (e.g. B/C)
 - The average time cosmic-rays propagate before they escape (eg. $^{10}\text{Be}/^{9}\text{Be}$).



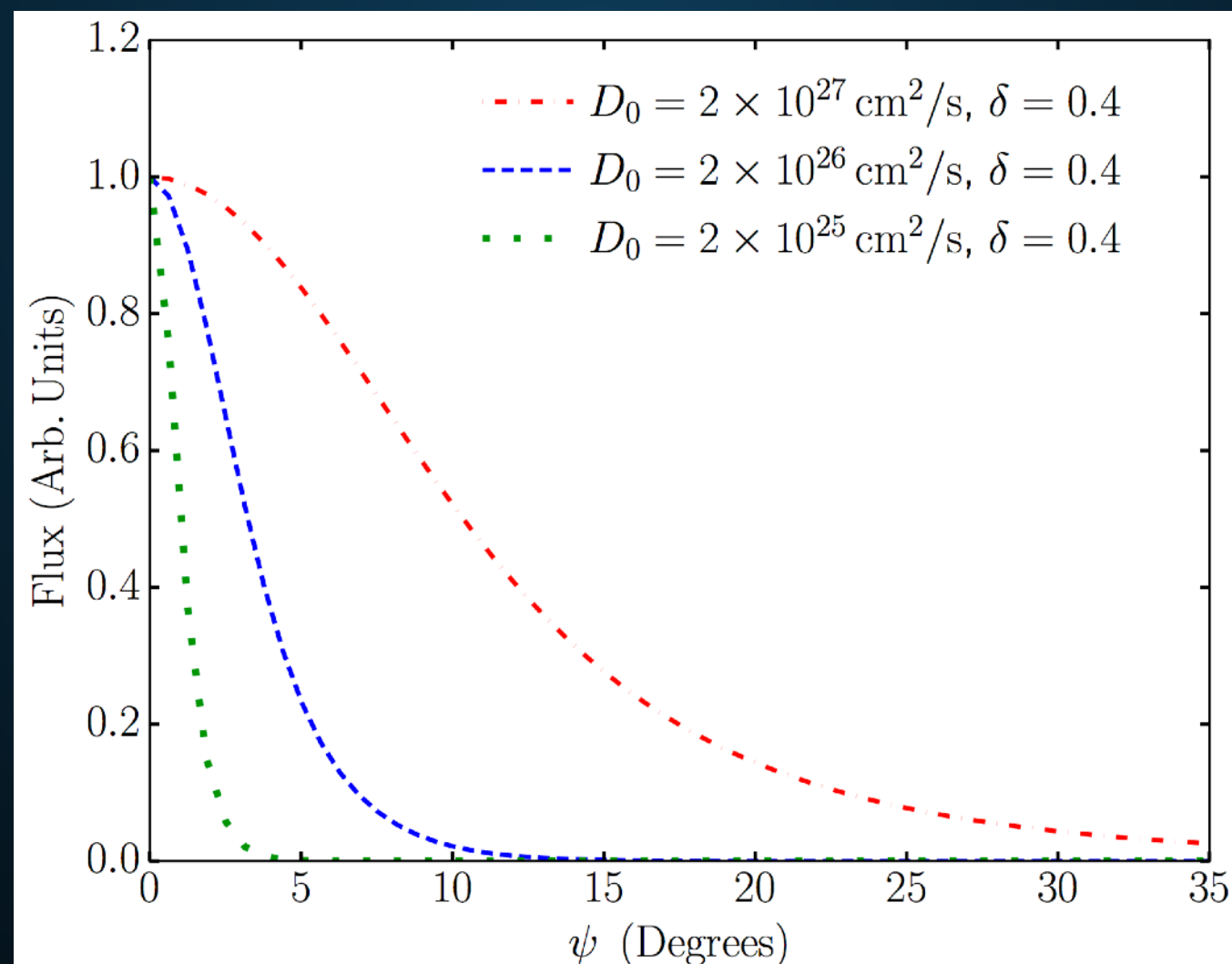
Fool me once.... shame on, shame on you...

Fool me..... you can't get fooled again!

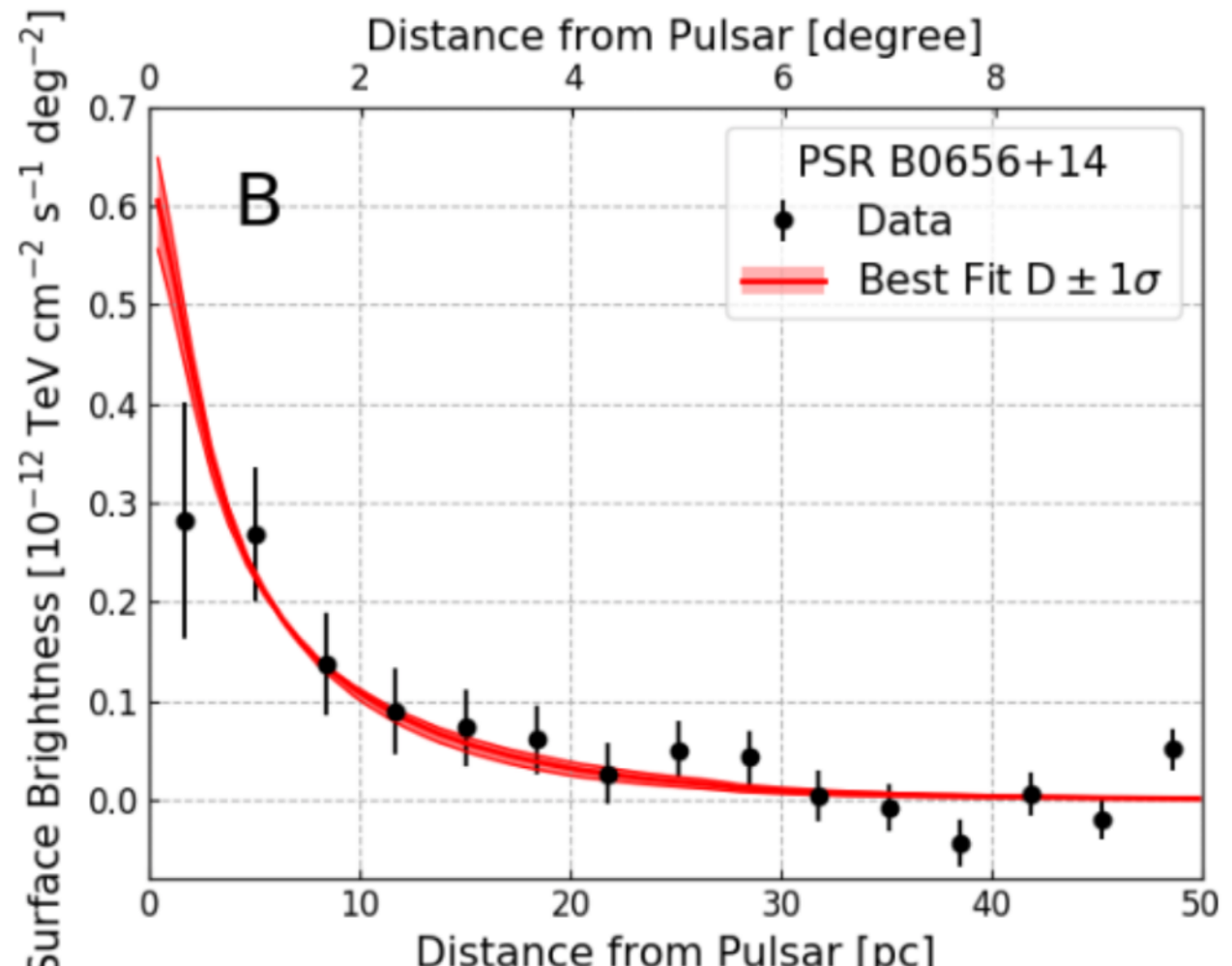
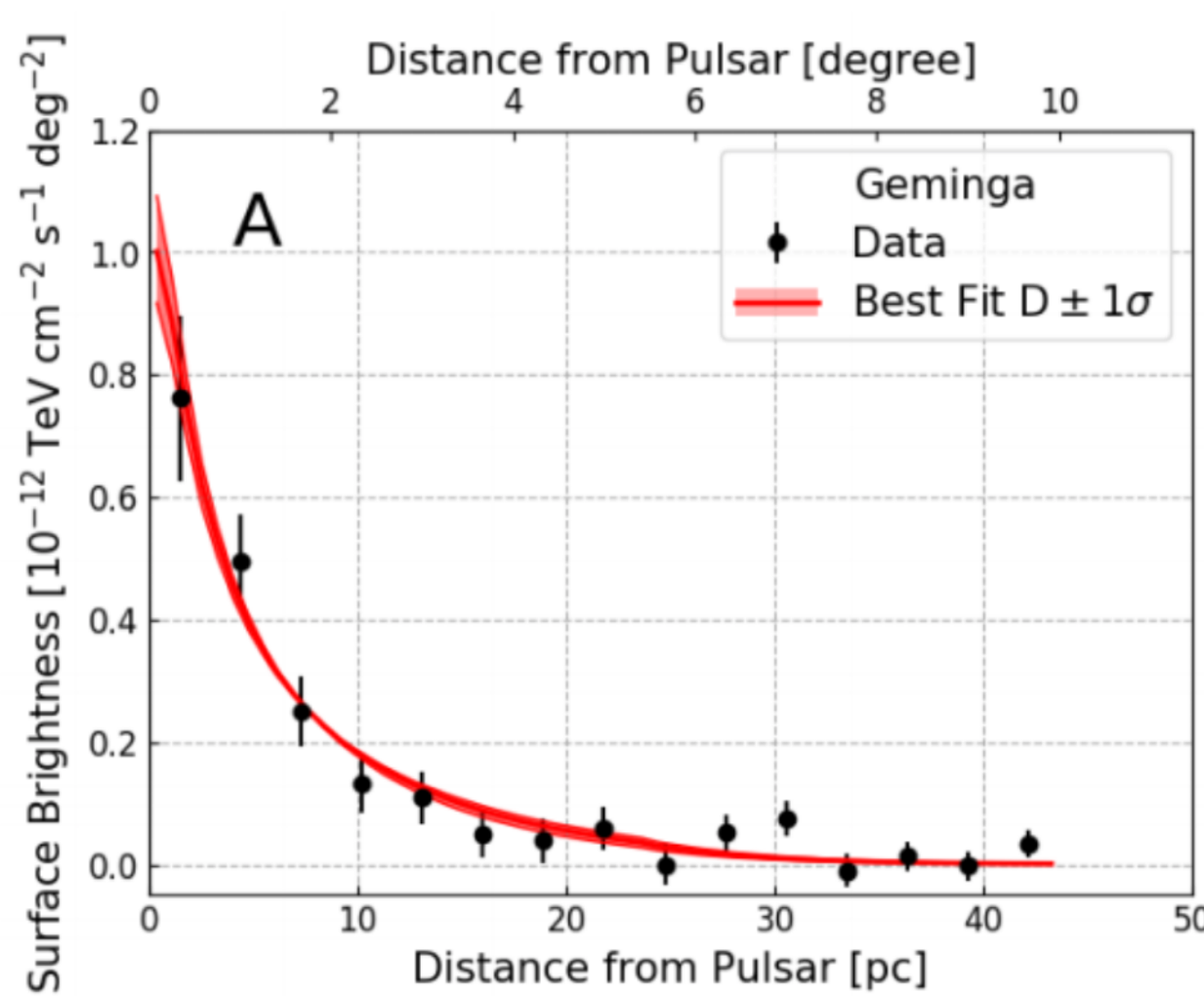
- The energy loss timescale in the ISM ($5 \mu\text{G}$; 1 eV cm^{-3}) is:

$$\tau_{\text{loss}} \approx 2 \times 10^4 \text{ yr} \left(\frac{10 \text{ TeV}}{E_e} \right)$$

- Can calculate the profile for different diffusion constants:

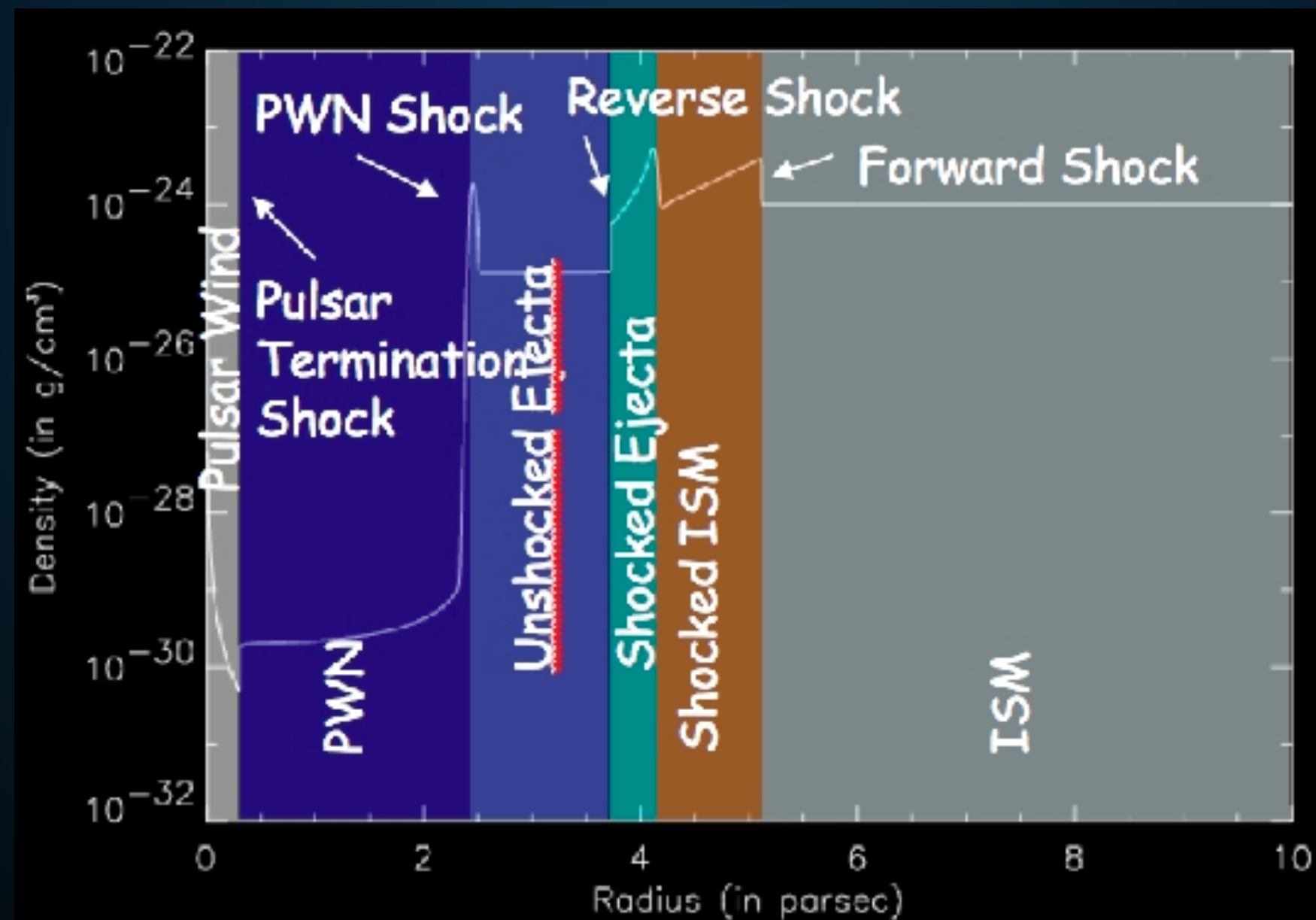


AN ENERGETICS PROBLEM

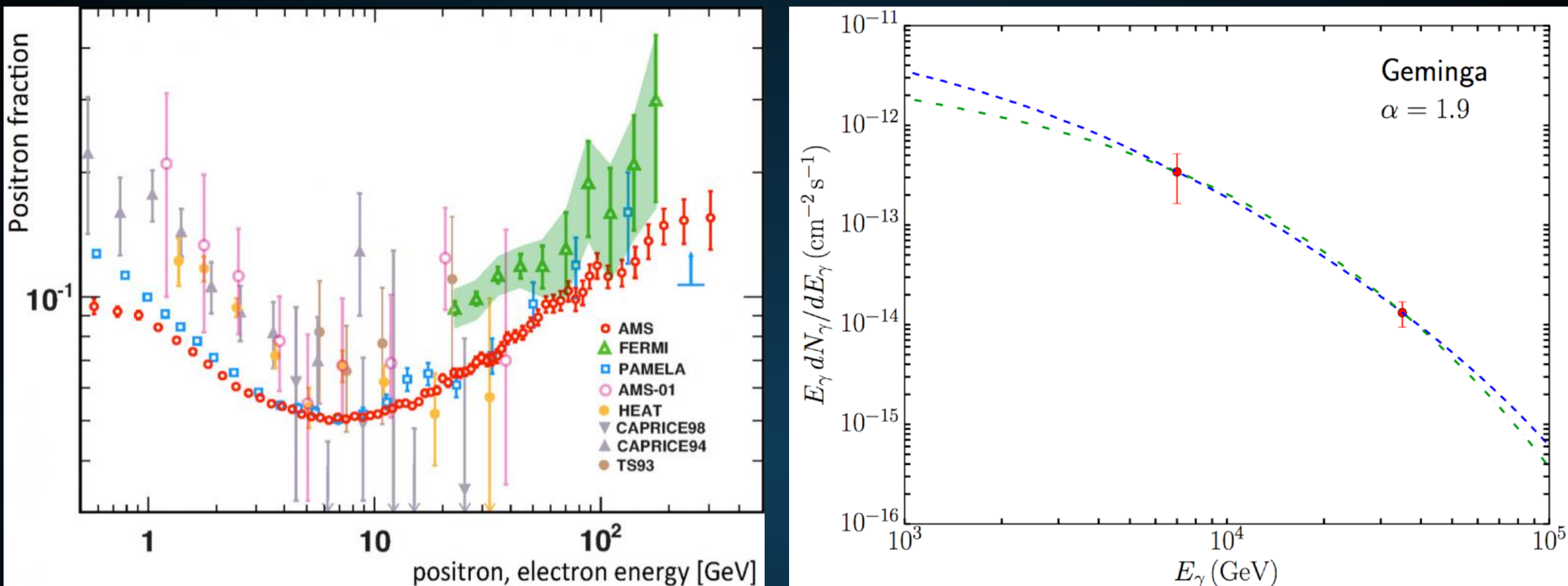


- Morphology of each pulsar fit by diffusion.
- If diffusion continued to 250 pc, would require >100% efficiency.

Pulsar Parameters		Geminga	PSR B0656+14
(Right ascension, declination) (J2000 source location)	[degrees]	(98.48, 17.77)	(104.95, 14.24)
τ_c (characteristic age)	[years]	342,000	110,000
D ₁₀₀ (Diffusion coefficient of 100TeV electrons from joint fit of two PWNe)	[x10 ²⁷ cm ² /sec]	4.5 ± 1.2	4.5 ± 1.2



LOW-ENERGY COSMIC-RAY DIFFUSION

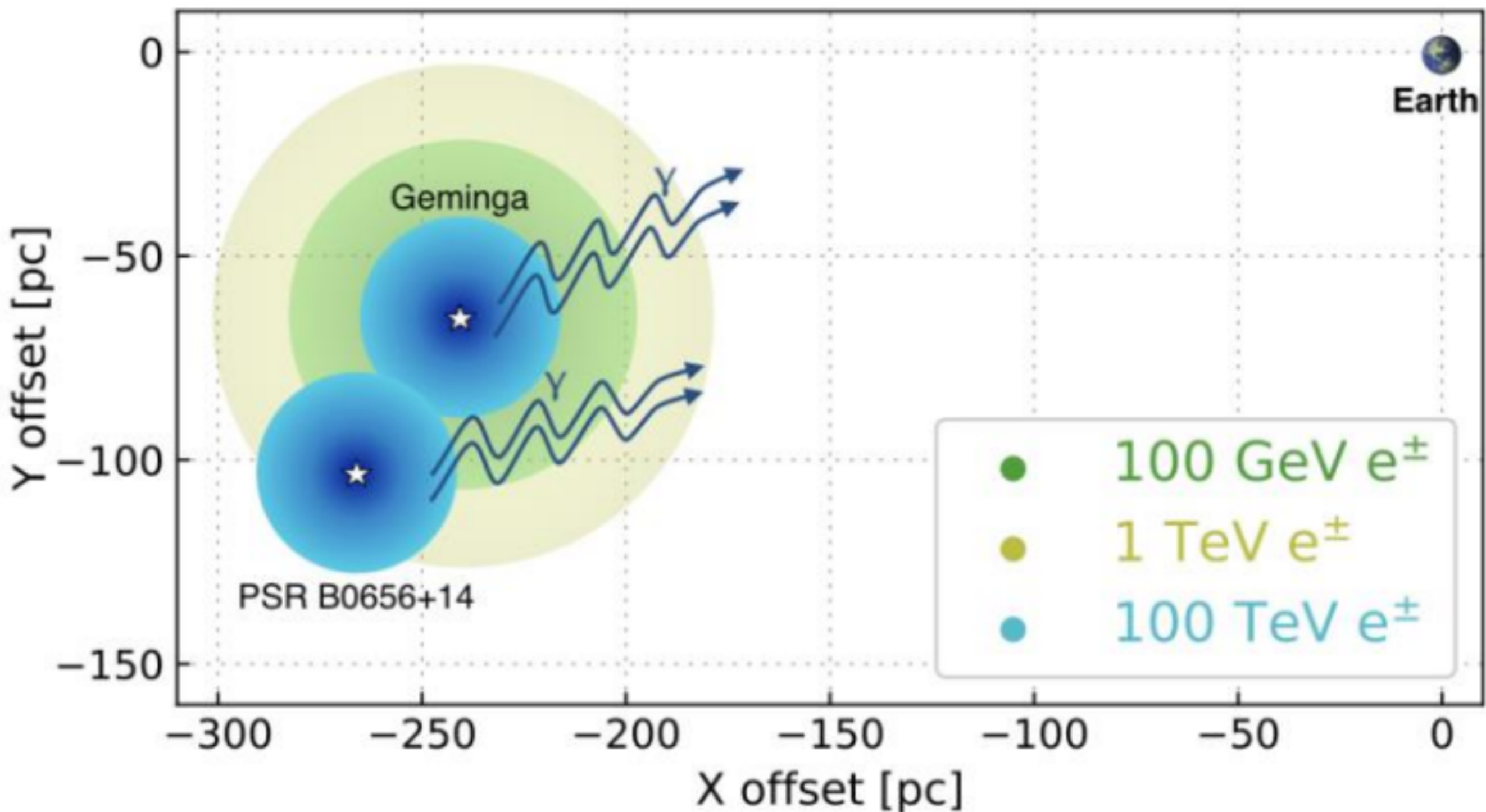


$$\tau_{\text{Diff}} \propto \frac{l^2}{D_0 E^\delta}$$

$$\tau_{\text{loss}} \propto E^{-1}$$

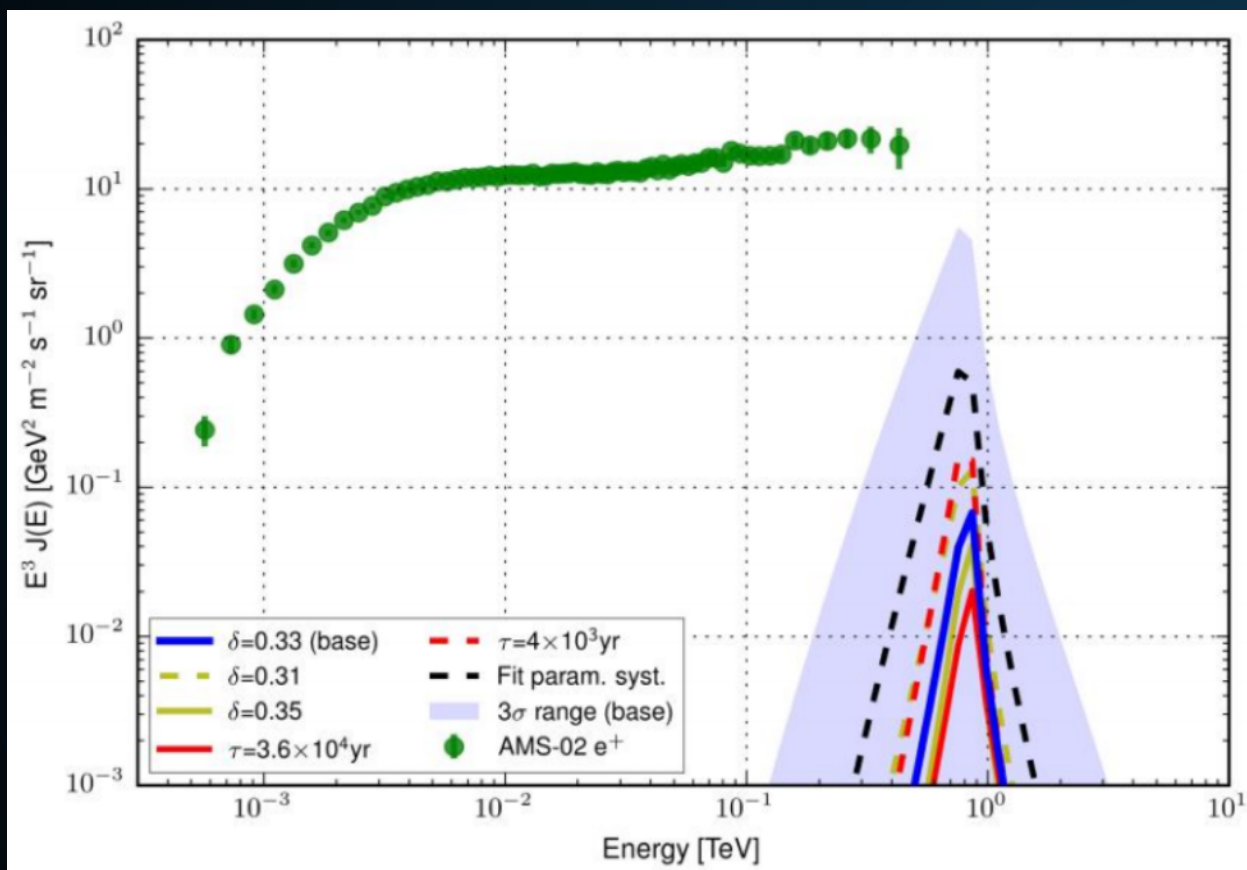
$$\left(\frac{\Delta E}{E}\right) \propto \frac{\tau_{\text{Diff}}}{\tau_{\text{loss}}} \propto E^{1-\delta}$$

AVERAGE COSMIC-RAY DIFFUSION



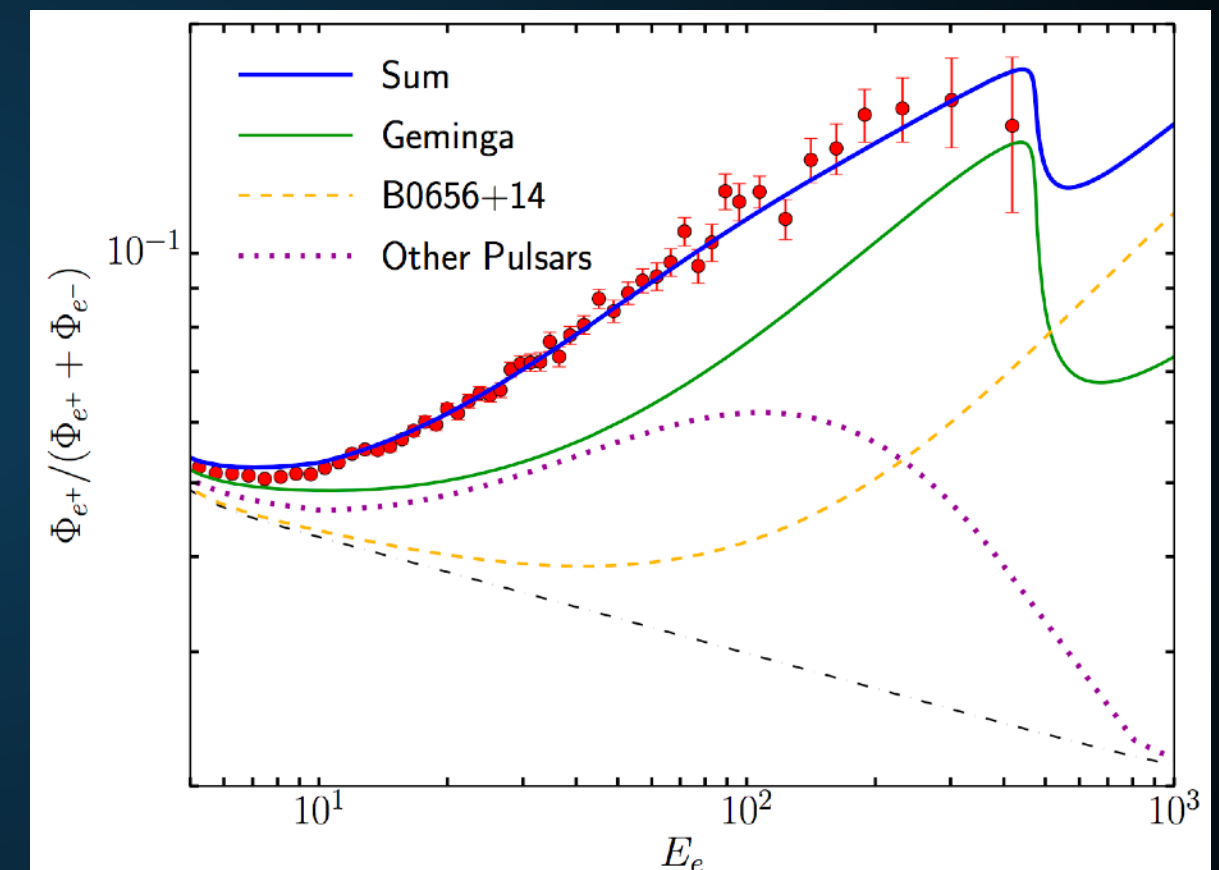
TWO POSSIBLE ASSUMPTIONS

Extrapolate Low-Diffusion Constant
UP to Earth:



100 GeV positrons do not make it to
Earth

Extrapolate the High Diffusion
Constant DOWN to Earth:



100 GeV positrons do make it to Earth

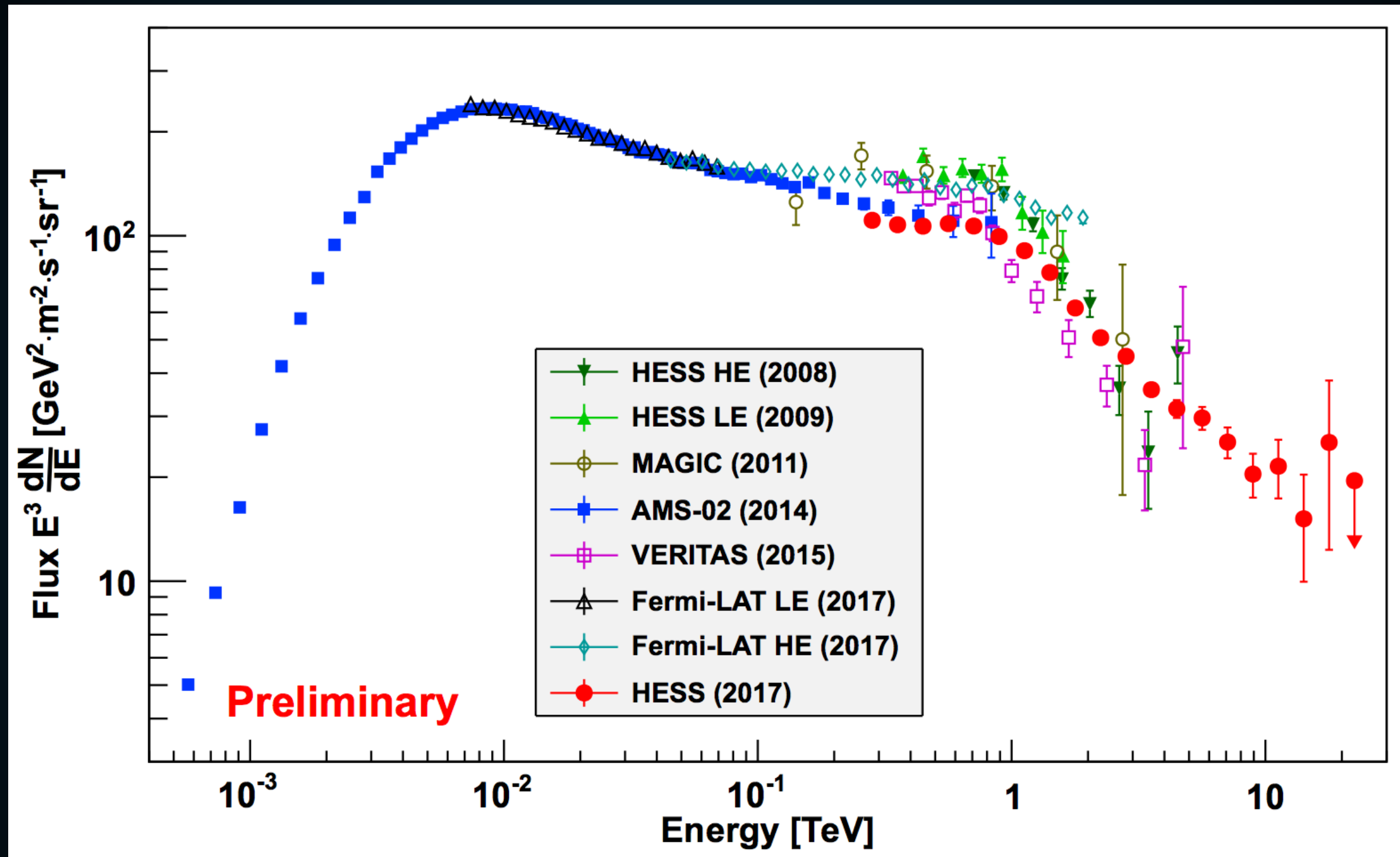
Hooper et al. (1702.08436)

Profumo et al. (1803.09731)

Fang et al. (1803.02640)

CAN THE LOCAL DIFFUSION CONSTANT BE LOW?

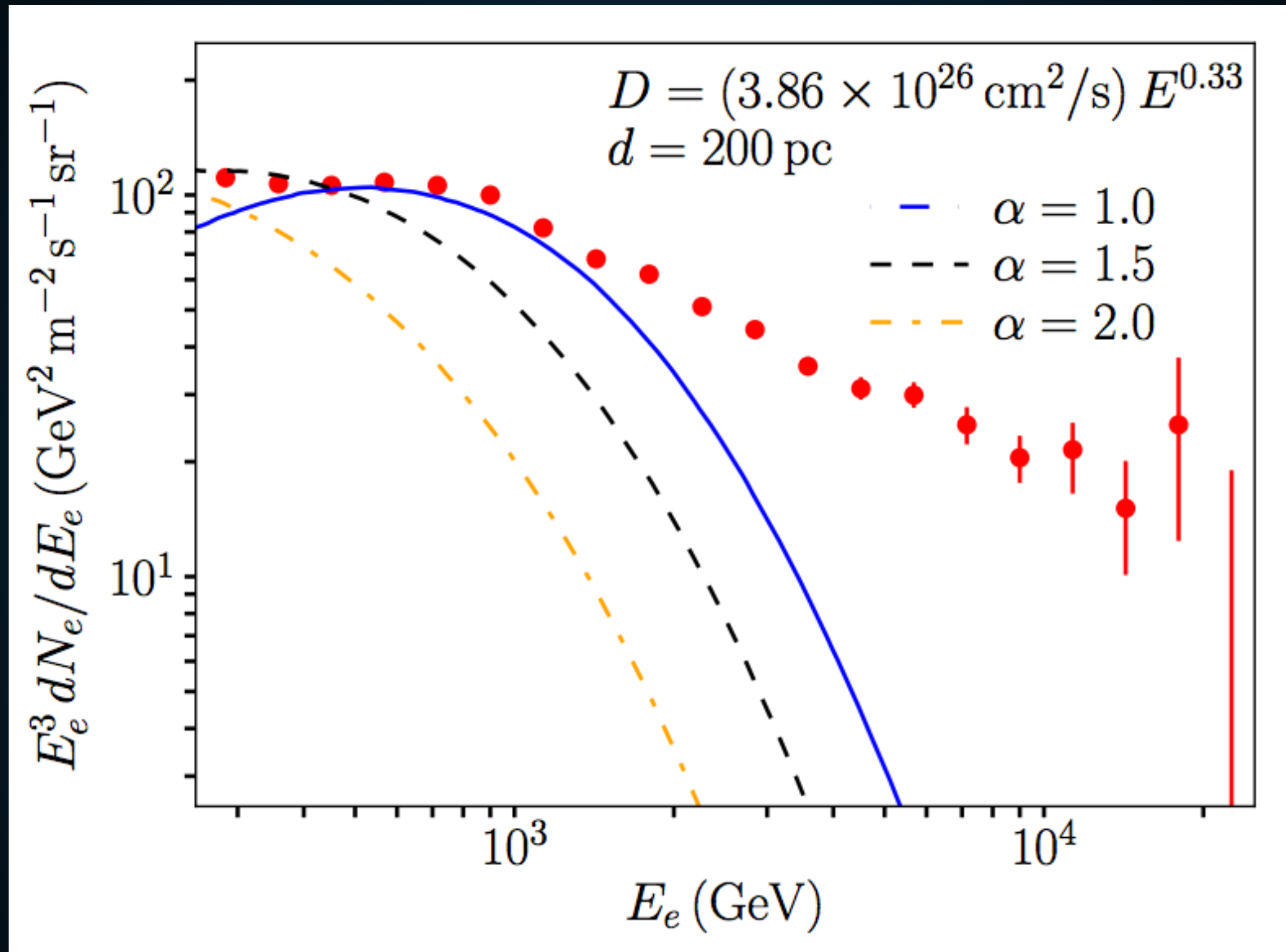
Hooper & Linden (1711.07482)



- Recently the HESS telescope detected 20 TeV electrons near Earth.

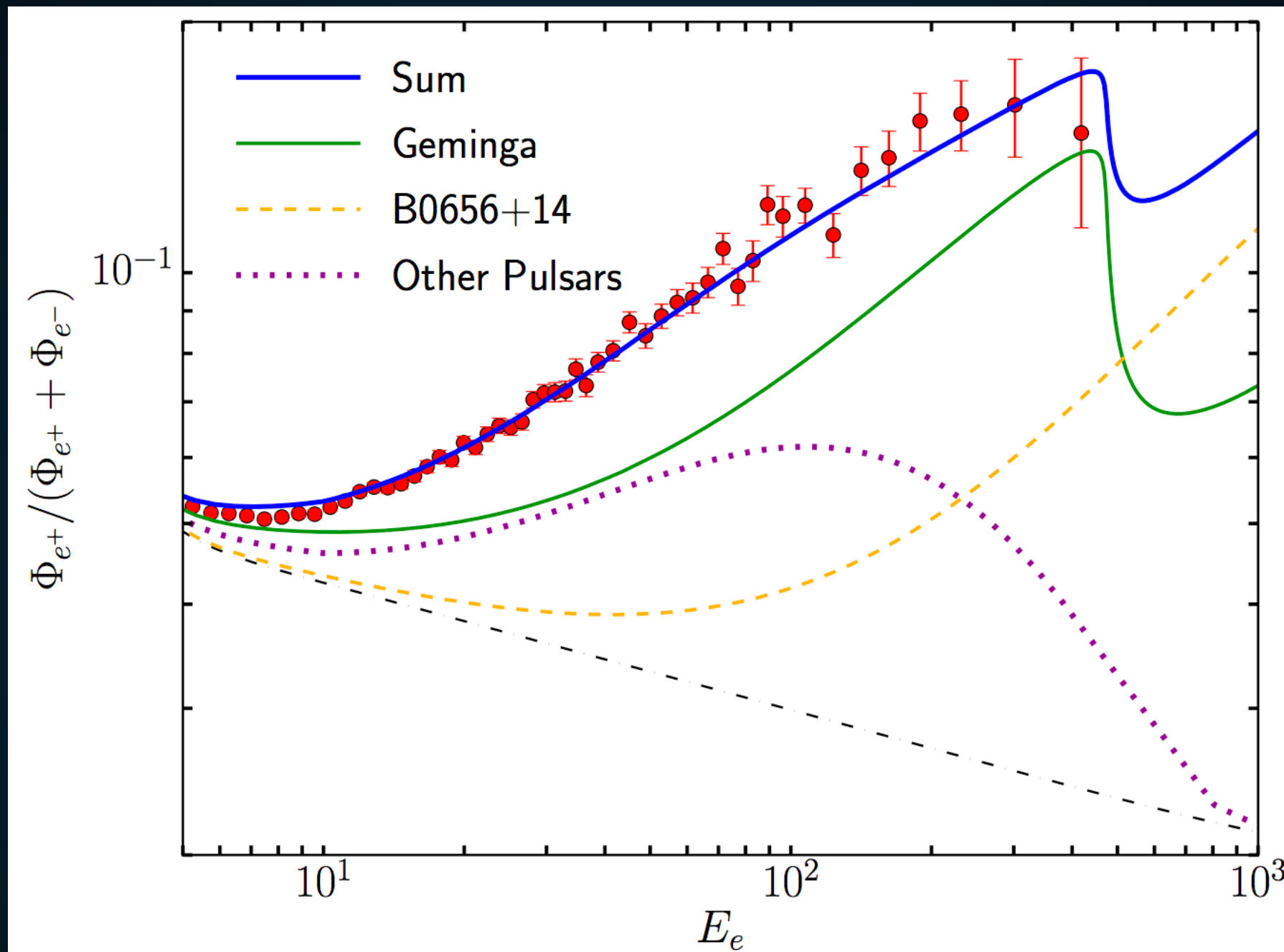
CAN THE LOCAL DIFFUSION CONSTANT BE LOW?

Hooper & Linden (1711.07482)



- If diffusion near Earth is low, then there is no source for these particles.

THE POSITRON FRACTION FROM TEV HALOS



- Reasonable models can be exactly fit to the excess.

*Braking index slightly changed to fit model to data.

ASSUMPTIONS

TeV Gamma-Ray Luminosity Roughly Proportional to Spindown Power

= Pulsars explain the Milagro TeV Excess

+ High Energy
electrons trapped in
TeV halos

= HAWC Sources
are TeV halos

+ Low energy
electrons escape
from TeV halos

= Pulsars explain
the positron excess

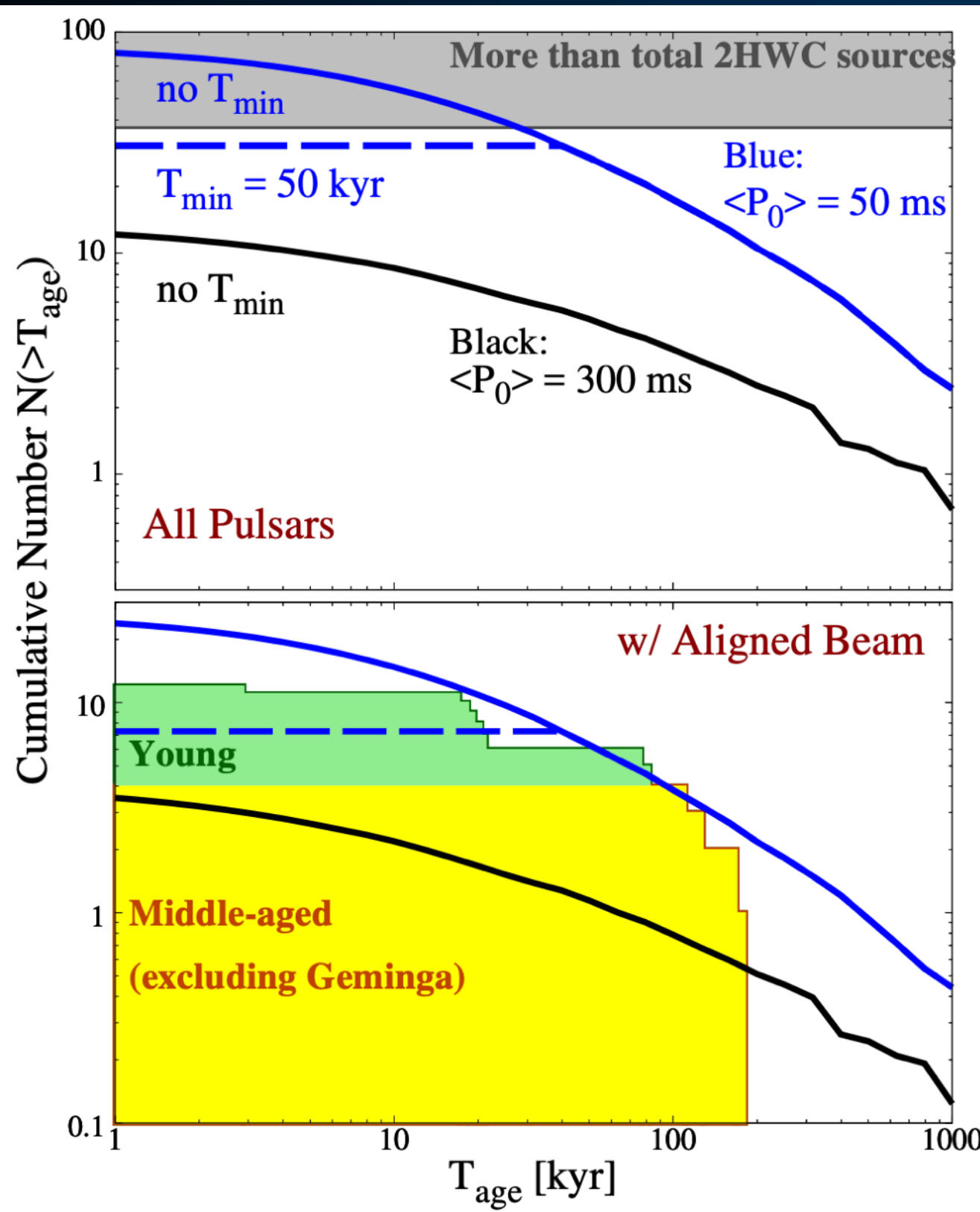
+ GC pulsars
consistent with
massive star formation

= TeV halos explain
the HESS pevatron

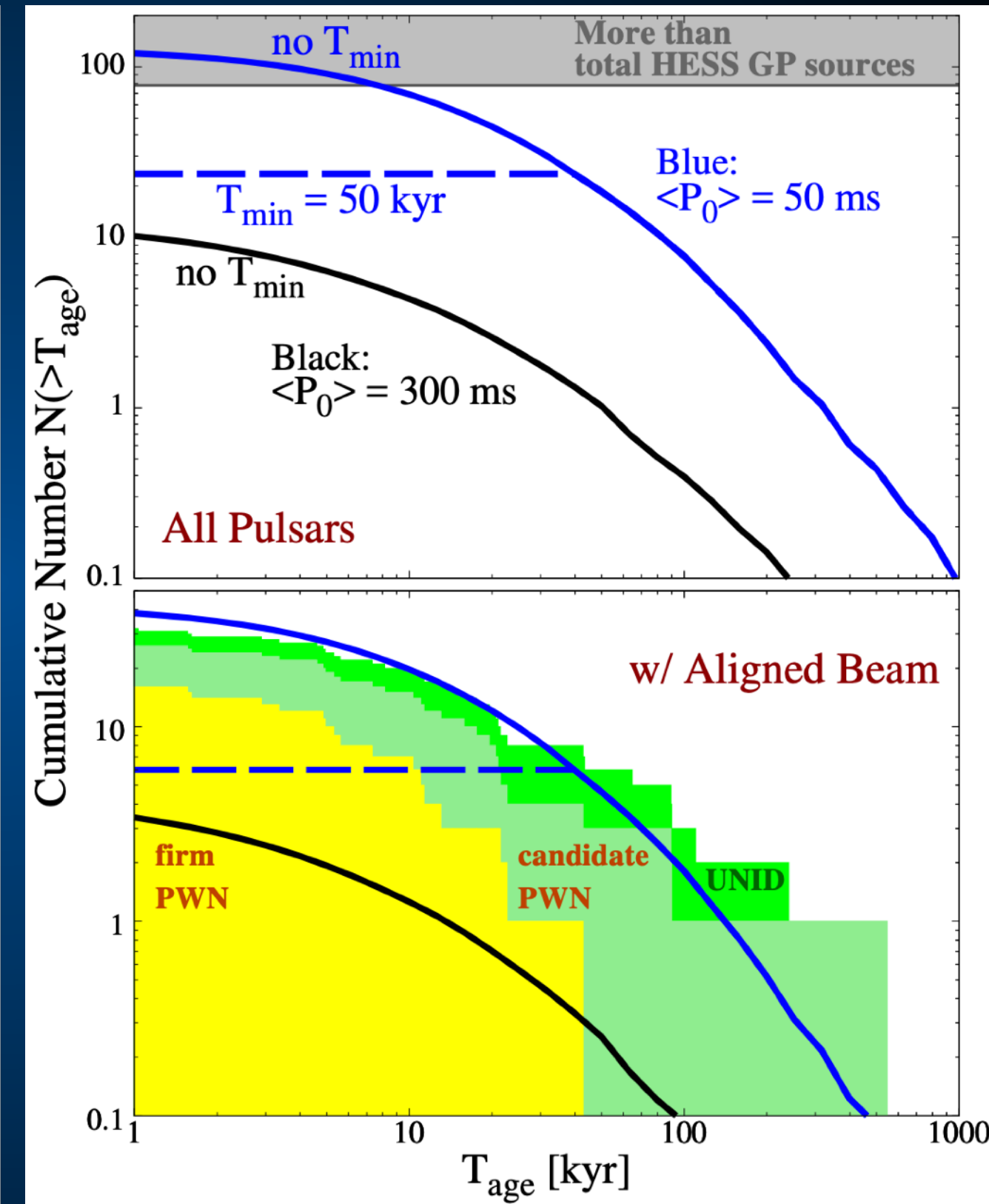


Understanding Pulsars

Sudoh, TL, Beacom (TBS)



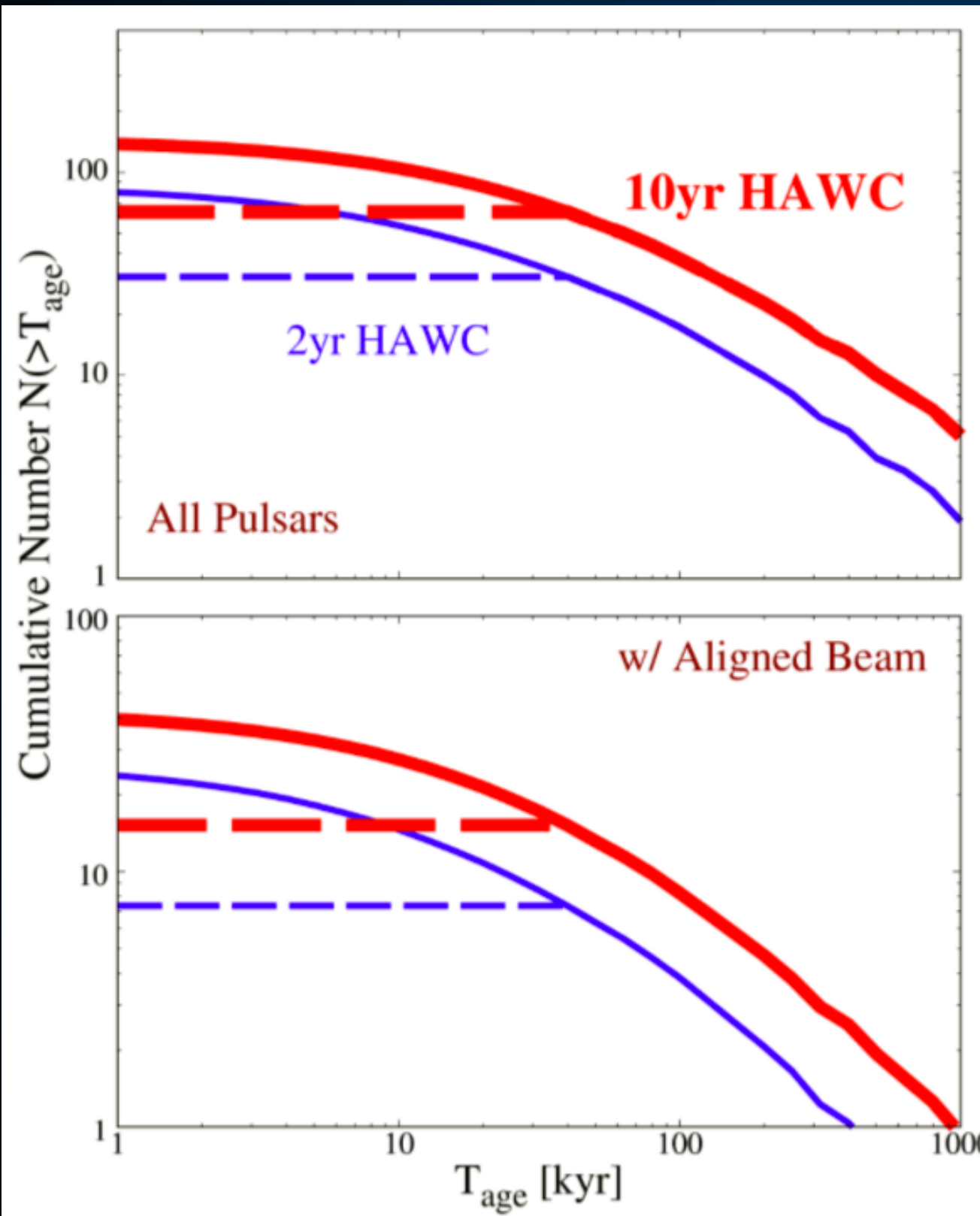
HAWC



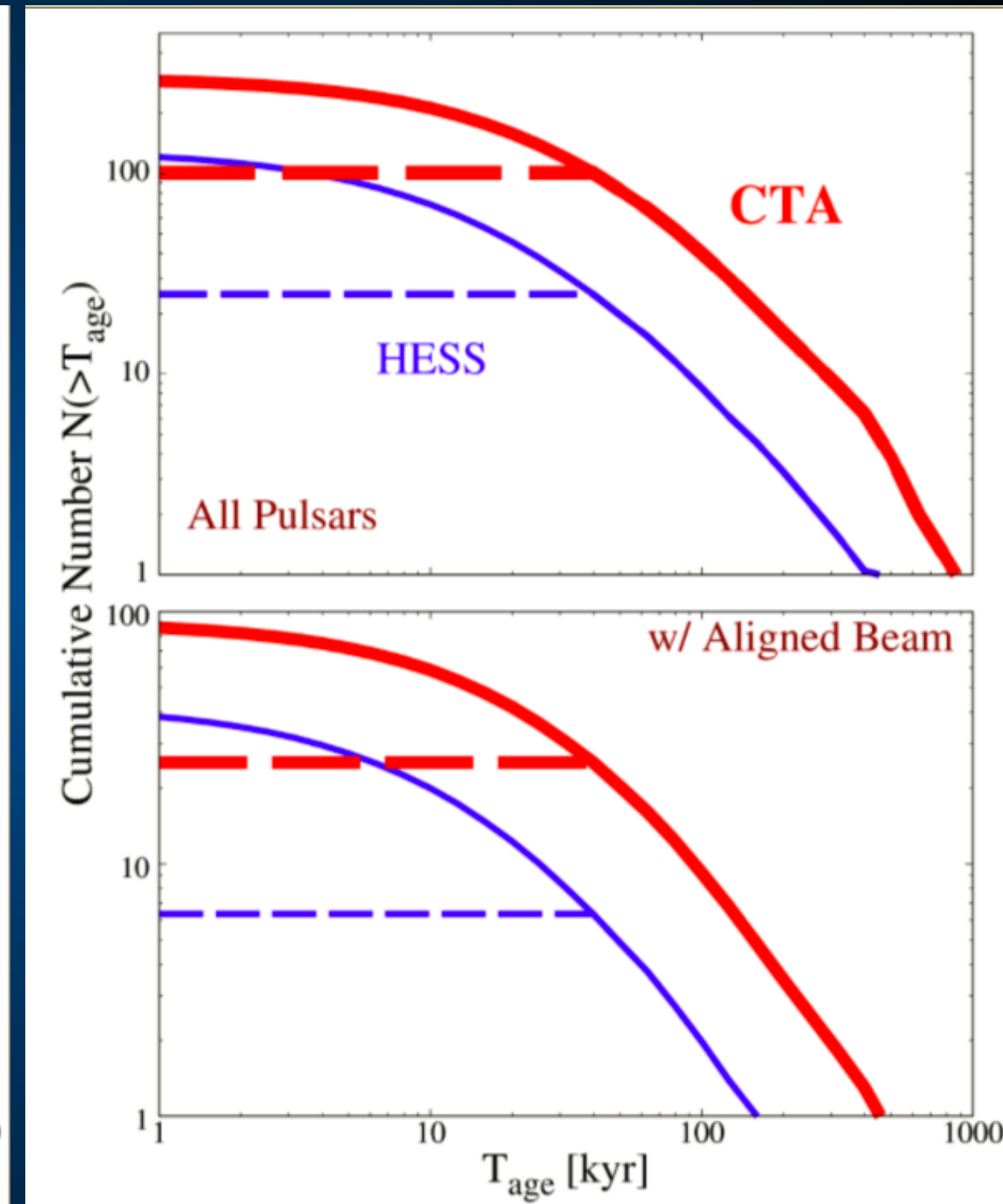
HESS

Detecting New Pulsars

Sudoh, TL, Beacom (TBS)



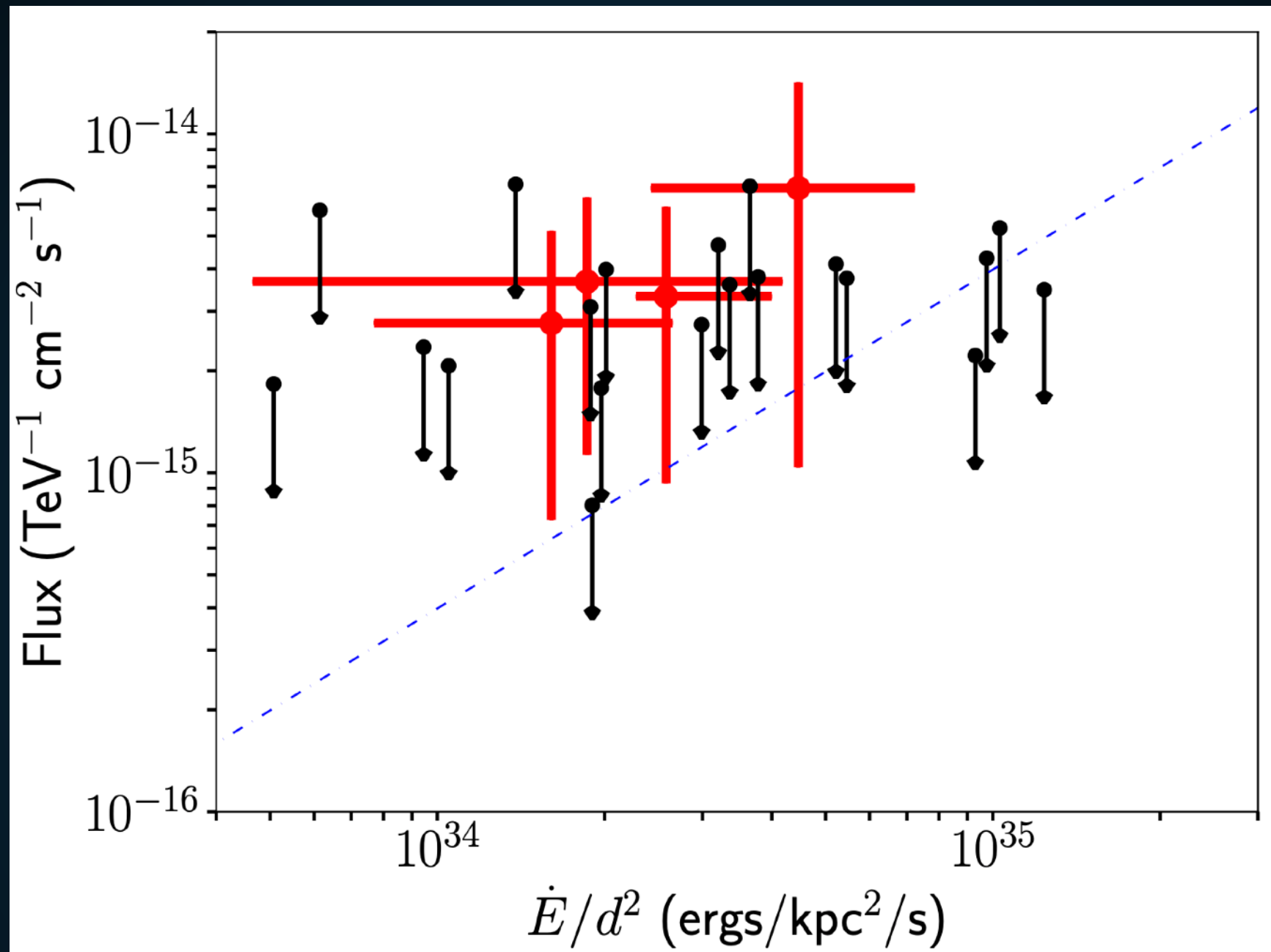
HAWC (10 yr)



HESS/CTA

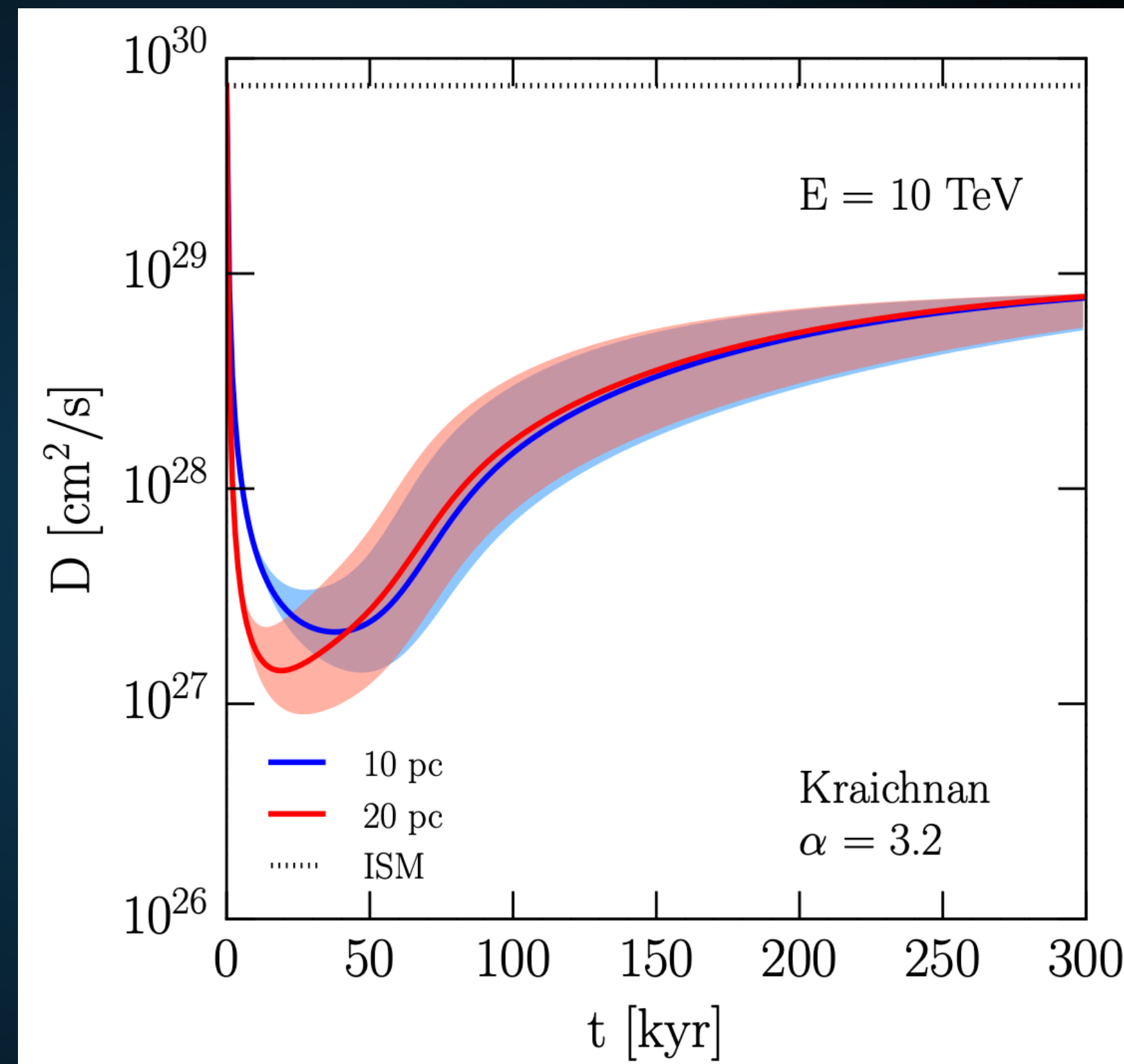
WHAT ABOUT MILLISECOND PULSARS?

Hooper & TL (2018; 1803.08046)



- Early evidence that millisecond pulsars also produce TeV halos.
- New opportunities to understand binary evolution.

- First models that explain low diffusion constant.
- New opportunities to understand galactic magnetic fields.



- Should observe coincident synchrotron Halo
- Possible Detection! (G327-1.1)

	Region	Area (arcsec ²)	Cts (1000)	N _H (10 ²² cm ⁻²)	Photon Index	Amplitude (10 ⁻⁴)	kT (keV)	τ (10 ¹² s cm ⁻³)	Norm. (10 ⁻³)	F ₁ (10 ⁻¹²)	F ₂	Red. χ^2
1	Compact Source	84.657	6.34	1.93 ^{+0.08} -0.08	1.61 ^{+0.08} -0.07	1.05 ^{+0.11} -0.10	0.45	...	0.80
2	Cometary PWN	971.22	7.75	1.93	1.62 ^{+0.08} -0.07	1.47 ^{+0.16} -0.14	1.09
3	Trail East	537.42	2.13	1.93	1.84 ^{+0.12} -0.12	0.44 ^{+0.07} -0.06	0.27
4	Trail West	766.56	3.12	1.93	1.80 ^{+0.11} -0.11	0.61 ^{+0.09} -0.08	0.39
5	Trail 1	424.45	1.98	1.93	1.76 ^{+0.12} -0.12	0.39 ^{+0.05} -0.05	0.26
6	Trail 2	588.19	2.13	1.93	1.95 ^{+0.11} -0.11	0.49 ^{+0.07} -0.06	0.28
7	Trail 3	994.92	2.99	1.93	2.09 ^{+0.10} -0.10	0.78 ^{+0.09} -0.08	0.42
8	Trail 4	839.48	2.38	1.93	2.28 ^{+0.12} -0.12	0.74 ^{+0.09} -0.09	0.37
9	Prong East	828.58	1.66	1.93	1.72 ^{+0.14} -0.14	0.30 ^{+0.06} -0.05	0.27
10	Prong West	971.22	2.06	1.93	1.85 ^{+0.14} -0.14	0.44 ^{+0.08} -0.07	1.09
11	Diffuse PWN*	20007	27.7	1.93	2.11 ^{+0.04} -0.05	6.91 ^{+0.37} -0.74	0.23 ^{+0.14} -0.05	0.21 ^{+0.88} -0.16	6.0 ⁺¹⁶ -4.0	3.68	17.7	0.82
12	Relic PWN*	26787	17.2	1.93	2.58 ^{+0.07} -0.10	6.51 ^{+0.53} -0.71	0.23	0.21	6.9 ⁺¹⁸ -5.5	3.14	20.3	...
13	Total	31476	1.00	1.93 ^{+0.23} -0.20	2.00 ^{+0.20} -0.52	1.00 ^{+0.52} -0.51	0.74

- New opportunities for studying TeV halo morphologies!

CONCLUSIONS (1/2)

- **TeV observations open up a new window into understanding Milky Way pulsars.**
- **Early indications:**
 - **TeV halos produce most of the TeV sources observed by ACTs and HAWC**
 - **TeV halos dominate the diffuse TeV emission in our galaxy.**
 - **Positron Excess is due to pulsar activity**

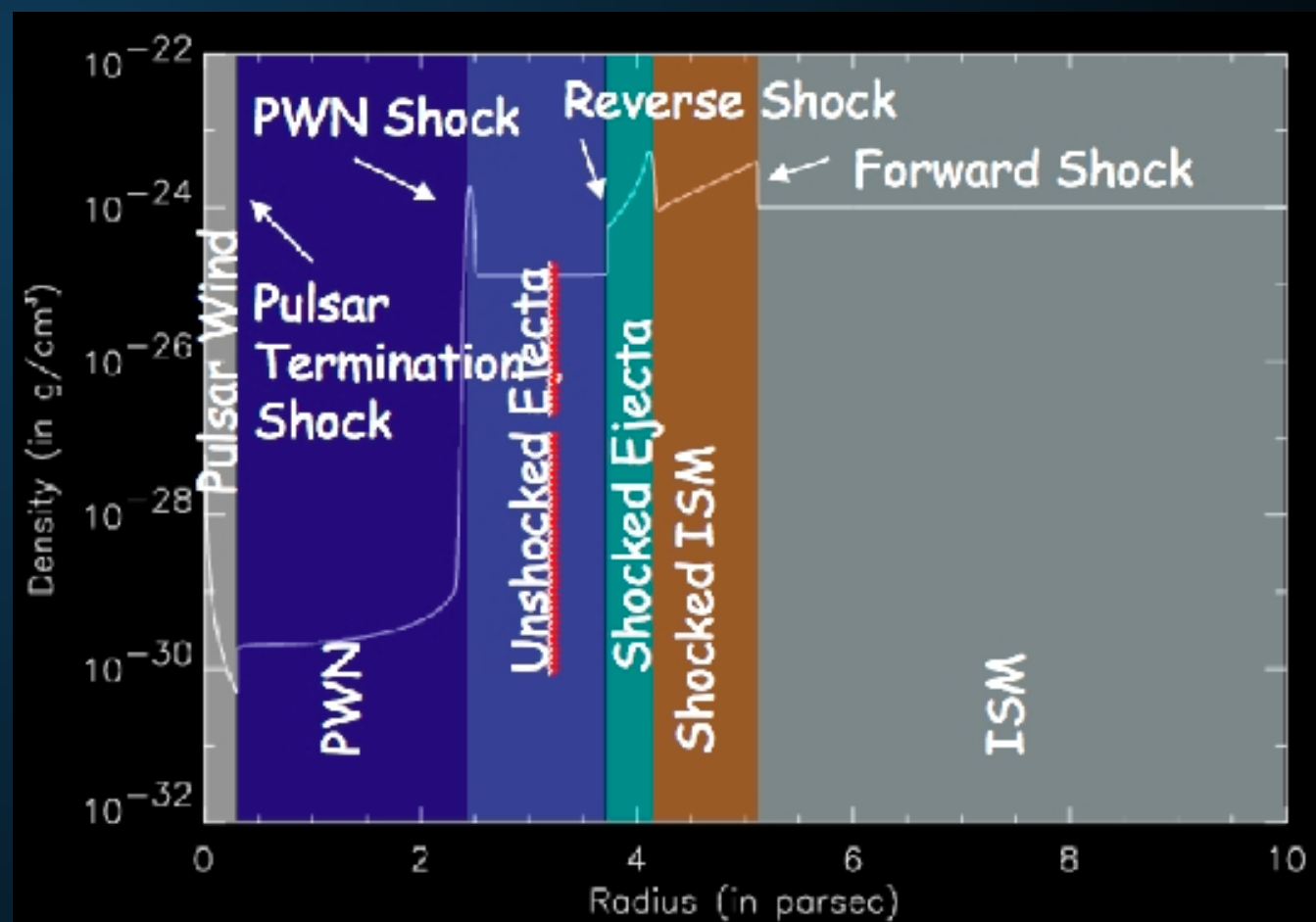
CONCLUSIONS (2/2)

- Additional implications:
 - Young pulsar braking index
 - MSPs?
 - Galactic cosmic-ray diffusion
 - Source of IceCube neutrinos
 - TeV Dark Matter Constraints

**What is a
TeV halo?**

WHAT ARE TEV HALOS

- TeV halos are a new feature
 - 3 orders of magnitude larger than PWN in volume
 - Opposite energy dependence
- PWN are morphologically connected to the physics of the termination shock
- TeV halos need a similar morphological description.



**Strong evidence that Milky Way
diffusion is extremely inhomogeneous!**

CONFIRMING TEV HALOS

- Several Methods to confirm TeV halo detections:
 - X-Ray PWN
 - X-Ray Halos
 - Thermal Pulsar Emission (see yesterday's talk)

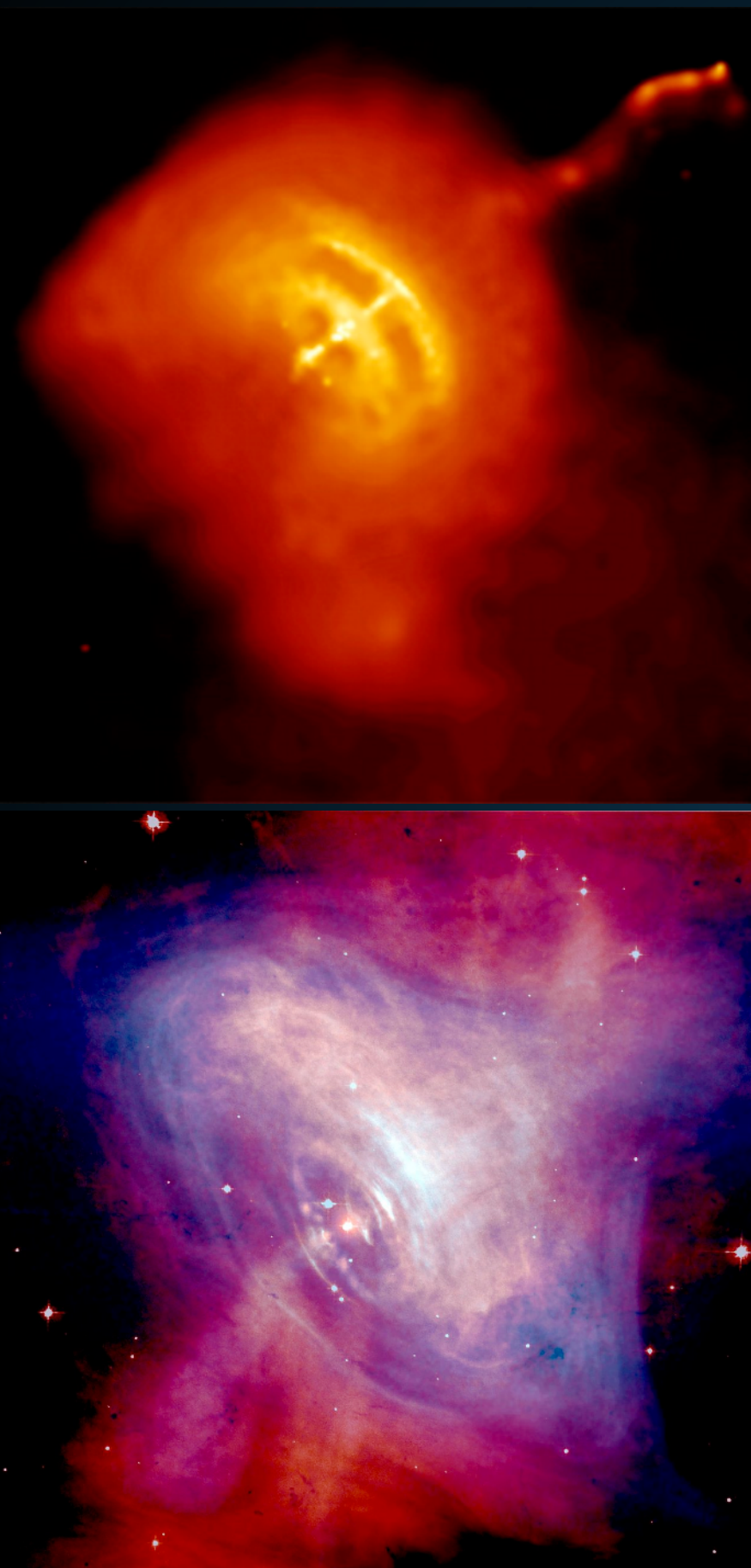
X-RAY HALOS

- An X-Ray halo with an identical morphology as the TeV halo must exist.

$$E_{\text{sync,critical}} = 22 \text{ eV} \left(\frac{B}{5 \mu G} \right) \left(\frac{E_e}{10 \text{ TeV}} \right)^2$$

- However, the signal has a low surface brightness and peaks at a low energy.

X-RAY PULSAR WIND NEBULAE

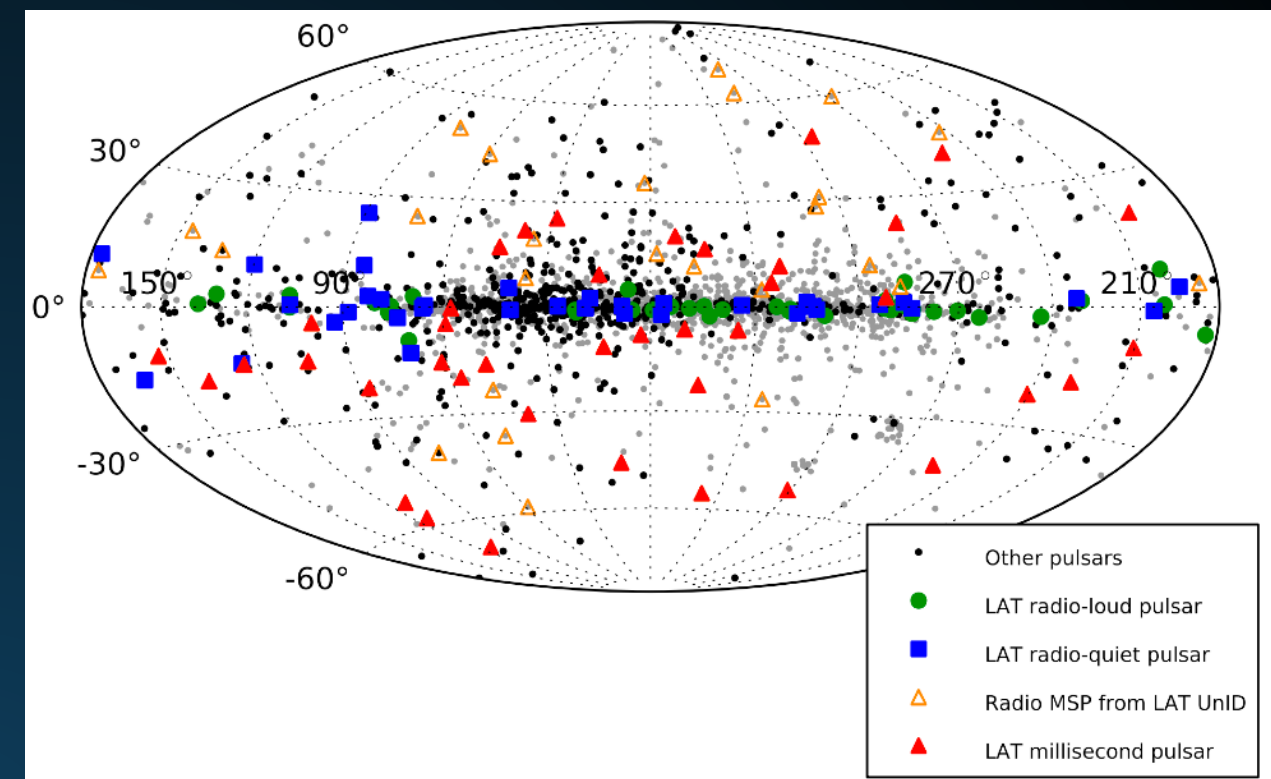


- Larger magnetic fields make compact PWN easier to observe
 - Synchrotron dominated
 - Higher energy peak
- More distant sources easier to see.
- Significant observation times require careful HAWC analysis.

Extra Slides

MISSING TEV HALOS

- Fermi-LAT has 5 middle-aged pulsars in the HAWC field.



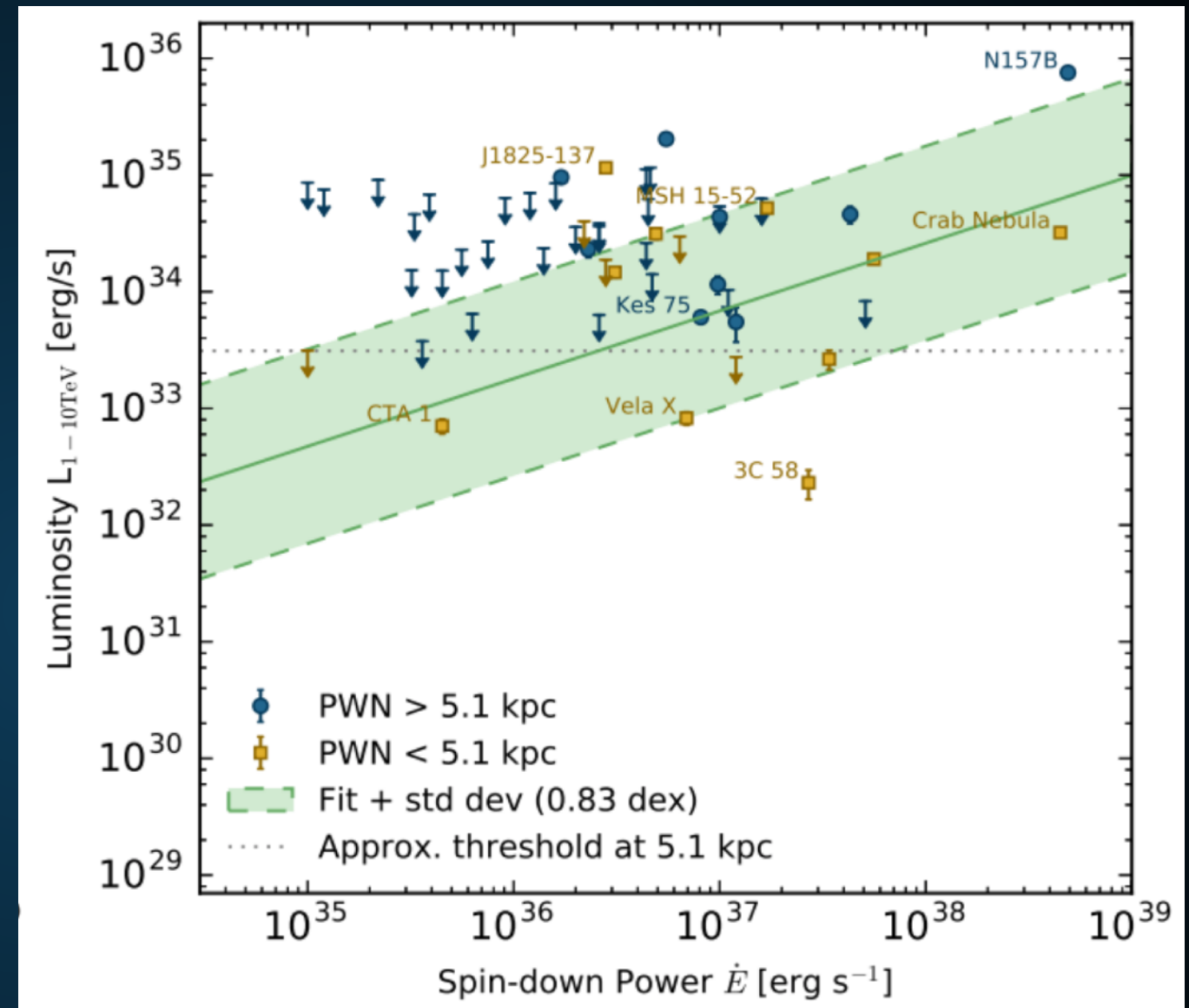
- X-Ray studies have only reported 6 X-Ray PWN without pulsars in the HAWC field of view.

PWNe With No Detected Pulsar						
Gname	other name(s)	R	X	Q	G	
G0.13-0.11					?	notes
G0.9+0.1					N	notes
G7.4-2.0	GeV J1809-2327, Tazzie				Y	notes
G16.7+0.1					N	notes
G18.5-0.4	GeV J1825-1310, Eel				Y	notes
G20.0-0.2					N	notes
G24.7+0.6					N	notes
G27.8+0.6					N	notes
G39.2-0.3	3C 396				Y	notes
G63.7+1.1					N	notes
G74.9+1.2	CTB 87				Y	notes
G119.5+10.2	CTA 1				Y	notes
G189.1+3.0	IC 443				?	notes
G279.8-35.8	B0453-685				N	notes
G291.0-0.1	MSH 11-62				Y	notes
G293.8+0.6					N	notes
G313.3+0.1	Rabbit				Y	notes
G318.9+0.4					N	notes
G322.5-0.1					N	notes
G326.3-1.8	MSH 15-56				N	notes
G327.1-1.1					N	notes
G328.4+0.2	MSH 15-57				N	notes
G358.6-17.2	RX J1856.5-3754	N	N		N	notes
G359.89-0.08					Y	notes

**What if the “Geminga”-like
model is wrong?**

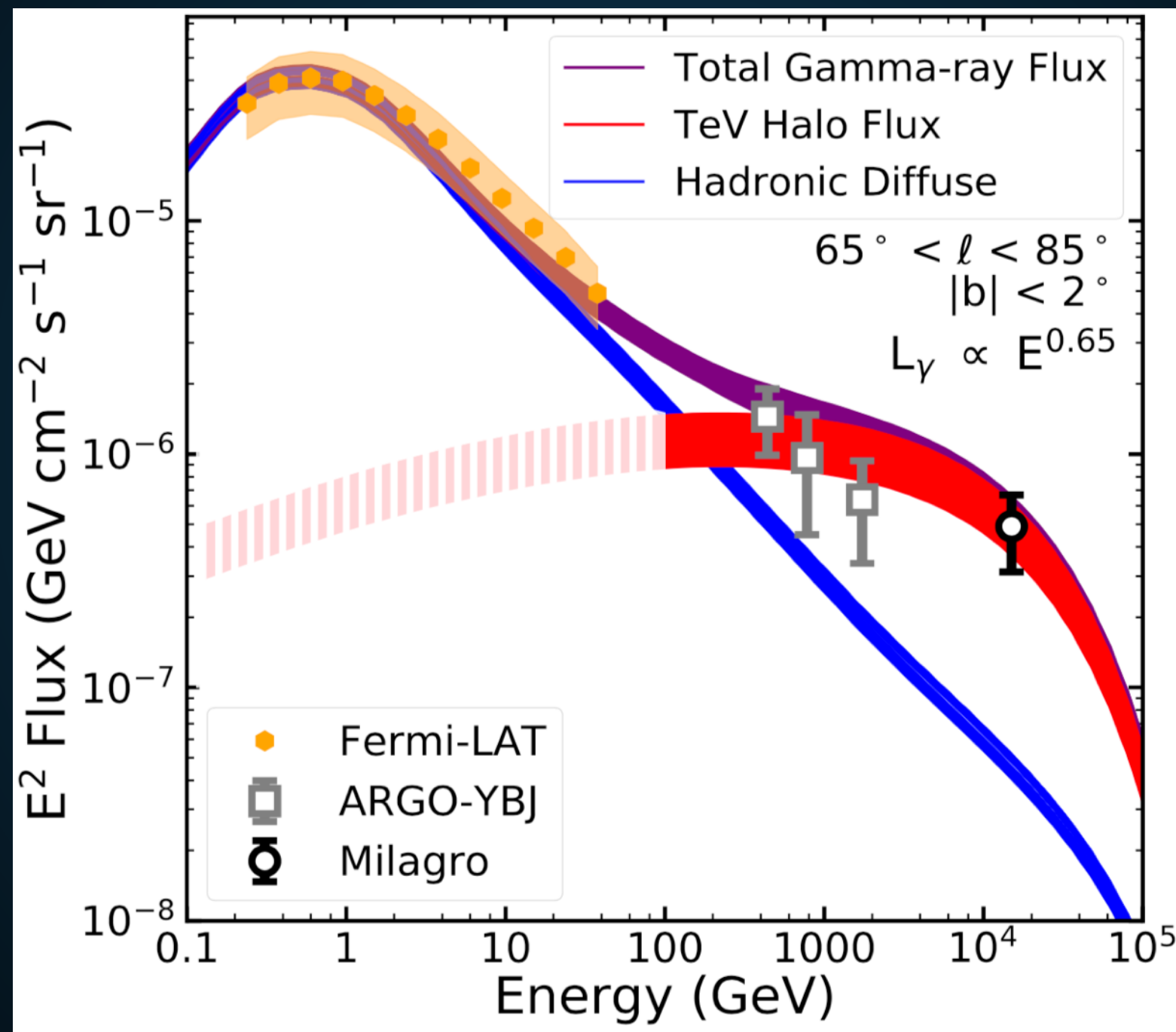
- ▶ Alternatively can utilize HESS results which find:

$$L = E_{\text{dot}}^{0.59}$$



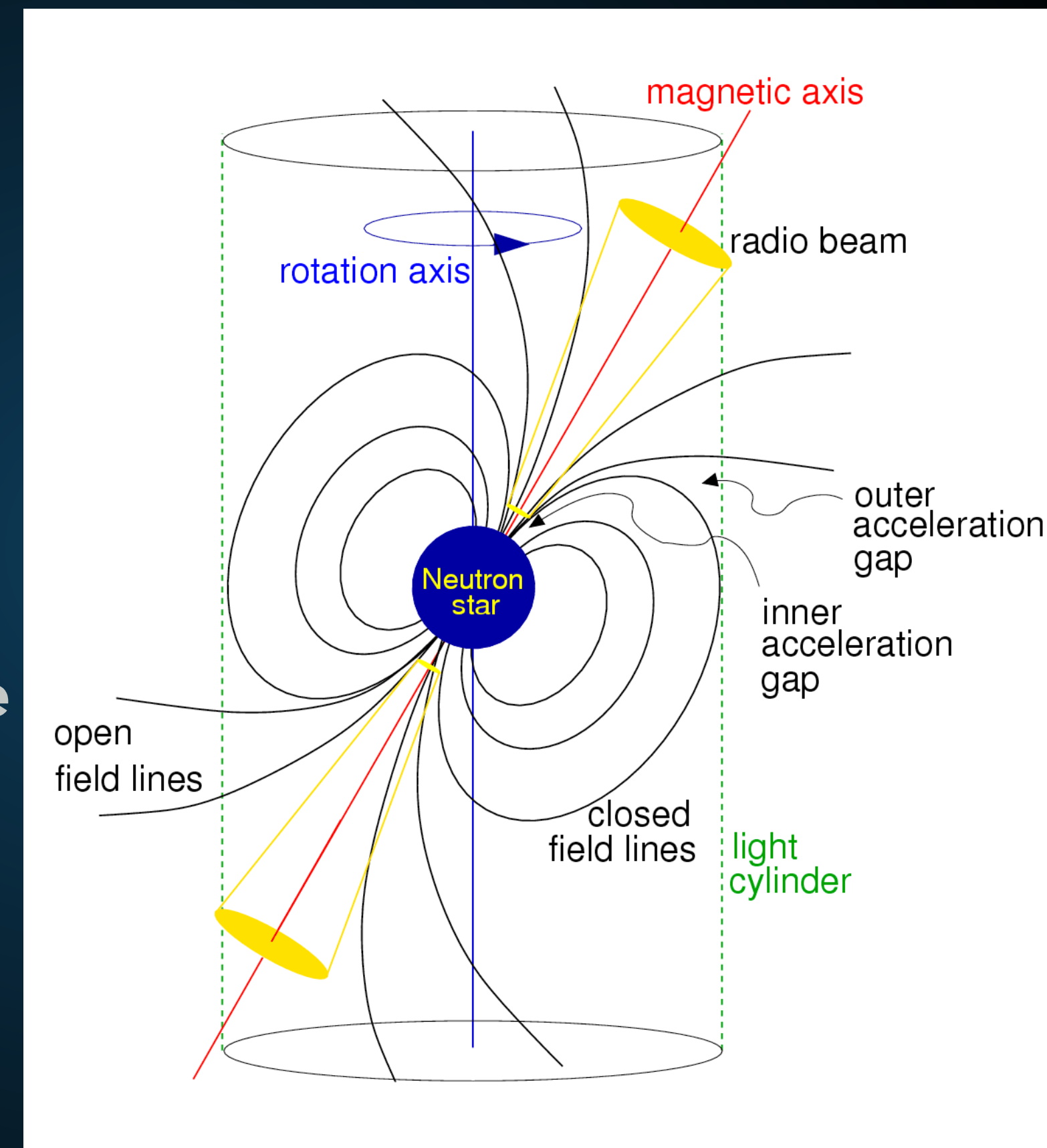
$$\phi_{\text{TeV halo}} = \left(\frac{\dot{E}_{\text{psr}}}{\dot{E}_{\text{Geminga}}} \right) \left(\frac{d_{\text{Geminga}}^2}{d_{\text{psr}}^2} \right) \phi_{\text{Geminga}}$$

► TeV halos naturally explain the TeV excess!

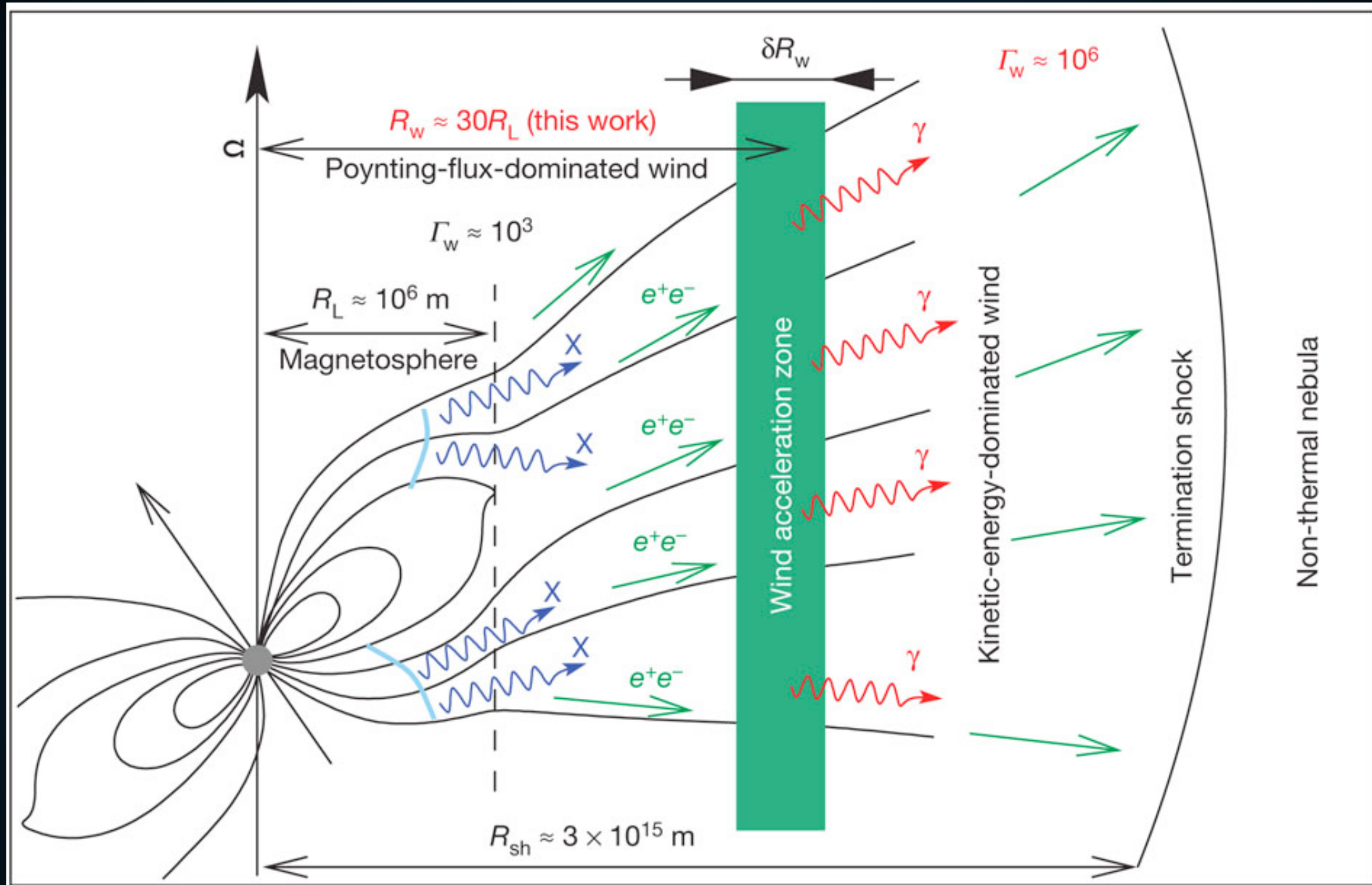


PULSARS AS ASTROPHYSICAL ACCELERATORS

- ▶ **radio beam**
- ▶ **gamma-ray beam**
- ▶ **e⁺e⁻ acceleration in pulsar magnetosphere**
- ▶ **e⁺e⁻ acceleration at termination shock**



PRODUCTION OF ELECTRON AND POSITRON PAIRS



- ▶ Final e⁺e⁻ spectrum is model dependent.
- ▶ Understanding this is important for MSPs.

ENERGY LOSSES ARE DOMINATED BY THE ISM

- It is not energetically possible for Geminga to produce the magnetic field or ISRF that these electrons interact with.

$$U = \frac{1}{8\pi} \beta^2 = \frac{(10 \mu G)^2}{8\pi}$$
$$= 4 \times 10^{-12} \frac{\text{erg}}{\text{cm}^3}$$
$$\int_0^{10 \rho c} U dV = 5 \times 10^{47} \text{ erg}$$
$$\hookrightarrow \text{Magnetic Flux} \approx 5 \times 10^{38} \frac{\text{ergs}}{\text{s}}$$

$$\text{ISRF} = 1 \frac{\text{eV}}{\text{cm}^3}$$
$$\int \text{ISRF} dV = 8 \times 10^{47} \text{ erg}$$
$$\hookrightarrow \text{Flux} = 8 \times 10^{38} \frac{\text{ergs}}{\text{s}}$$

- We can use typical ISM values ($5 \mu G$; 1 eV cm^{-3}) to characterize interactions.
- Nearly equal energy to synchrotron and ICS.

X-RAY PWN DETECTIONS

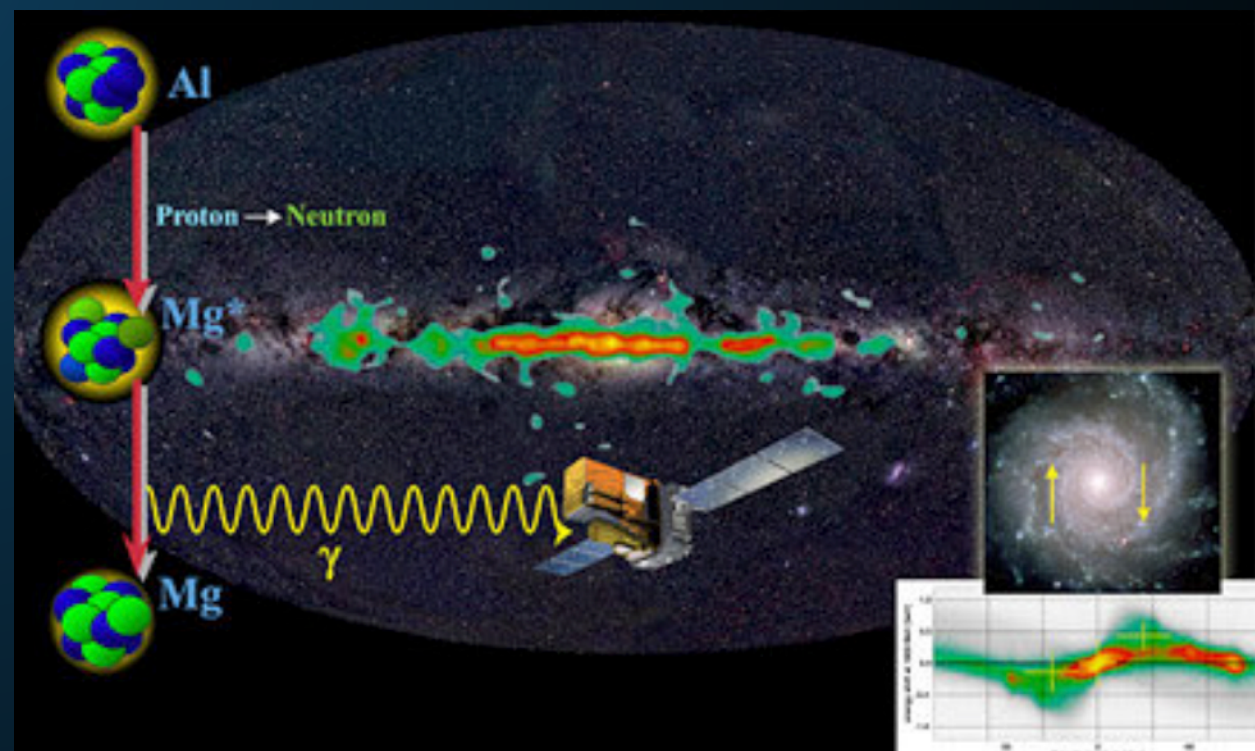
PWNe With No Detected Pulsar						
Gname	other name(s)	R	X	Q	G	
G0.13-0.11					?	notes
G0.9+0.1					N	notes
G7.4-2.0	GeV J1809-2327, Tazzie				Y	notes
G16.7+0.1					N	notes
G18.5-0.4	GeV J1825-1310, Eel				Y	notes
G20.0-0.2					N	notes
G24.7+0.6					N	notes
G27.8+0.6					N	notes
G39.2-0.3	3C 396				Y	notes
G63.7+1.1					N	notes
G74.9+1.2	CTB 87				Y	notes
G119.5+10.2	CTA 1				Y	notes
G189.1+3.0	IC 443				?	notes
G279.8-35.8	B0453-685				N	notes
G291.0-0.1	MSH 11-62				Y	notes
G293.8+0.6					N	notes
G313.3+0.1	Rabbit				Y	notes
G318.9+0.4					N	notes
G322.5-0.1					N	notes
G326.3-1.8	MSH 15-56				N	notes
G327.1-1.1					N	notes
G328.4+0.2	MSH 15-57				N	notes
G358.6-17.2	RX J1856.5-3754	N	N		N	notes
G359.89-0.08					Y	notes

- ▶ X-Ray PWN have detected only ~6 of these 37 systems.

GEMINGA ISN'T SPECIAL

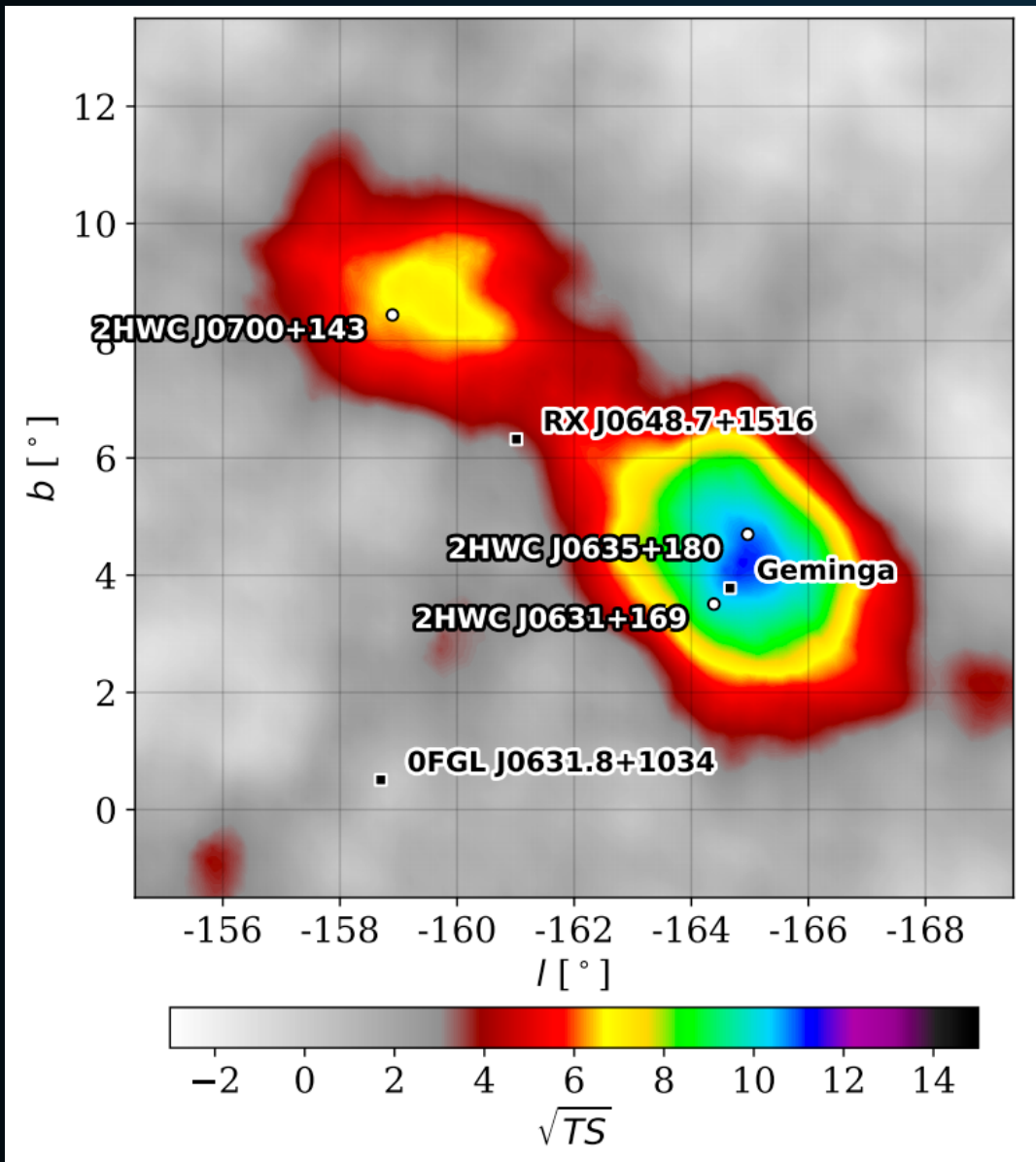
$$f \sim \frac{N_{\text{region}} \times \frac{4\pi}{3} r_{\text{region}}^3}{\pi R_{\text{MW}}^2 \times 2z_{\text{MW}}}$$
$$\sim 0.25 \times \left(\frac{r_{\text{region}}}{100 \text{ pc}} \right)^3 \left(\frac{\dot{N}_{\text{SN}}}{0.03 \text{ yr}^{-1}} \right) \left(\frac{\tau_{\text{region}}}{10^6 \text{ yr}} \right) \left(\frac{20 \text{ kpc}}{R_{\text{MW}}} \right)^2 \left(\frac{200 \text{ pc}}{z_{\text{MW}}} \right)$$

- **Galactic Supernova rate $\sim 0.02 \text{ yr}^{-1}$**
- **If each supernova (and natal pulsar) produces a large diffusion region, the diffusion constant should be low everywhere.**
- **Only alternative is that a very unique event produced the local bubble.**



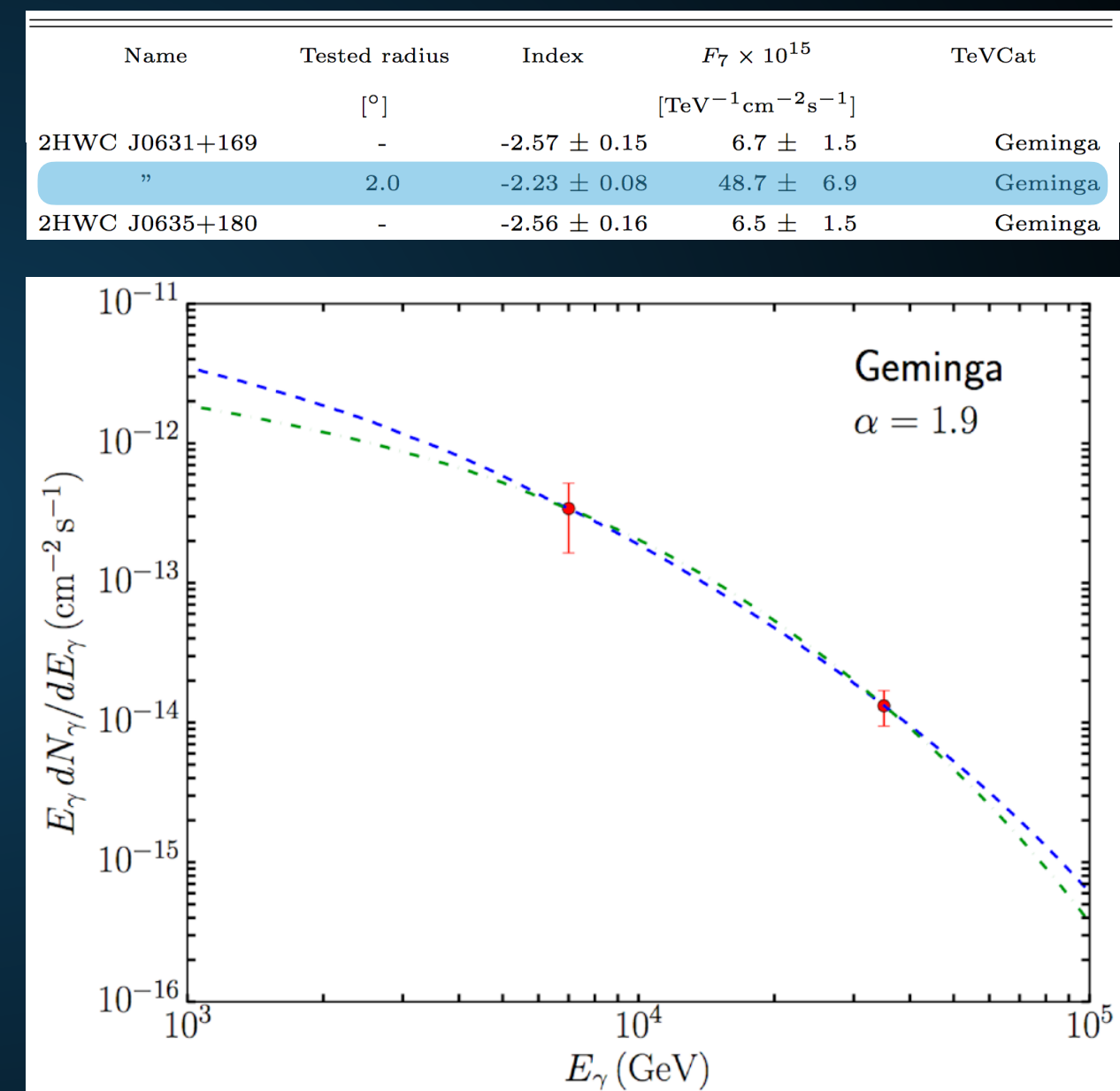
TWO CONTRASTING OBSERVABLES

Geminga is Bright



Indicative of significant
electron cooling

Geminga has a hard-spectrum



Indicative of minimal
electron cooling

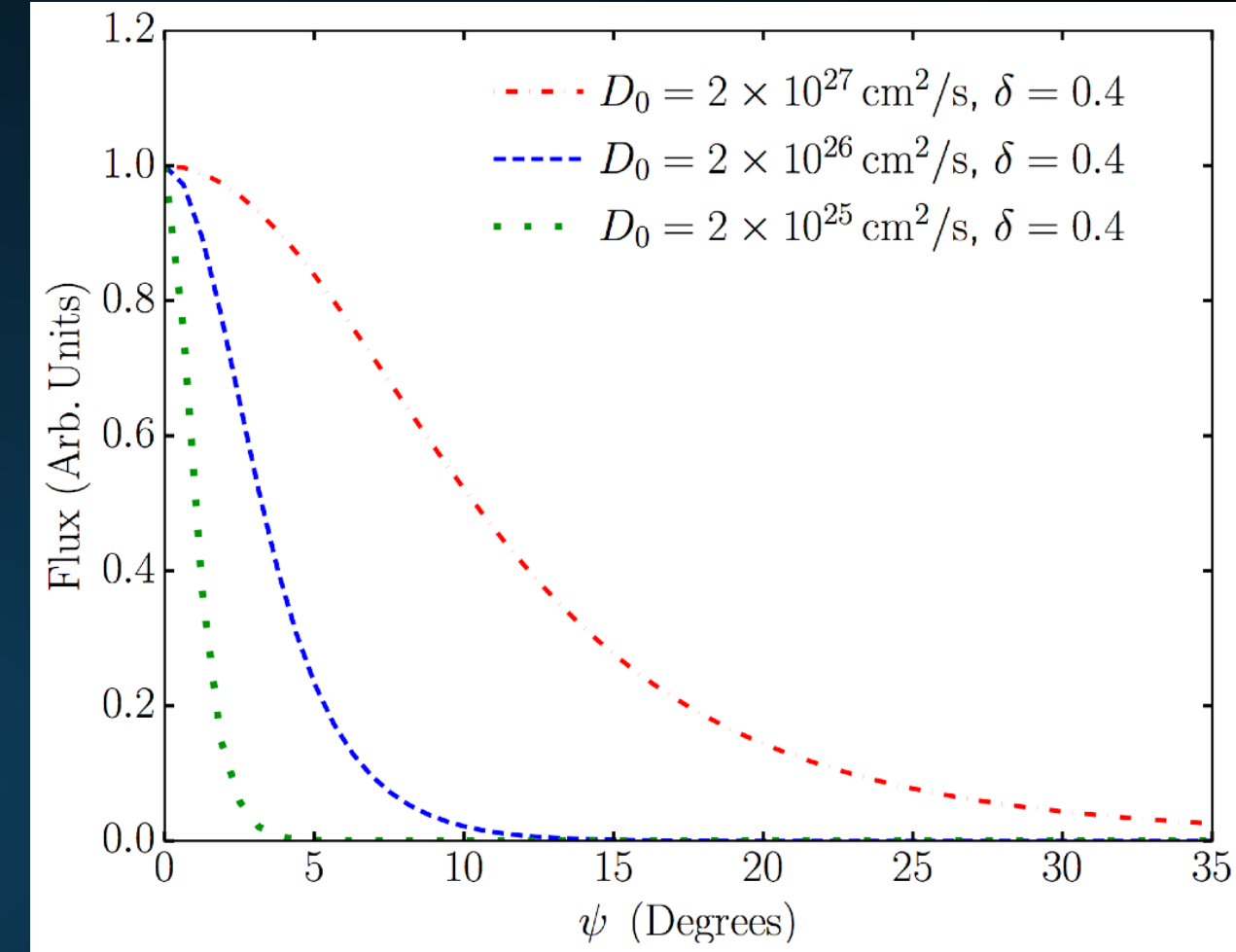
TOTAL POWER OF TEV HALOS

- ▶ Measured Geminga flux translates to an intensity:
 $2.86 \times 10^{31} \text{ erg s}^{-1}$ at 7 TeV
- ▶ For the best-fit spectrum, this requires an e^+e^- injection:
 $3.8 \times 10^{33} \text{ erg s}^{-1}$
- ▶ Total Spindown Power of Geminga is:
 $3.4 \times 10^{34} \text{ erg s}^{-1}$
- ▶ Roughly 10% conversion efficiency to e^+e^- !

COSMIC-RAY DIFFUSION IN A TEV HALO

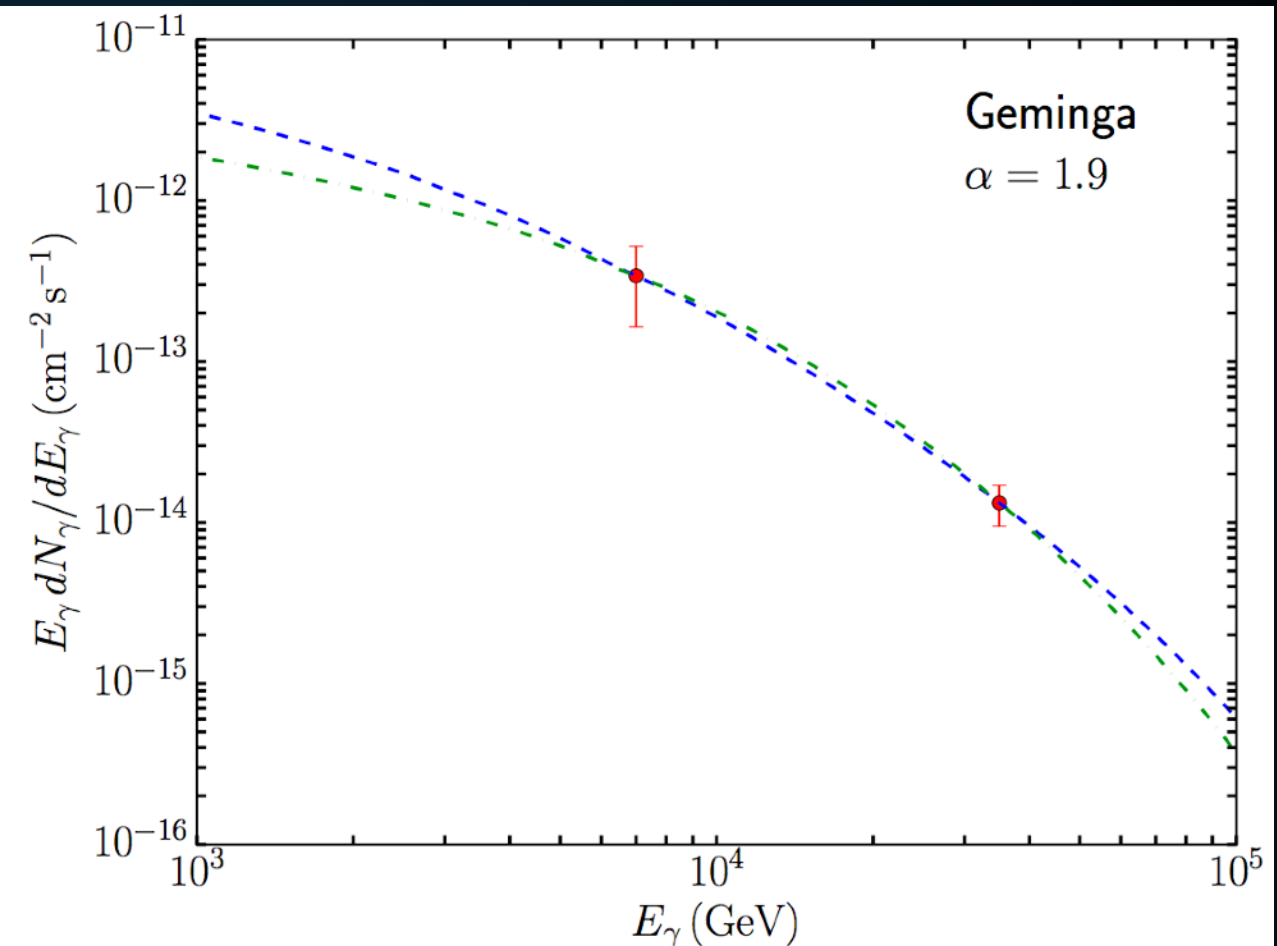
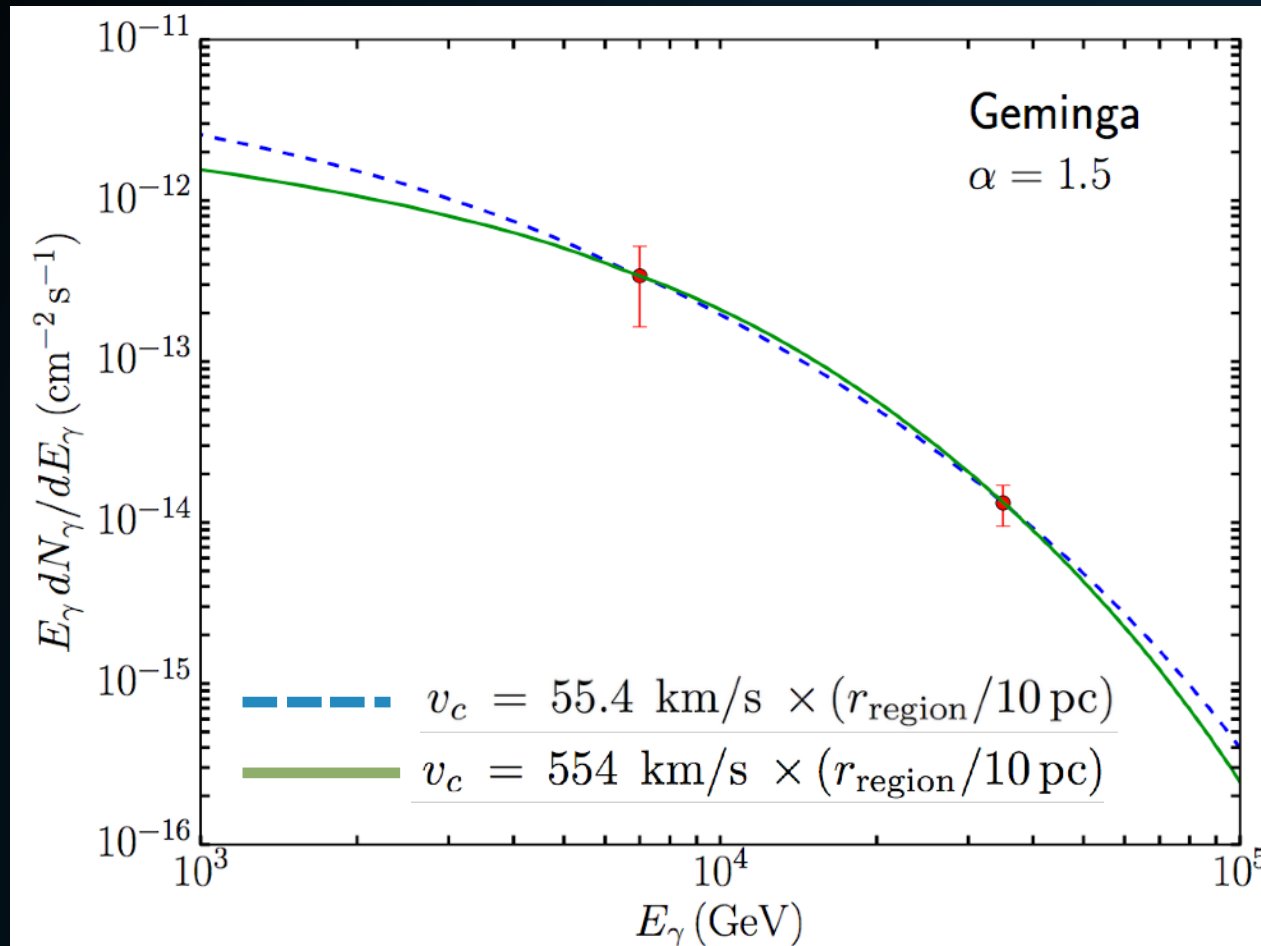
- ▶ Actual source of particle propagation is unknown:

- ▶ Diffusion
- ▶ Advection



- ▶ Particle propagation near pulsars must be orders of magnitude less efficient than typical for the ISM.
- ▶ Continues far outside the termination shock of a pulsar with no SNR.

GEMINGA SPECTRUM INDICATIVE OF CONVECTION

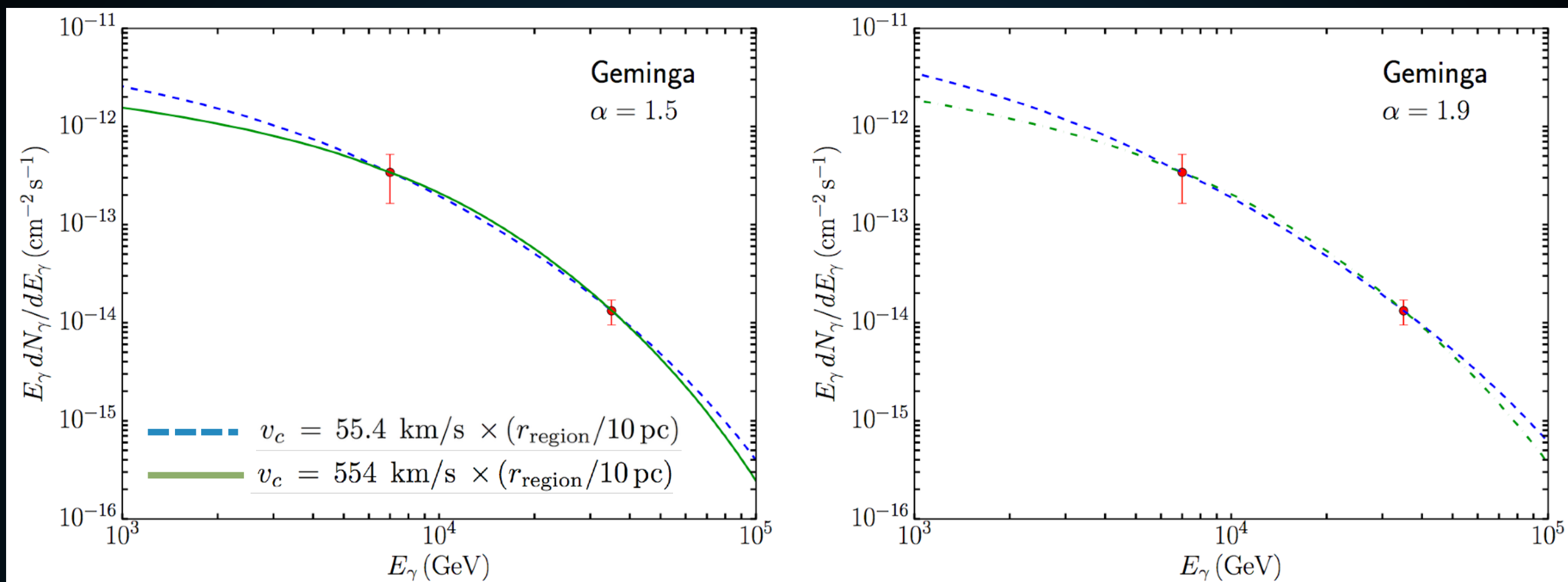


- ▶ However, Bohmian diffusion is incompatible with the gamma-ray spectrum.
- ▶ If low-energy electrons are cooled, the spectrum at 7 TeV should be significantly softer.

AN UPPER LIMIT ON THE TEV HALO SIZE

- ▶ These arguments only set a lower limit on the TeV halo size.
- ▶ What if TeV halos are much larger, but the TeV electrons die at ~ 10 pc?
- ▶ Will need to answer this question on the population level.

GEMINGA SPECTRUM INDICATIVE OF CONVECTION



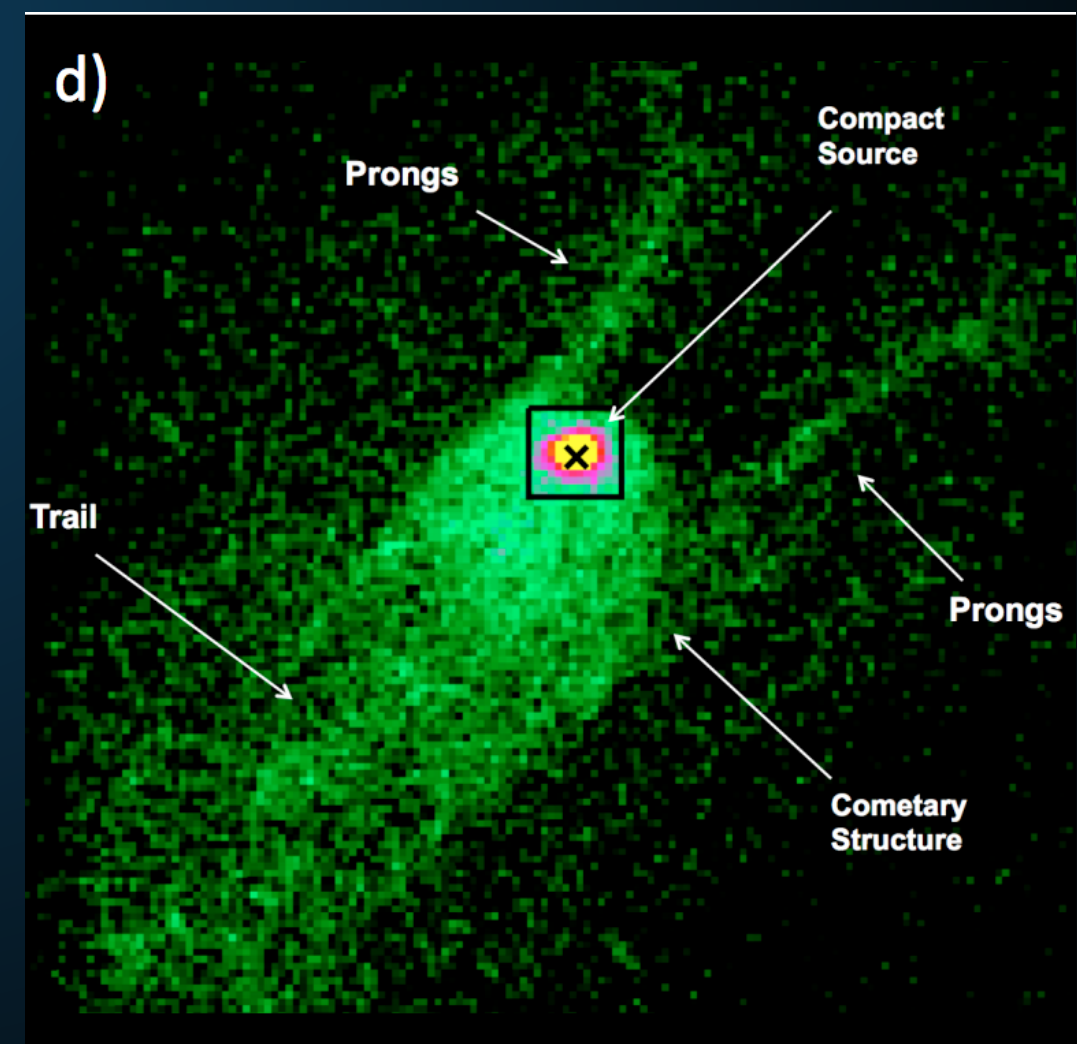
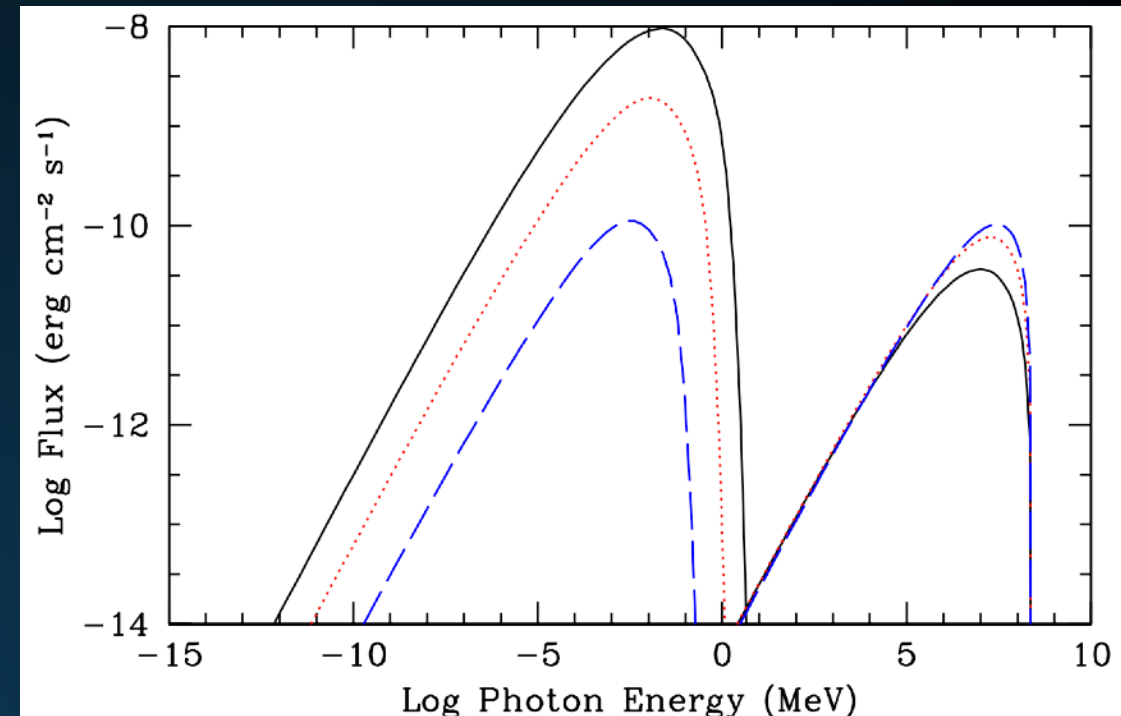
- ▶ **Geminga spectrum is fit better with convective models.**
- ▶ **Energy-independent diffusion provides identical results**
- ▶ **Best-fit spectral-index (-2.23 +/- 0.08) prefers high convection**

- ▶ Cooling dominated by $20 \mu\text{G}$ magnetic field.

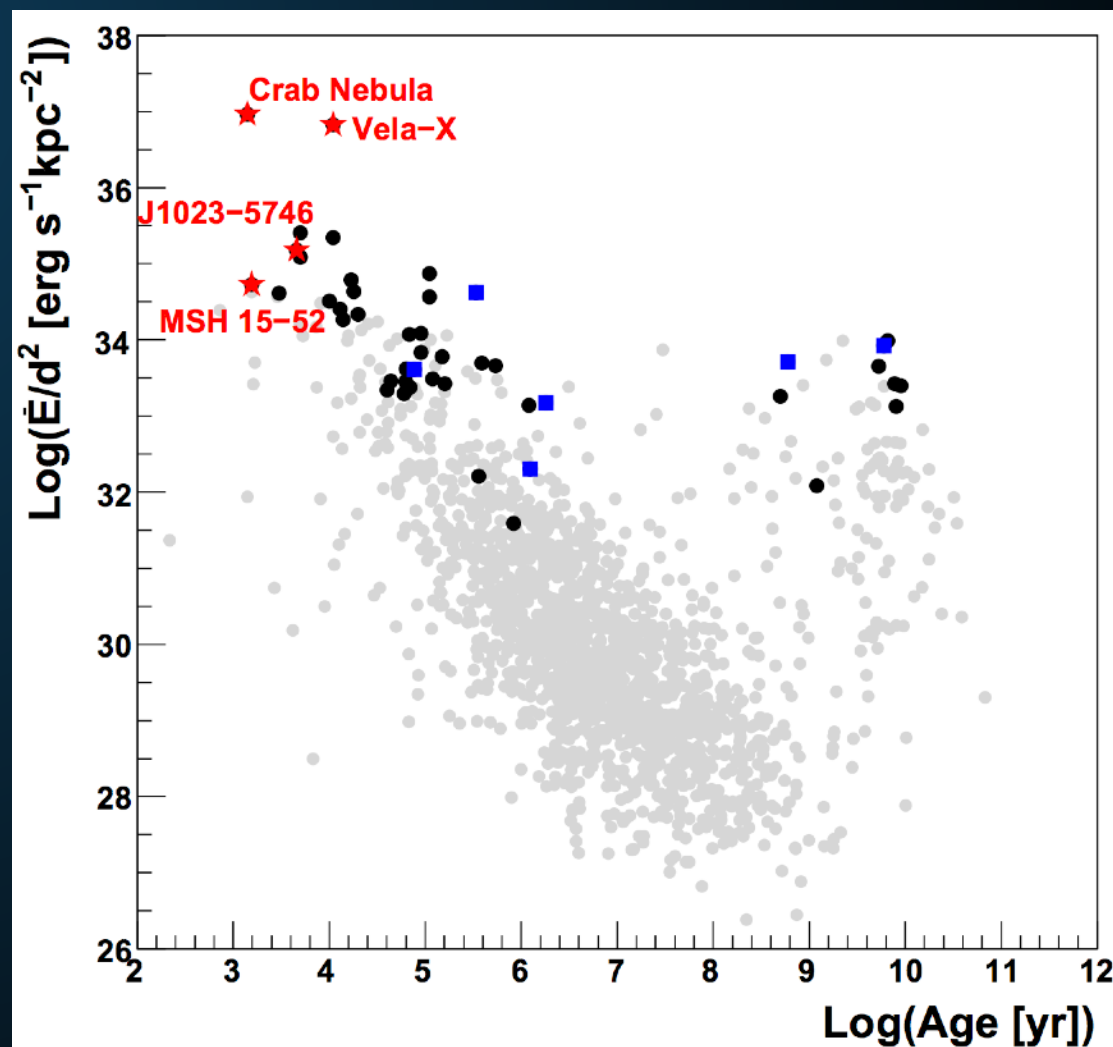
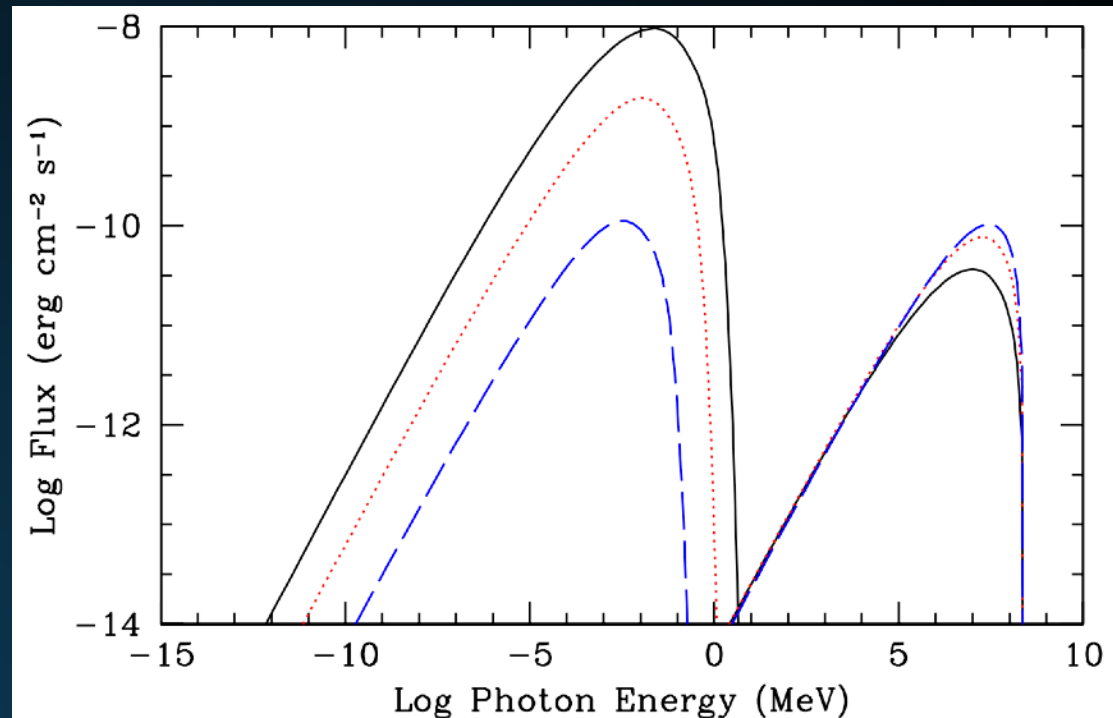
- ▶ Energy loss time: ~ 40 years

- ▶ Distance Traveled: ~ 6 pc for standard diffusion constant. Real diffusion must be slower.

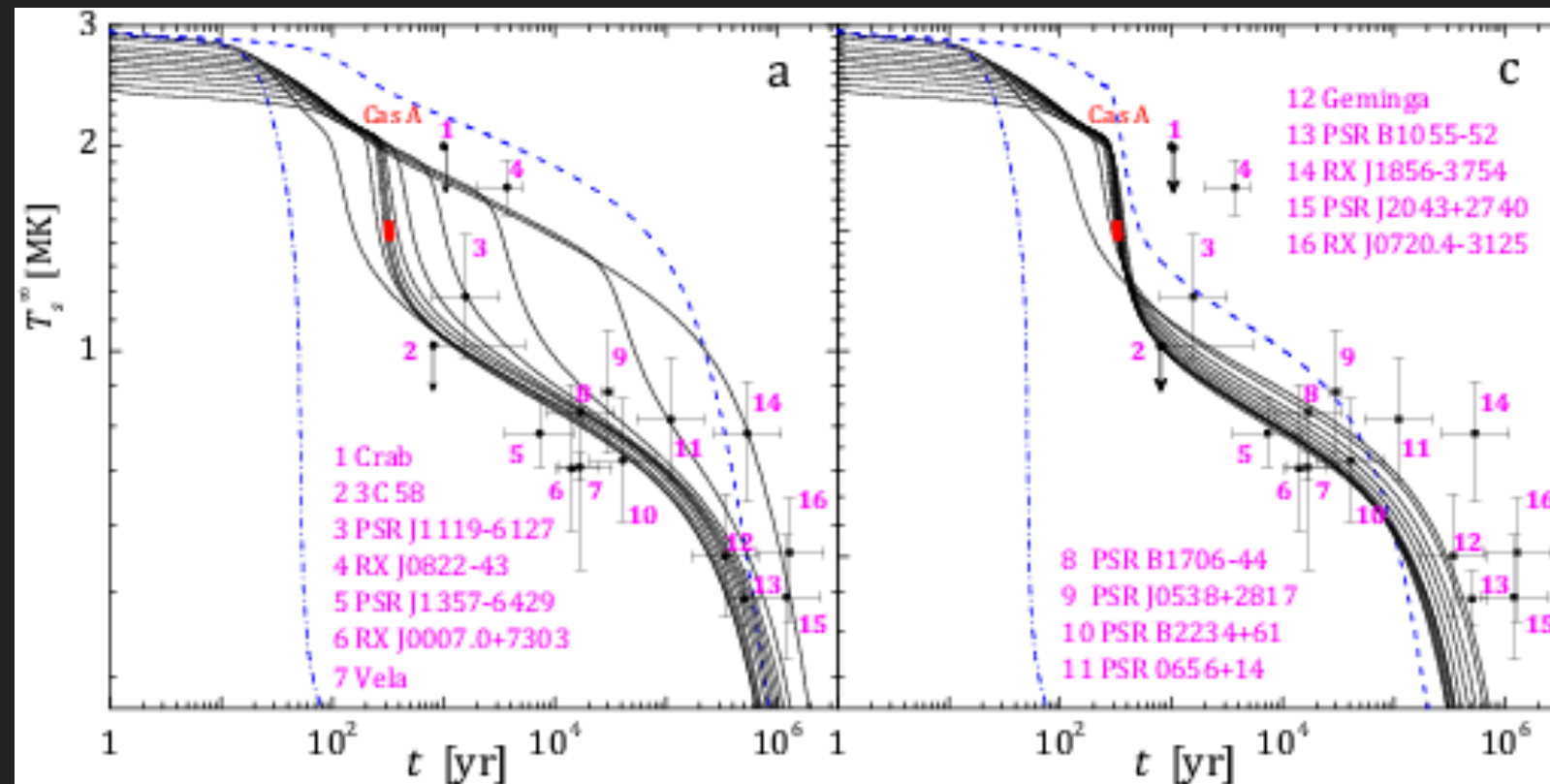
- ▶ The spectrum changes as a function of distance and time.



- ▶ Gamma-Ray produced through ICS should accompany synchrotron emission.
- ▶ Synchrotron observations imply very hard GeV gamma-ray spectrum.
- ▶ Conclusively prove leptonic nature of emission.

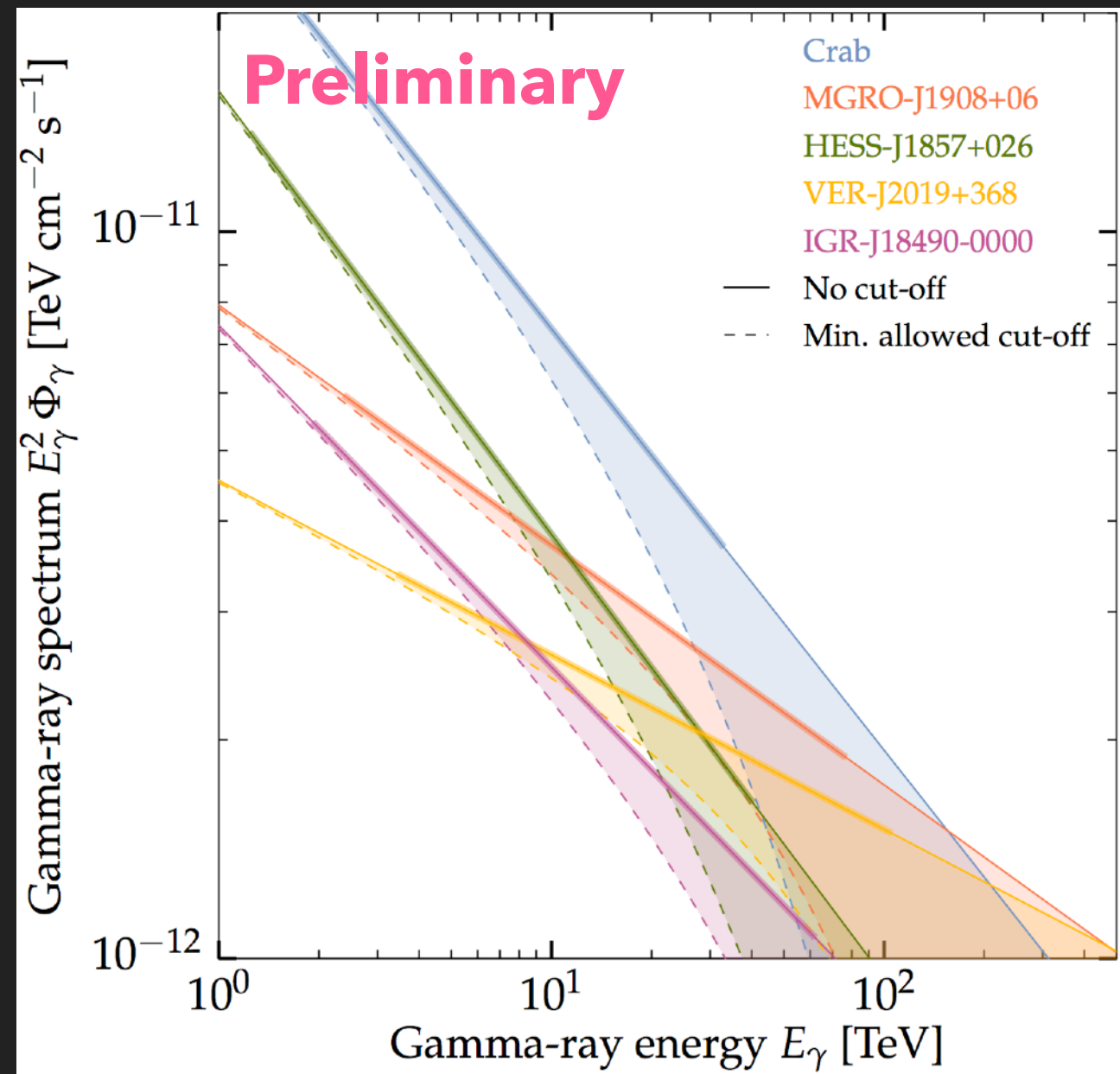


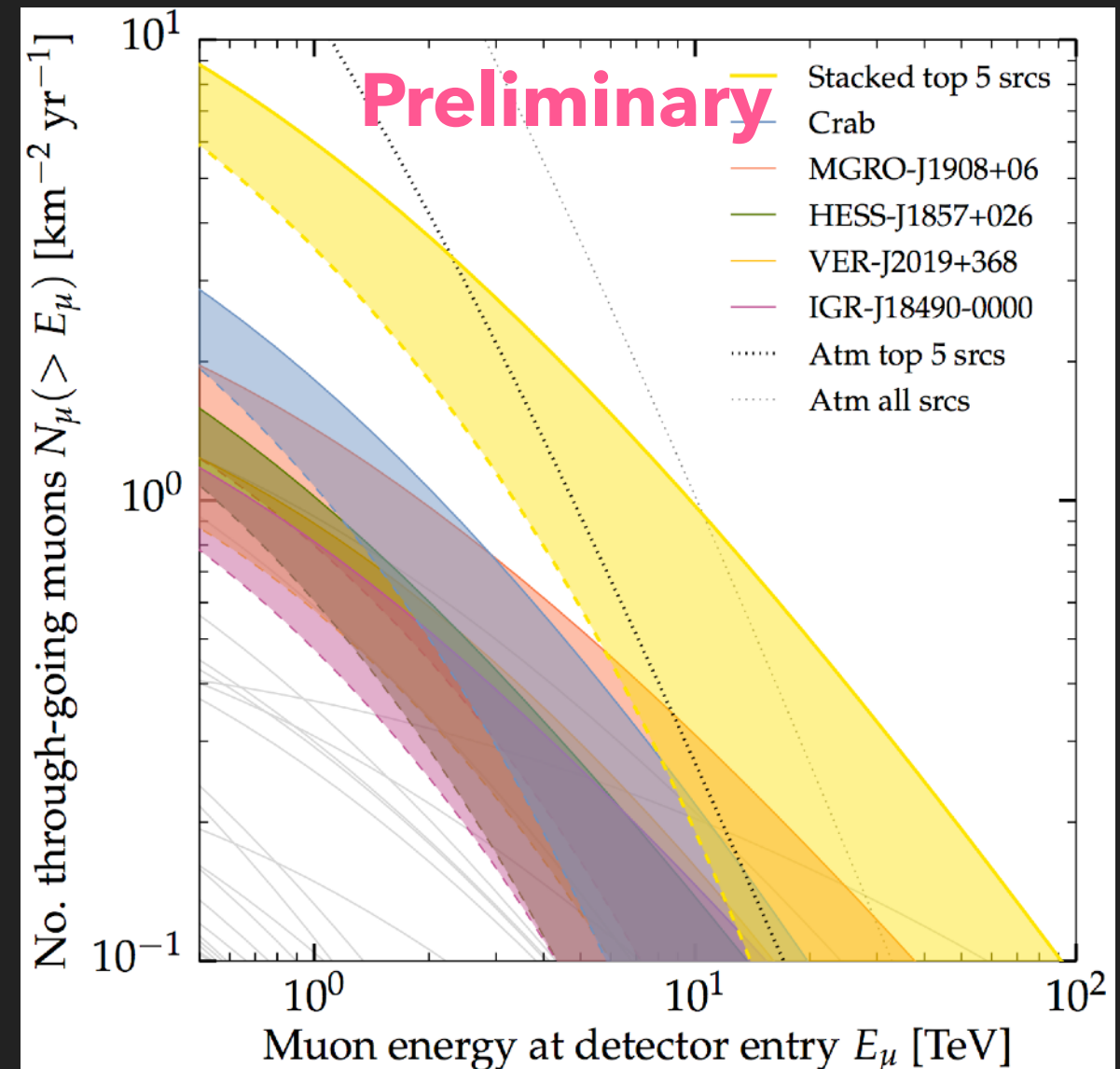
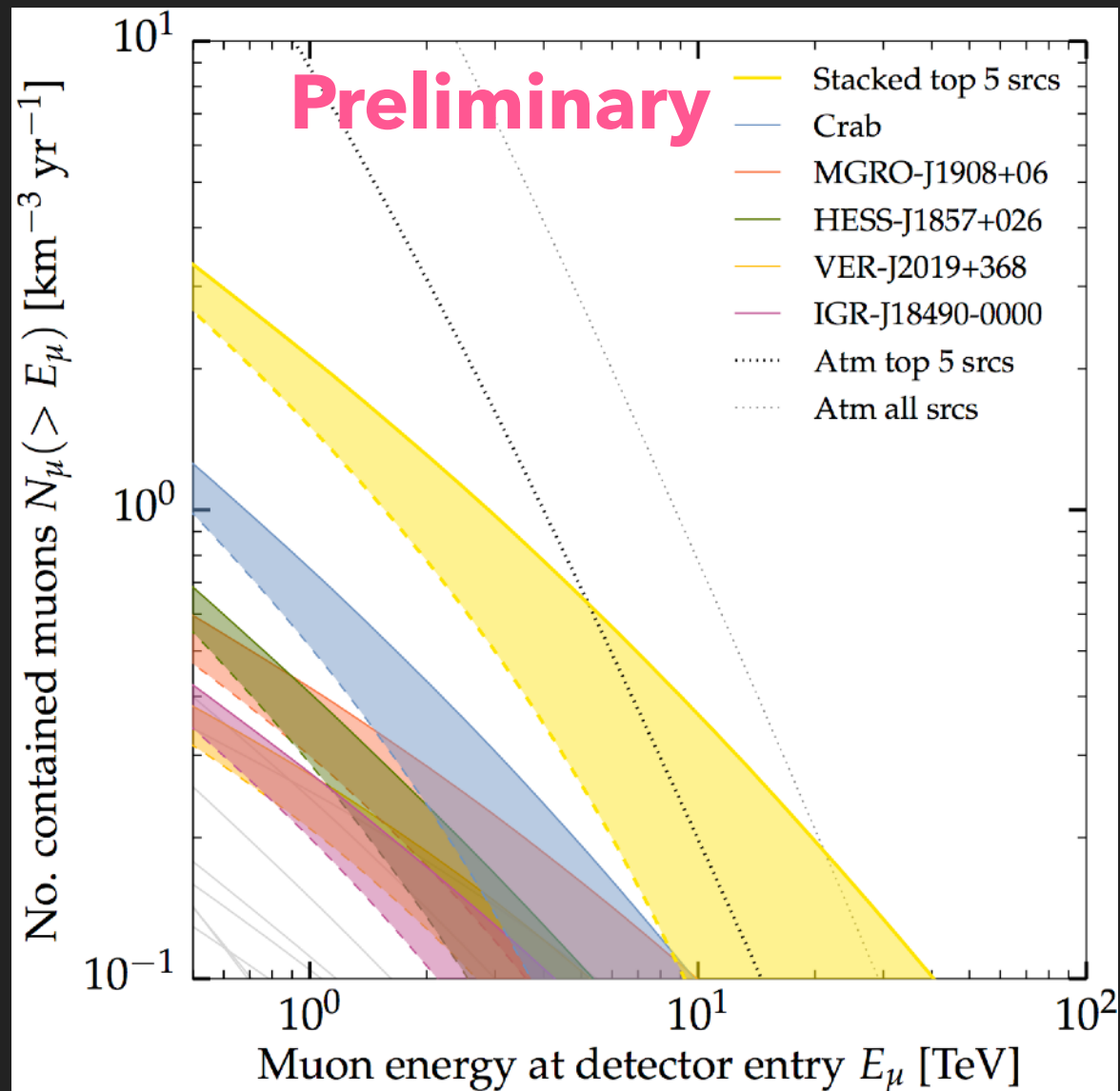
THERMAL PULSAR EMISSION



- ▶ Hot neutron stars can also be observed via their isotropic thermal emission.
- ▶ X-Ray observations can be sensitive to ~2 kpc for 10^6 K NS.
- ▶ Cooler NS extremely hard to see.
- ▶ Could potentially detect a system which has recently ceased producing TeV particles.

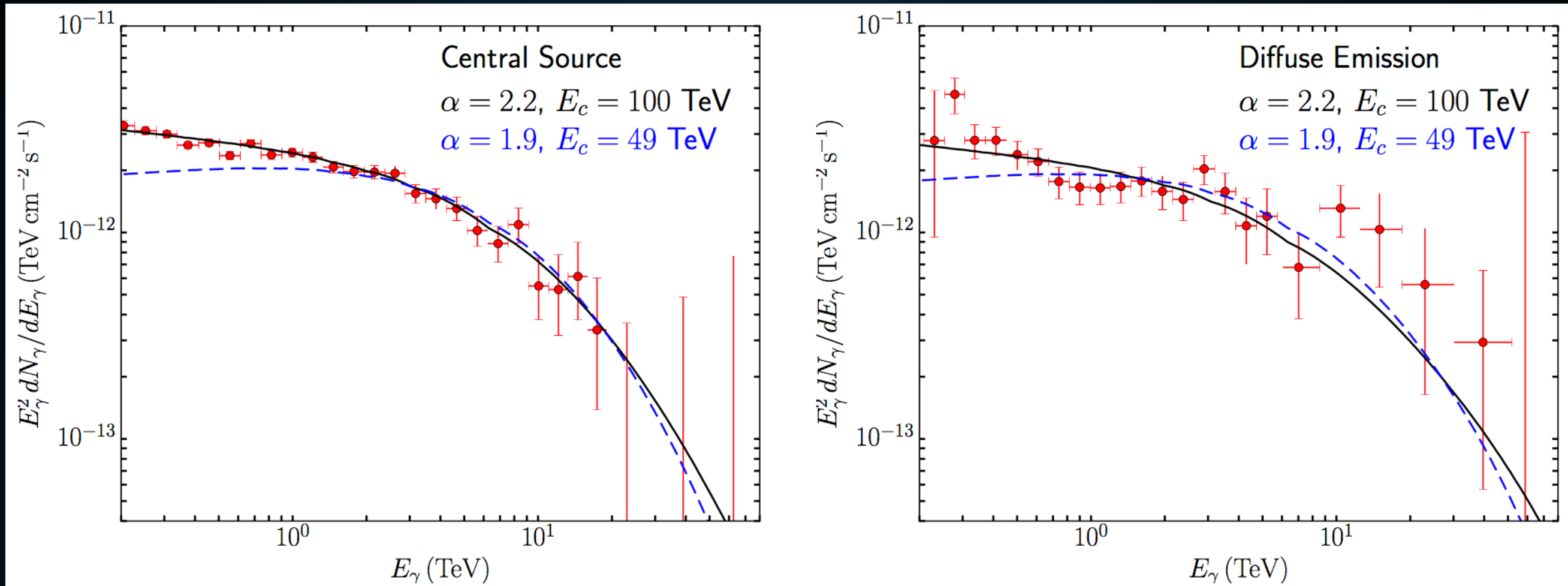
- ▶ HAWC sources are potential IceCube neutrino sources.
- ▶ Spectral measurements of HAWC sources are imperative to calculating the expected neutrino flux.
- ▶ Here we produce an analysis taking into account a 20% uncertainty in total flux, as well as spectral uncertainty due to an exponential cutoff.





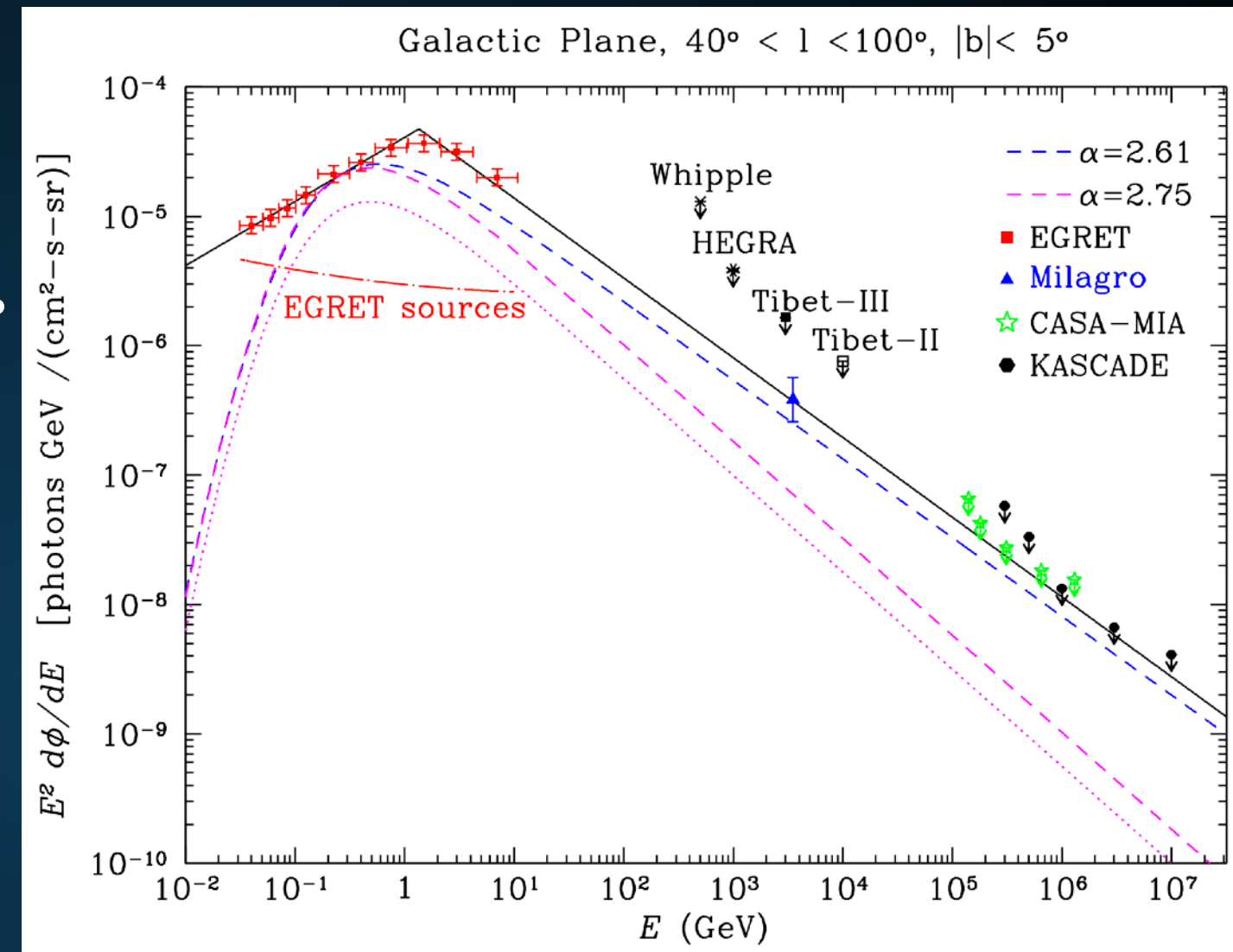
- ▶ If these sources are hadronic, their stacked neutrino flux is detectable in current IceCube data.
- ▶ Alternatively, can place a strong constraint on the hadronic fraction of the brightest HAWC sources.

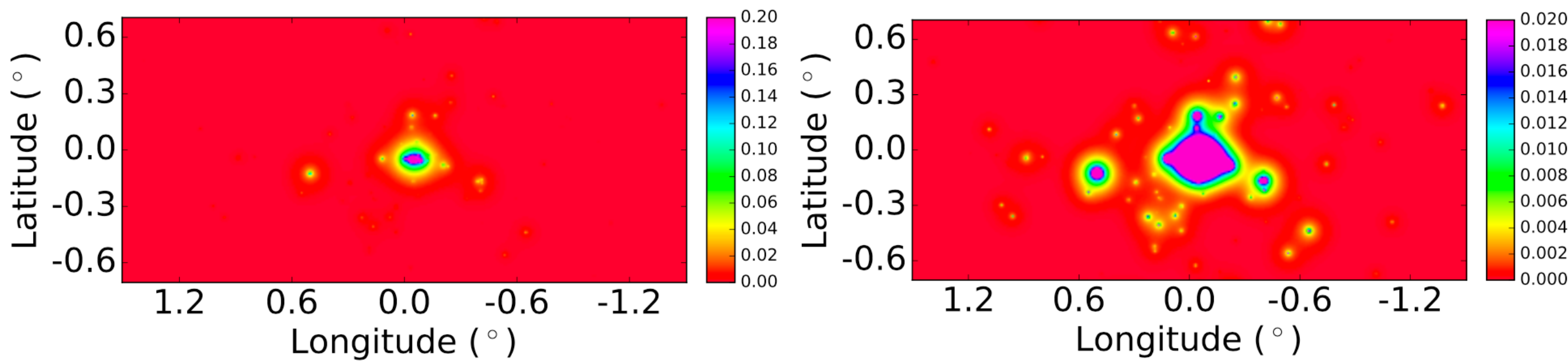
TEV HALOS PRODUCE THE PEVATRON SPECTRUM



- ▶ The TeV halo spectrum from Geminga naturally reproduces the HESS observations.
- ▶ Slightly softer spectra preferred.
- ▶ Some evidence that Geminga spectrum is particularly hard.
- ▶ Hadronic diffuse background contamination?

- Milagro detects bright diffuse TeV emission along the Galactic plane.
- Difficult to explain with pion decay, due to steeply falling local hadronic CR spectrum.
- Can harden gamma-ray emission to some extent using radially dependent diffusion constants (1504.00227).

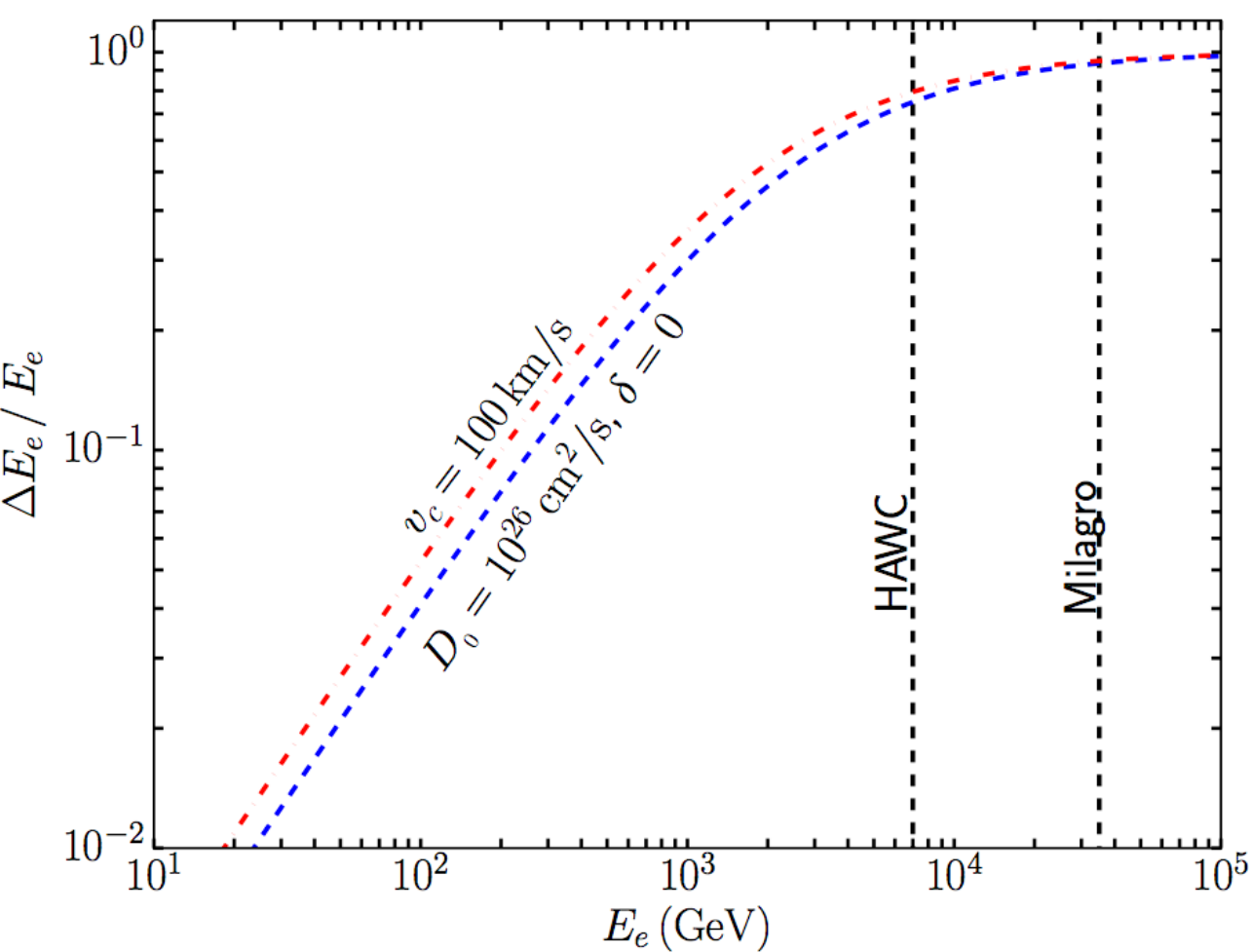
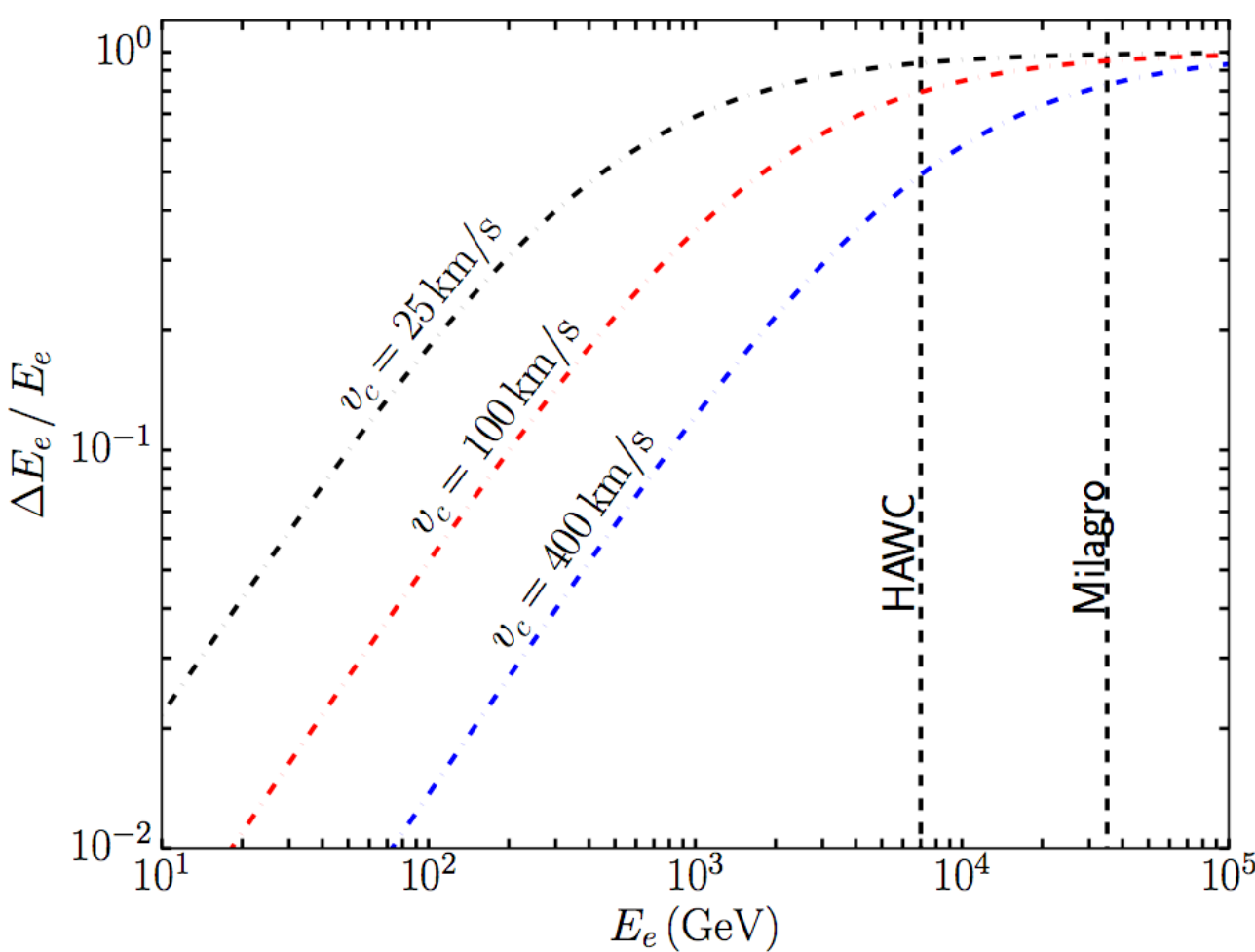




- **Significant star (pulsar) formation in the Galactic center**
- **Pulsars formed in the central parsec will be kicked into surrounding medium.**
- **Source of diffuse gamma-rays in the Galactic center.**

WHAT ABOUT THE LOW-ENERGY ELECTRONS?

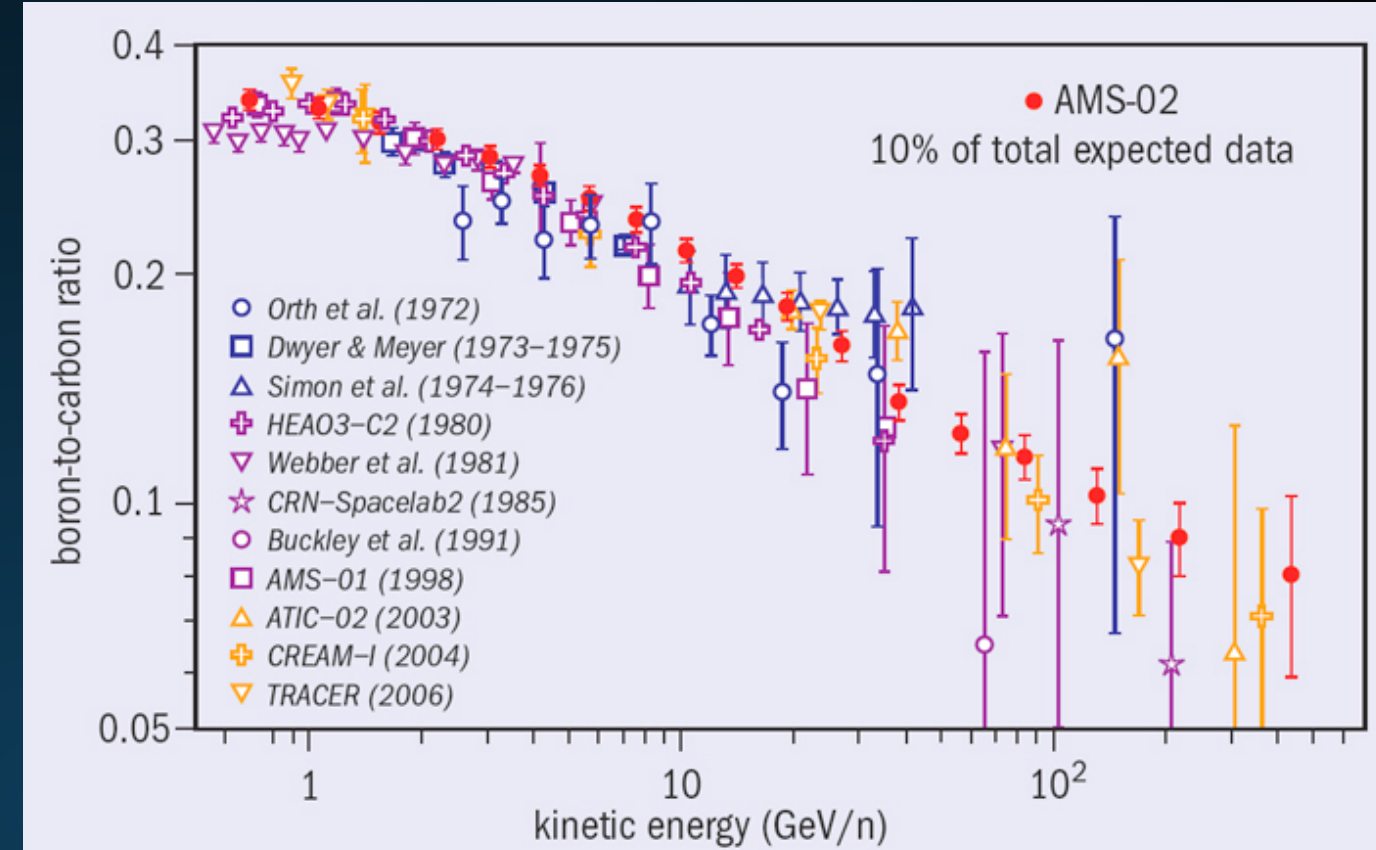
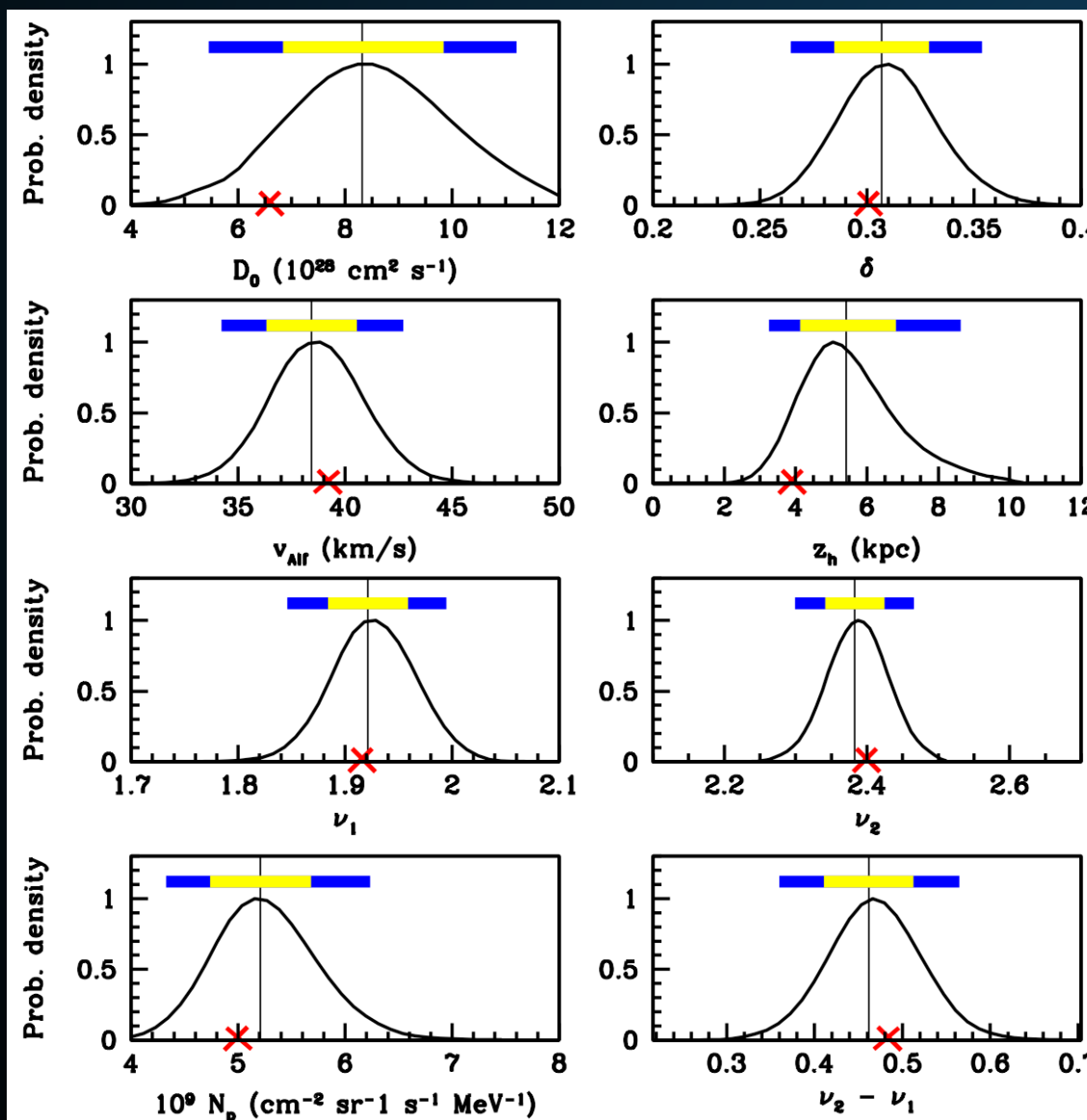
Fraction of energy lost before Electrons Travel a constant distance



- Low-energy electrons lose energy slower, must travel farther.
- This is true in both convective case (shown here) as well as most diffusive (e.g. Kolmogorov, Kraichnian) scenarios.
- Where do these electrons go?

EFFECT OF TEV HALOS ON ISM PROPAGATION

- Multiple cosmic-ray observations indicate that the average diffusion constant is $\sim 5 \times 10^{28} \text{ cm}^2 \text{s}^{-1}$



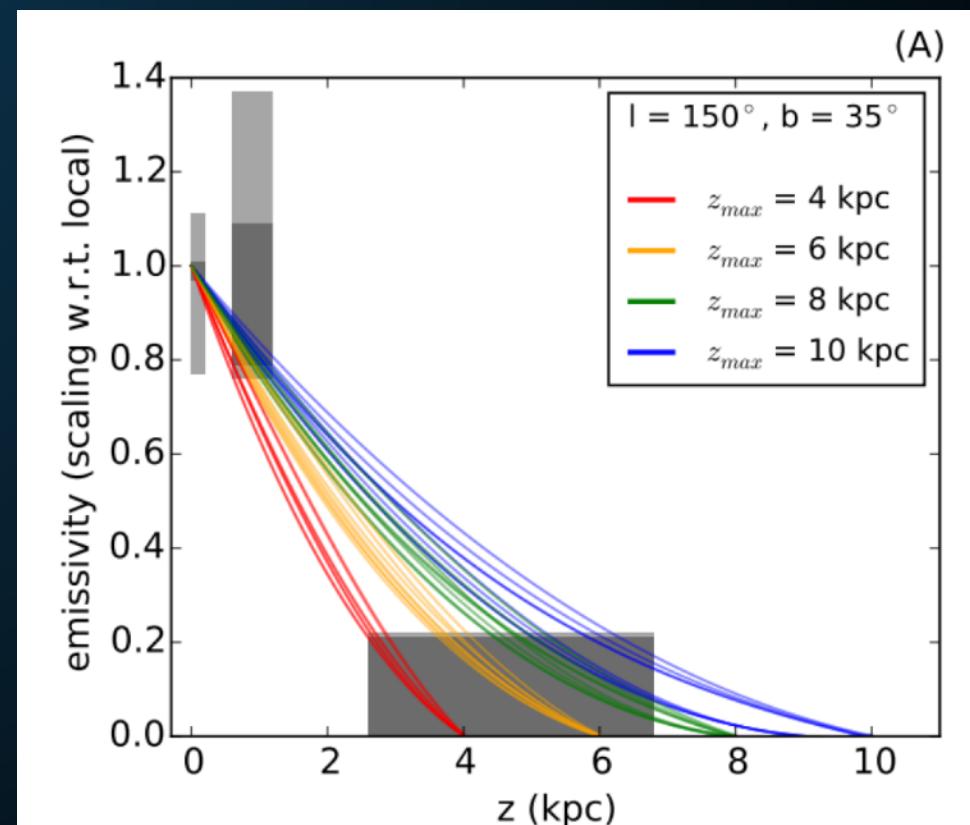
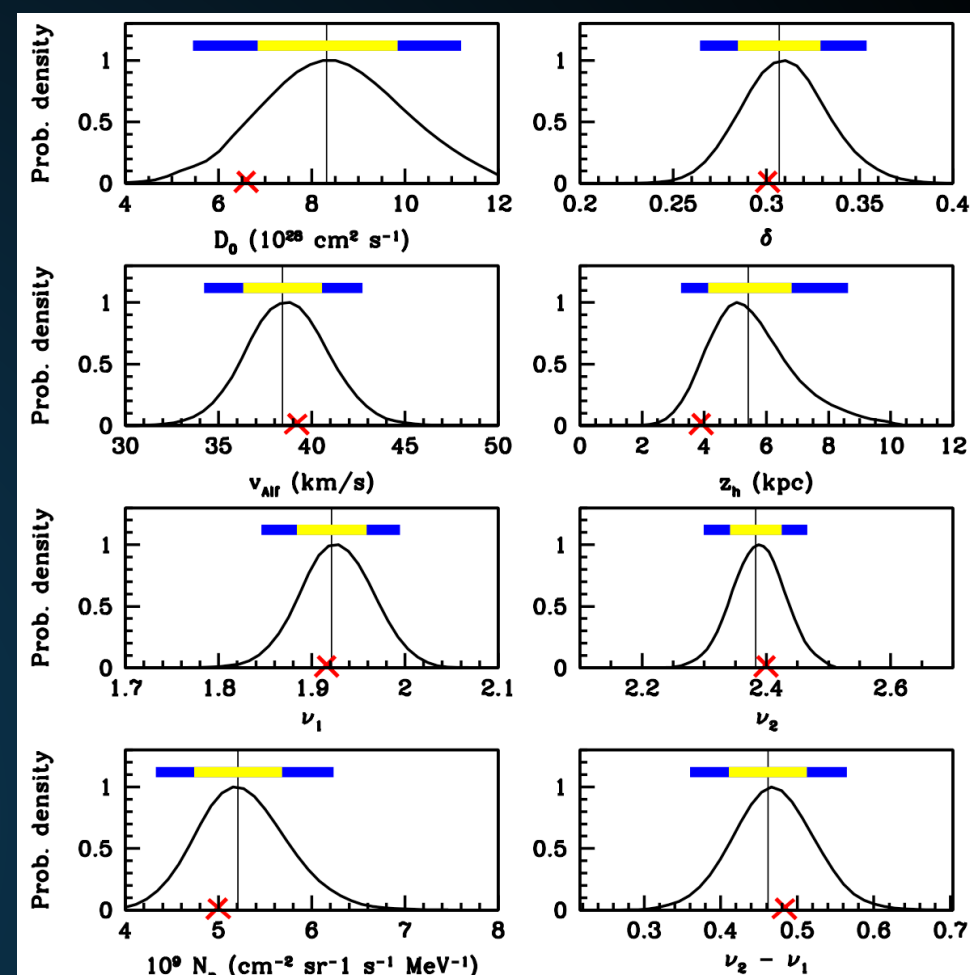
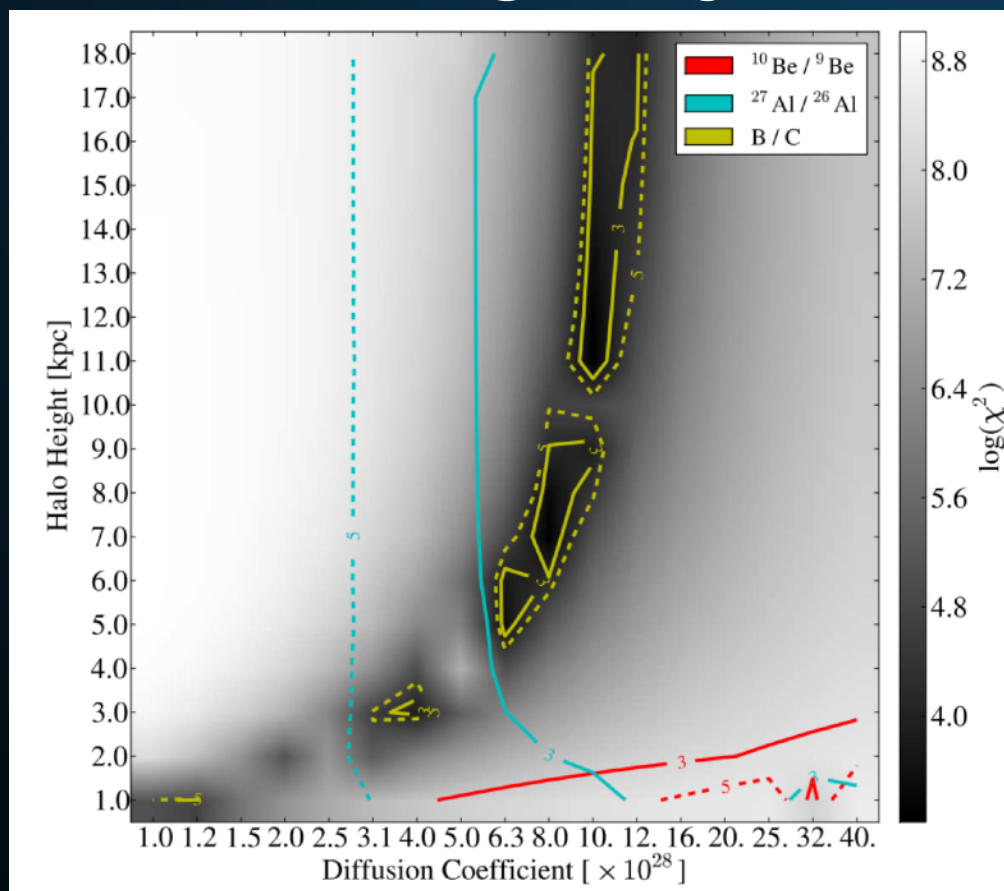
- Assume that diffusion reverts back to the standard case outside the TeV halo.
- Primary difference between our results and those from HAWC.

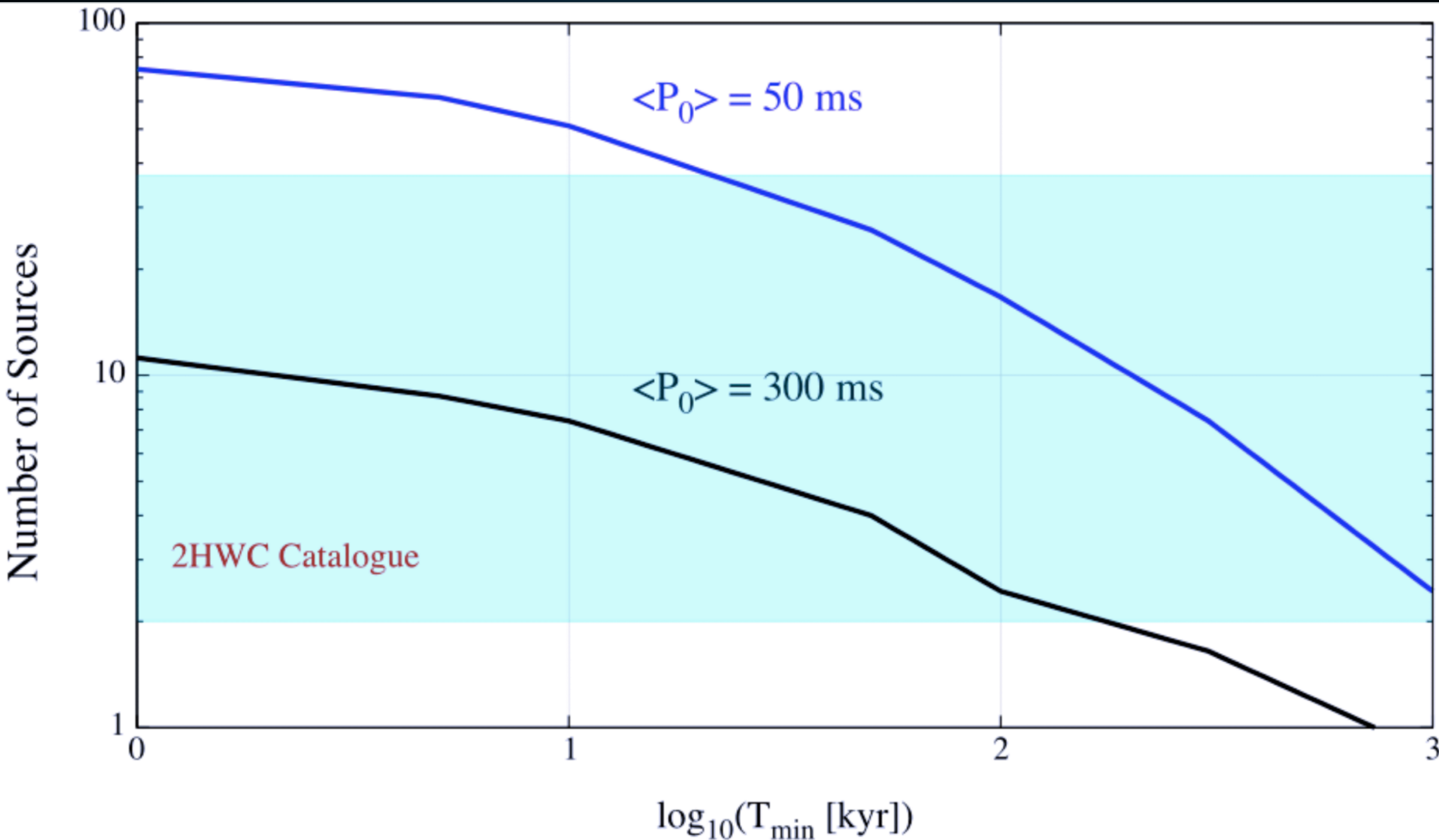
CAN THE DIFFUSION CONSTANT BETWEEN GEMINGA AND US BE LOW?

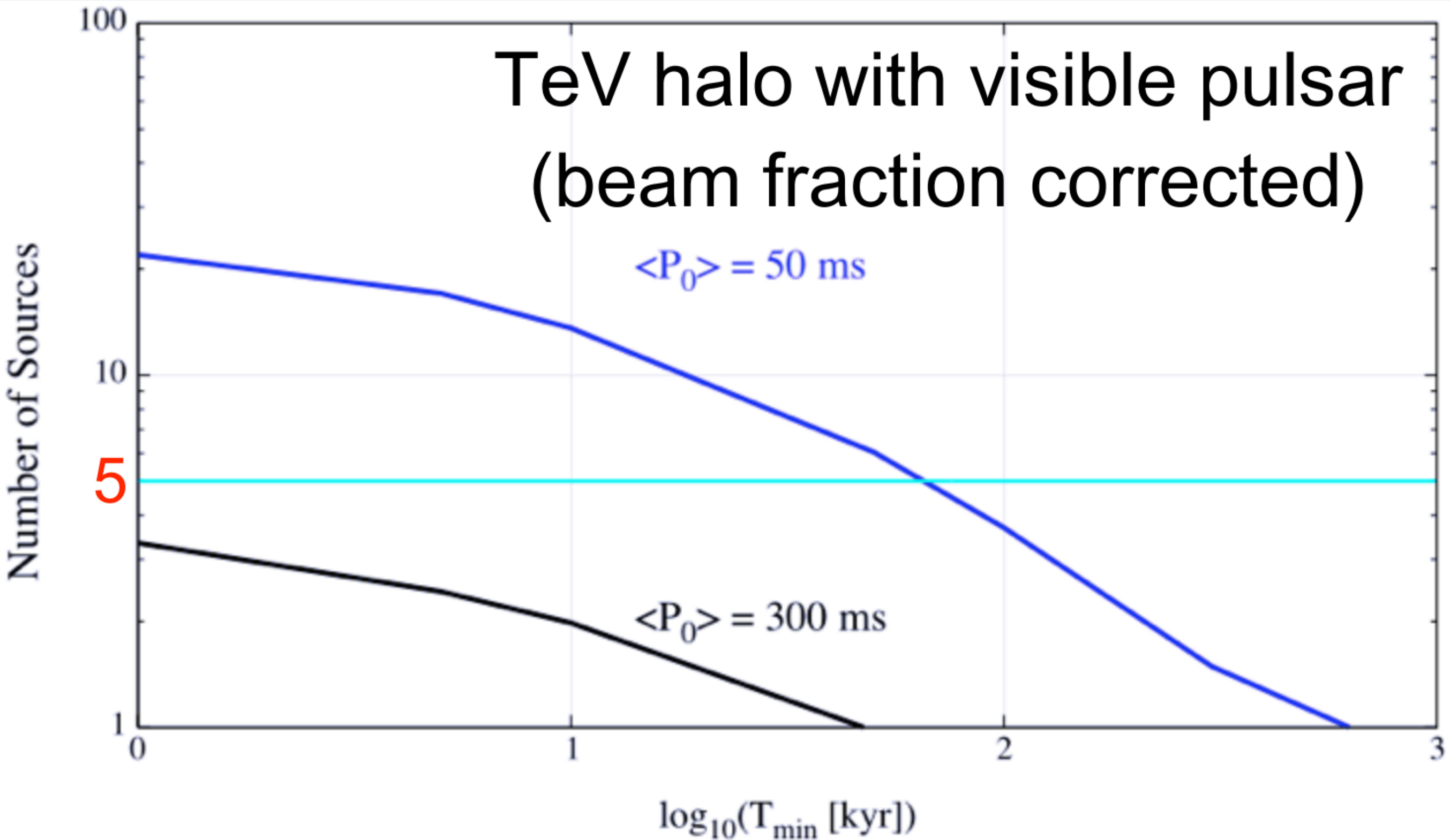


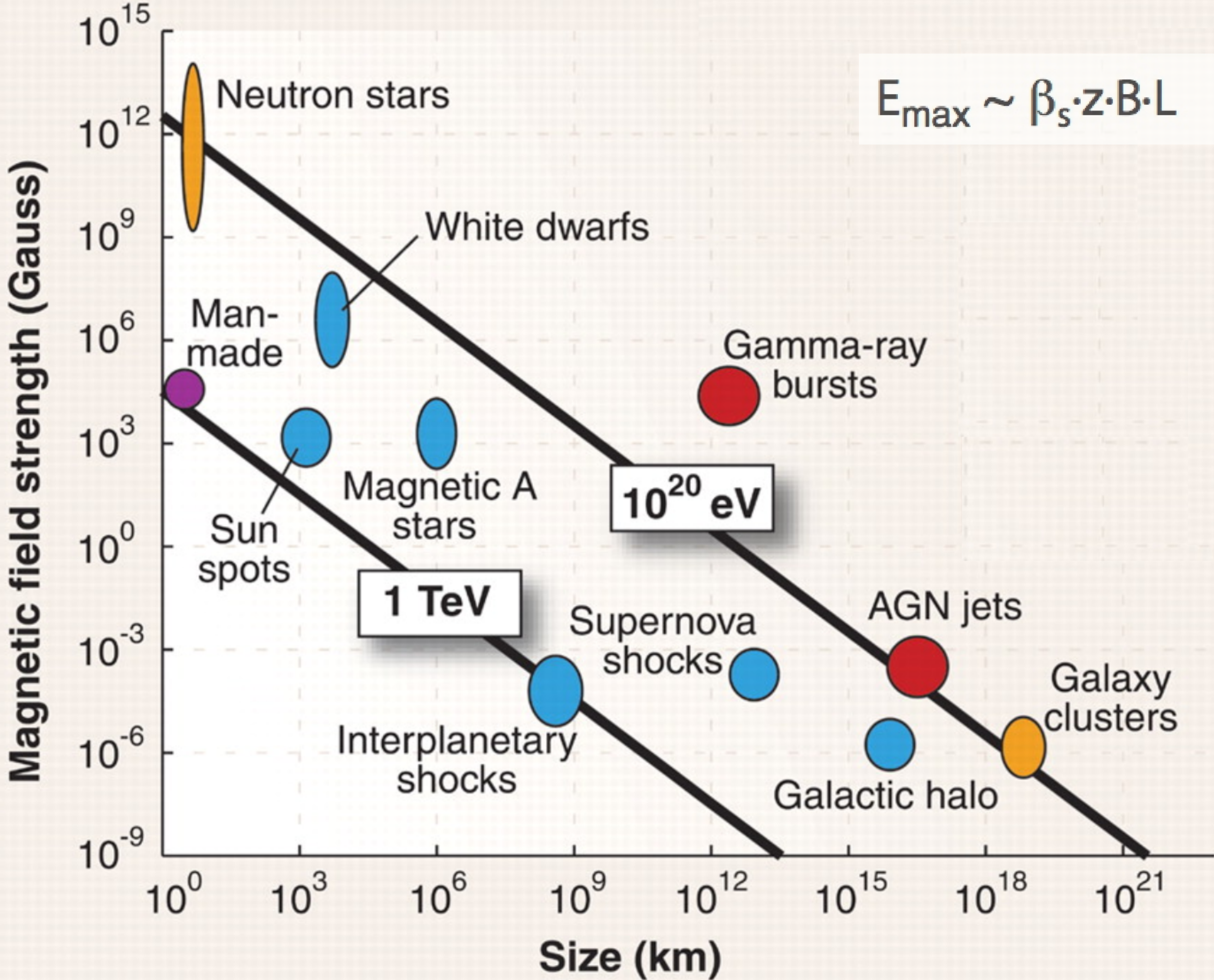
SCENARIO 1: THE MILKY WAY DIFFUSION CONSTANT IS LOW

- Cosmic-Ray primary to secondary ratios tell us about:
 - The average grammage encountered by cosmic-rays before they escape the galaxy (e.g. B/C)
 - The average time cosmic-rays are confined in the galaxy ($^{10}\text{Be}/^{9}\text{Be}$).

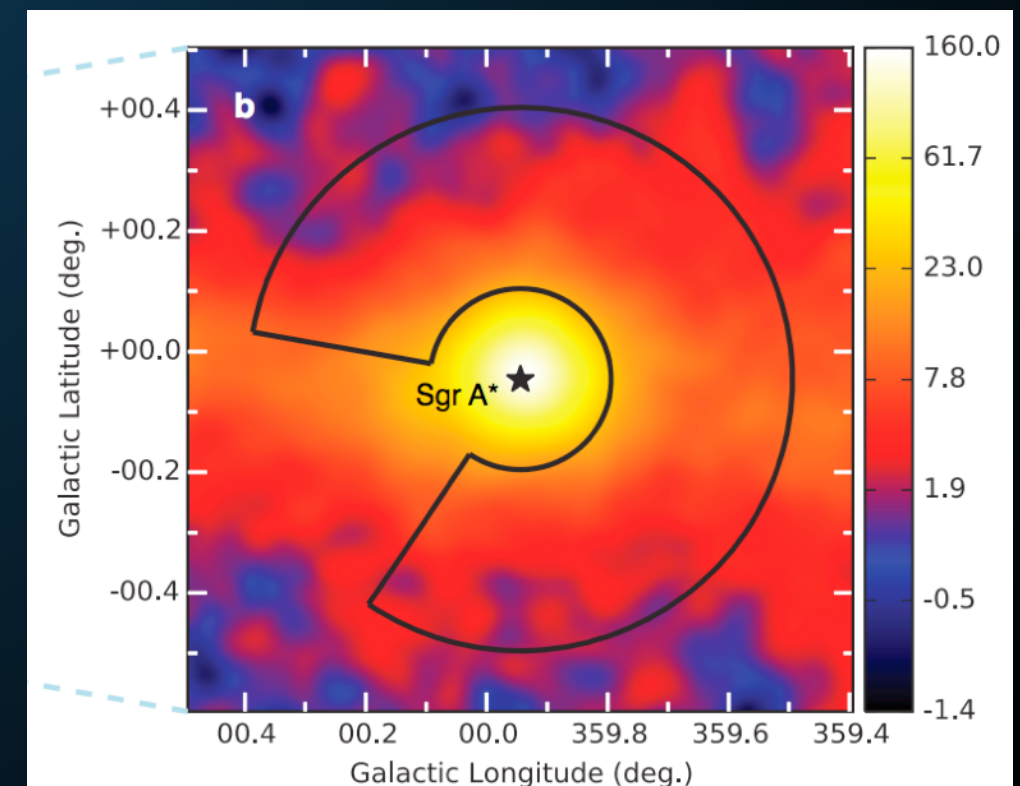
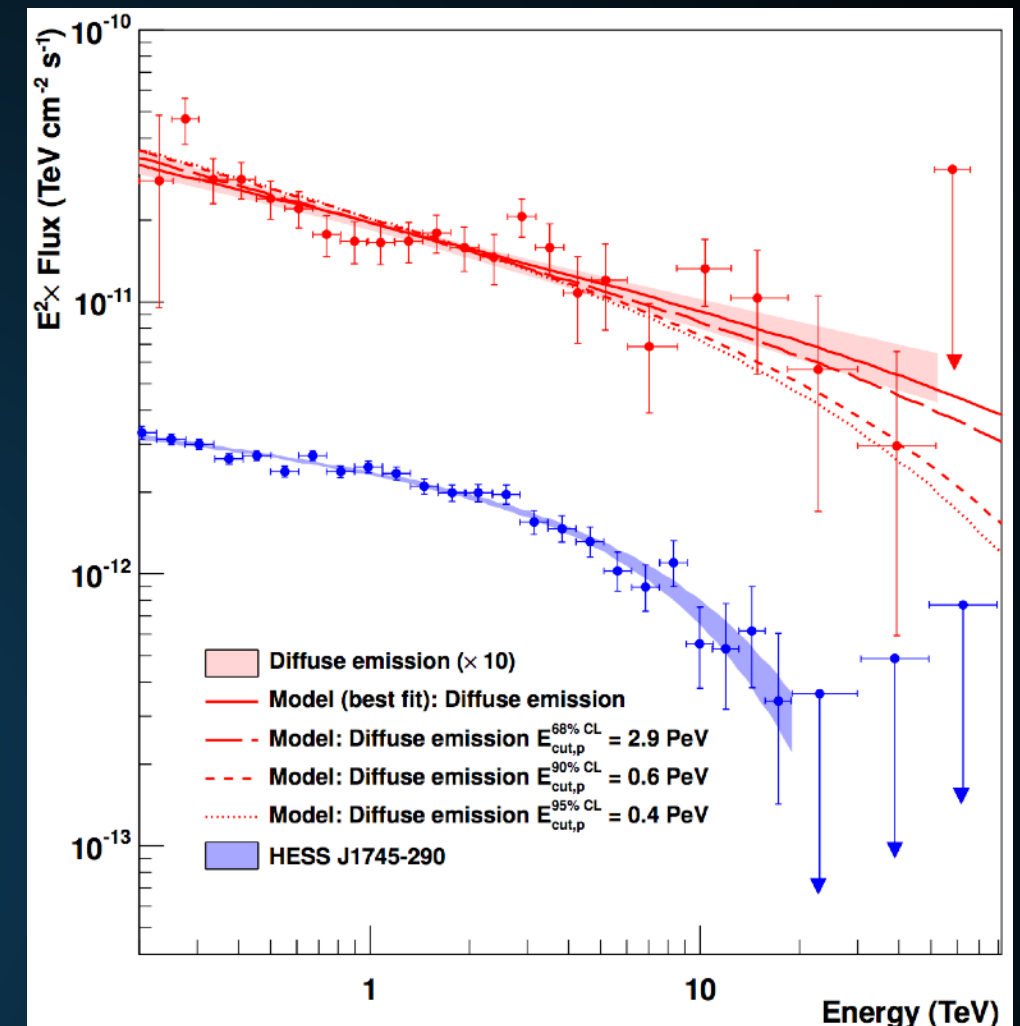




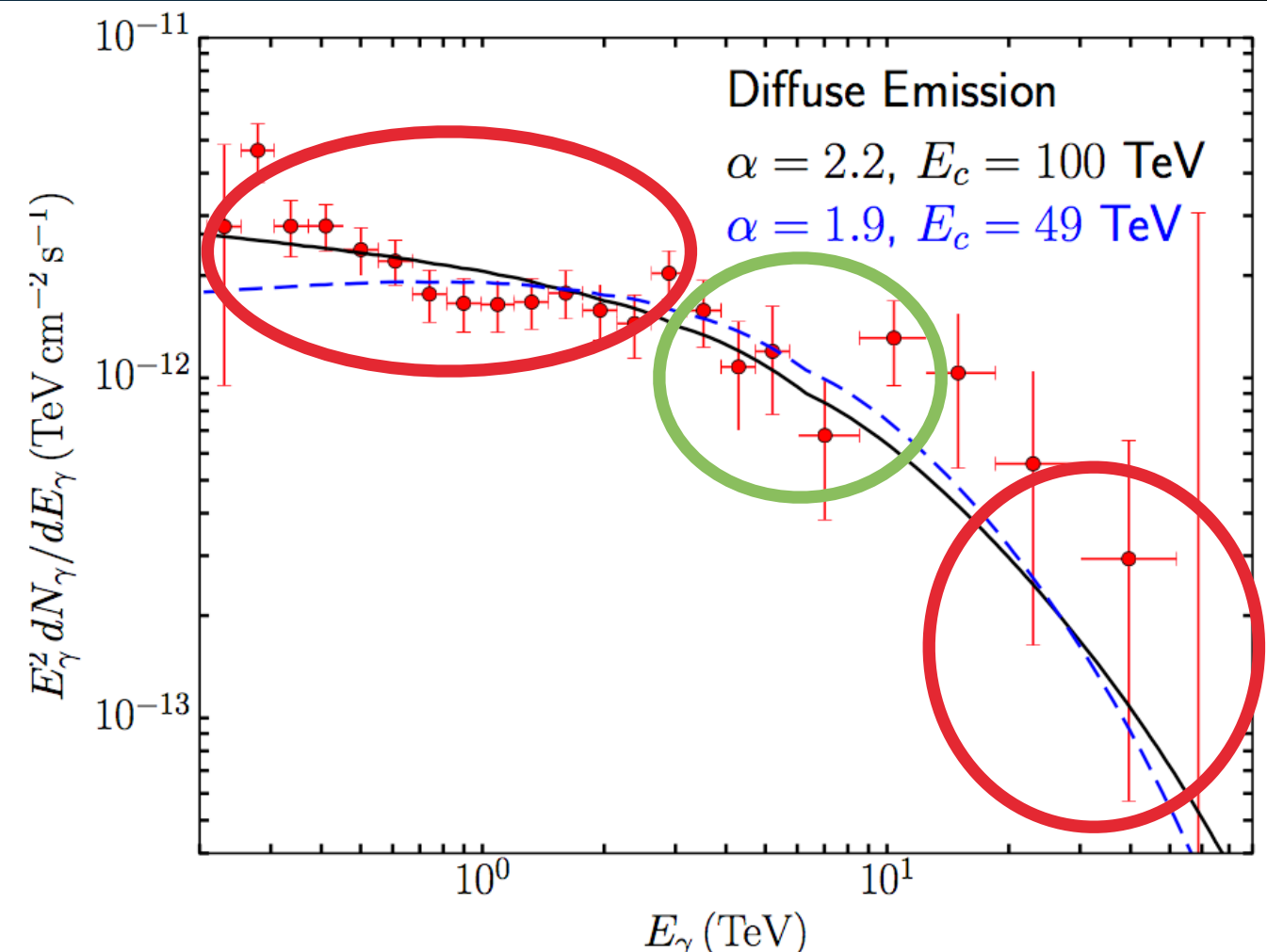
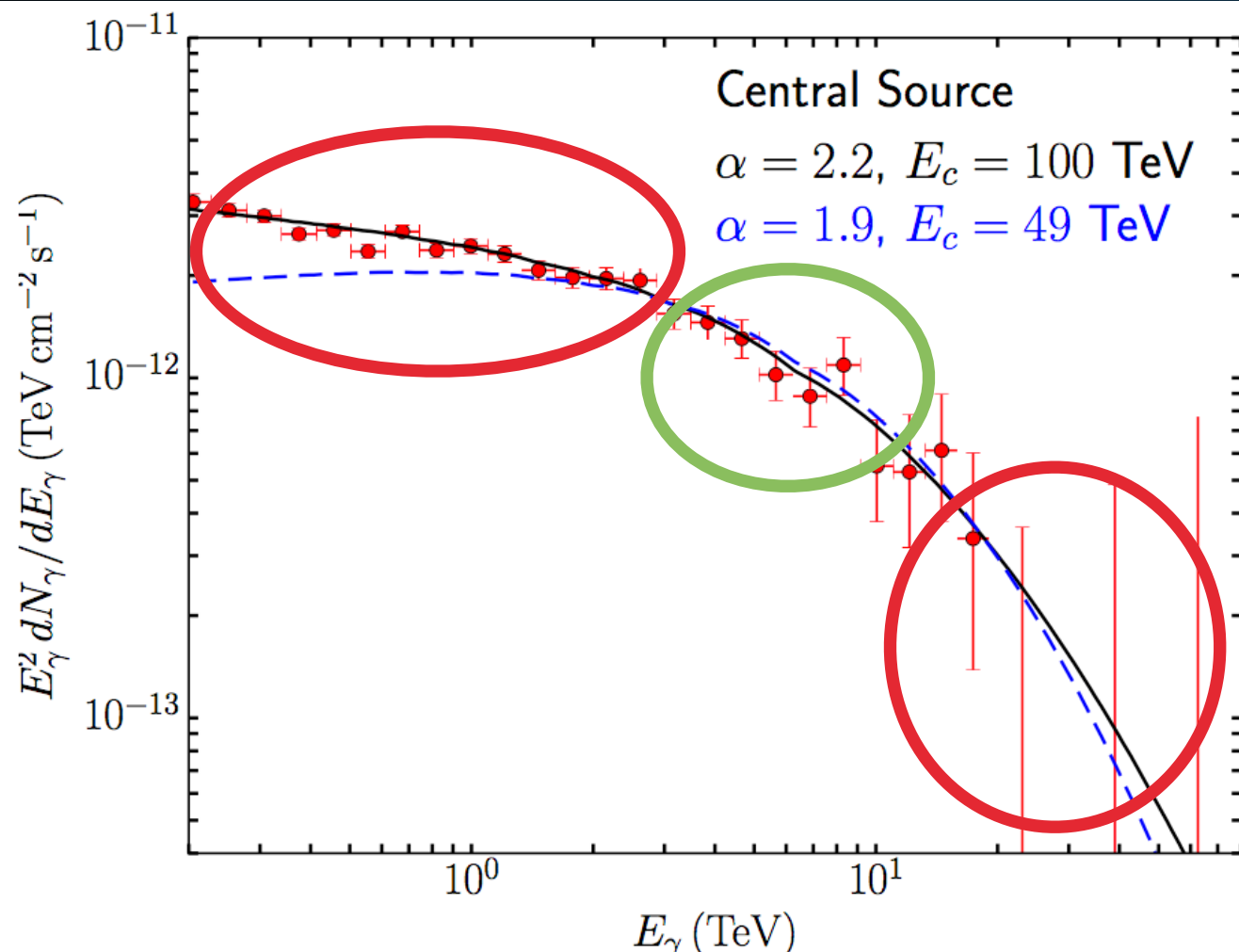




- HESS observed diffuse ~ 50 TeV emission from the Galactic center.
- If this emission is hadronic, it indicates PeV particle acceleration in the GC
- Spherical symmetry hints at Galactic Center source.



- **TeV halos naturally explain the data!**



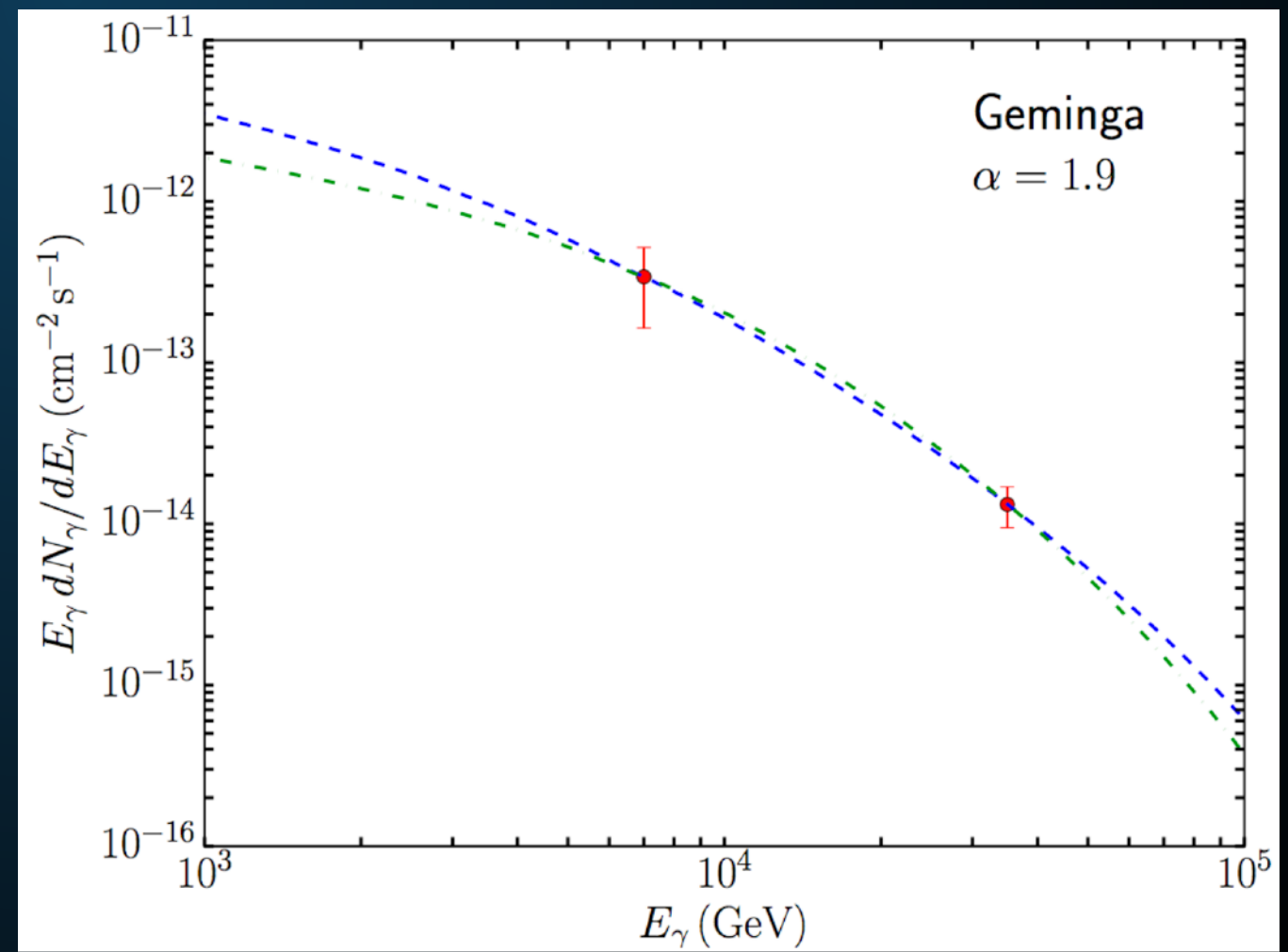
GEMINGA GAMMA-RAY SPECTRUM

Name	Tested radius [°]	Index	$F_7 \times 10^{15}$ [TeV $^{-1}$ cm $^{-2}$ s $^{-1}$]	TeVCat
2HWC J0631+169	-	-2.57 ± 0.15	6.7 ± 1.5	Geminga
”	2.0	-2.23 ± 0.08	48.7 ± 6.9	Geminga
2HWC J0635+180	-	-2.56 ± 0.16	6.5 ± 1.5	Geminga

- **We assume an electron injection spectrum following a power-law with an exponential cutoff.**

- **Best Fit:**

- $-1.9 < \alpha < -1.5$
- $E_{\text{cut}} \approx 50 \text{ TeV}$



**These conclusions stem merely from the
existence of these sources.**

So far - no modeling of what a TeV halo is...

Overview:

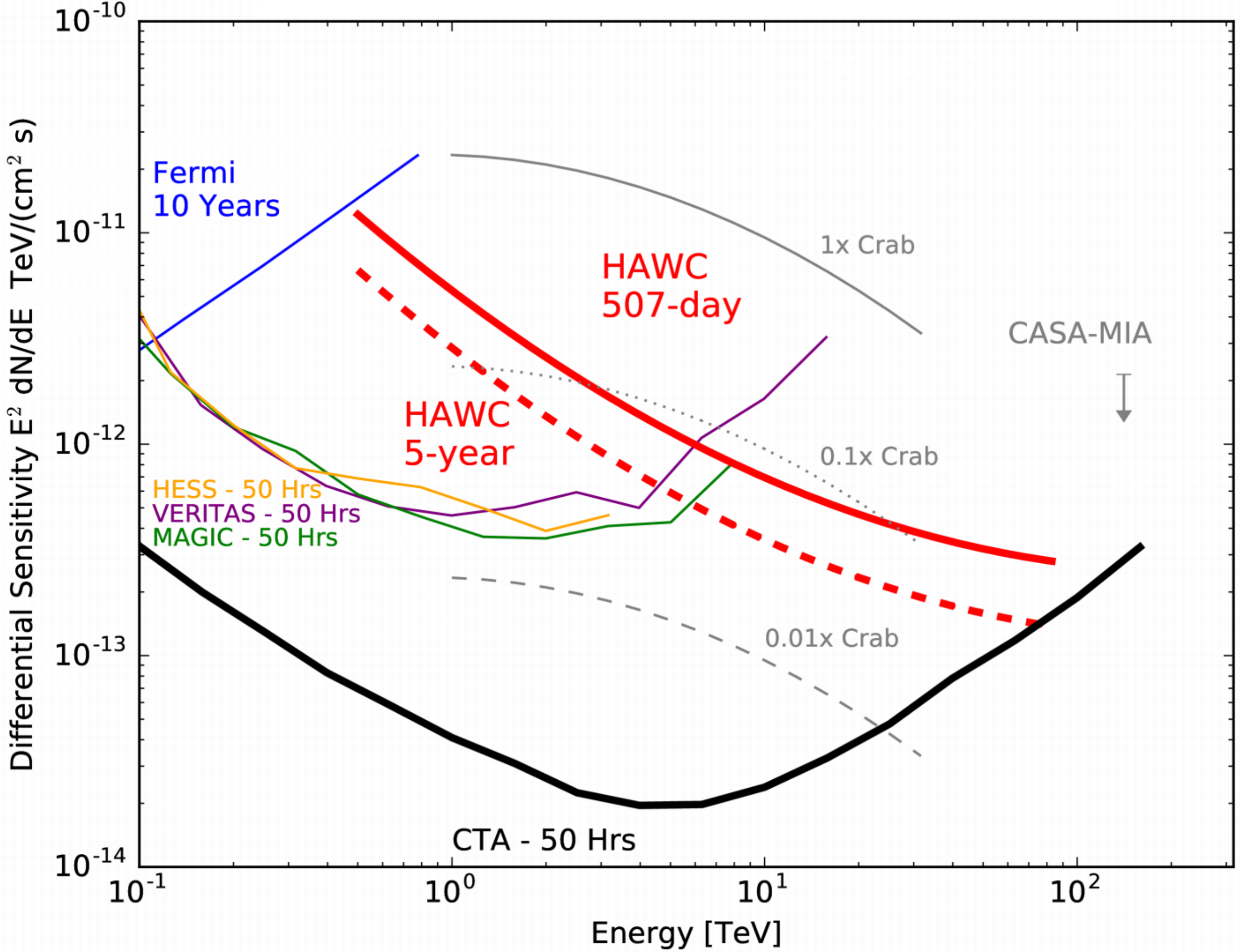
Assume that pulsars convert an the same fraction of their spindown power to e^+e^- as Geminga.

Assume that the e^+e^- spectrum is the same as Geminga.

Table 4 Candidate pulsar wind nebulae from the pre-selection.

HGPS name	ATNF name	$\lg \dot{E}$	τ_c	d	PSR offset	Γ	R_{PWN}	$L_{1-10 \text{ TeV}}$
			(kyr)	(kpc)	(pc)		(pc)	($10^{33} \text{ erg s}^{-1}$)
J1616–508 (1)	J1617–5055	37.20	8.13	6.82	< 26	2.34 ± 0.06	28 ± 4	162 ± 9
J1023–575	J1023–5746	37.04	4.60	8.00	< 9	2.36 ± 0.05	23.2 ± 1.2	67 ± 5
J1809–193 (1)	J1811–1925	36.81	23.3	5.00	29 ± 7	2.38 ± 0.07	35 ± 4	53 ± 3
J1857+026	J1856+0245	36.66	20.6	9.01	21 ± 6	2.57 ± 0.06	41 ± 9	118 ± 13
J1640–465	J1640–4631 (1)	36.64	3.35	12.8	< 20	2.55 ± 0.04	25 ± 8	210 ± 12
J1641–462	J1640–4631 (2)	36.64	3.35	12.8	50 ± 5	2.50 ± 0.11	< 14	17 ± 4
J1708–443	B1706–44	36.53	17.5	2.60	17 ± 3	2.17 ± 0.08	12.7 ± 1.4	6.6 ± 0.9
J1908+063	J1907+0602	36.45	19.5	3.21	21 ± 3	2.26 ± 0.06	27.2 ± 1.5	28 ± 2
J1018–589A	J1016–5857 (1)	36.41	21.0	8.00	47.5 ± 1.6	2.24 ± 0.13	< 4	8.1 ± 1.4
J1018–589B	J1016–5857 (2)	36.41	21.0	8.00	25 ± 7	2.20 ± 0.09	21 ± 4	23 ± 5
J1804–216	B1800–21	36.34	15.8	4.40	18 ± 5	2.69 ± 0.04	19 ± 3	42.5 ± 2.0
J1809–193 (2)	J1809–1917	36.26	51.3	3.55	< 17	2.38 ± 0.07	25 ± 3	26.9 ± 1.5
J1616–508 (2)	B1610–50	36.20	7.42	7.94	60 ± 7	2.34 ± 0.06	32 ± 5	220 ± 12
J1718–385	J1718–3825	36.11	89.5	3.60	5.4 ± 1.6	1.77 ± 0.06	7.2 ± 0.9	4.6 ± 0.8
J1026–582	J1028–5819	35.92	90.0	2.33	9 ± 2	1.81 ± 0.10	5.3 ± 1.6	1.7 ± 0.5
J1832–085	B1830–08 (1)	35.76	147	4.50	23.3 ± 1.5	2.38 ± 0.14	< 4	1.7 ± 0.4
J1834–087	B1830–08 (2)	35.76	147	4.50	32.3 ± 1.9	2.61 ± 0.07	17 ± 3	25.8 ± 2.0
J1858+020	J1857+0143	35.65	71.0	5.75	38 ± 3	2.39 ± 0.12	7.9 ± 1.6	7.1 ± 1.5
J1745–303	B1742–30 (1)	33.93	546	0.200	1.42 ± 0.15	2.57 ± 0.06	0.62 ± 0.07	0.014 ± 0.003
J1746–308	B1742–30 (2)	33.93	546	0.200	< 1.1	3.3 ± 0.2	0.56 ± 0.12	0.009 ± 0.003

- HESS systems have a higher spin down power, but are more distant.



- The energy loss timescale in the ISM ($5 \mu\text{G}$; 1 eV cm^{-3}) is approximately:

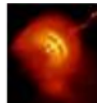
$$\tau_{\text{loss}} \approx 2 \times 10^4 \text{ yr} \left(\frac{10 \text{ TeV}}{E_e} \right)$$

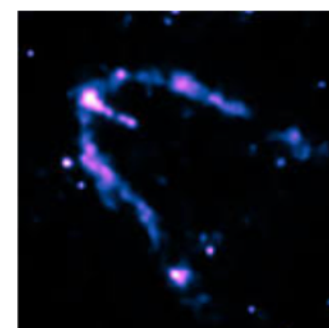
- In the ISM ($D_0 = 5 \times 10^{28} \text{ cm}^2 \text{s}^{-1}$ $\delta=0.33$), this implies a radial extent of ~ 250 pc.

Geminga / Distance to Earth

815.4 light years

People also search for

 Vela Pulsar 958.9 light years	 Crab Pulsar 7,175 light years	 RX J1856.5-3754 400 light years
--	--	--



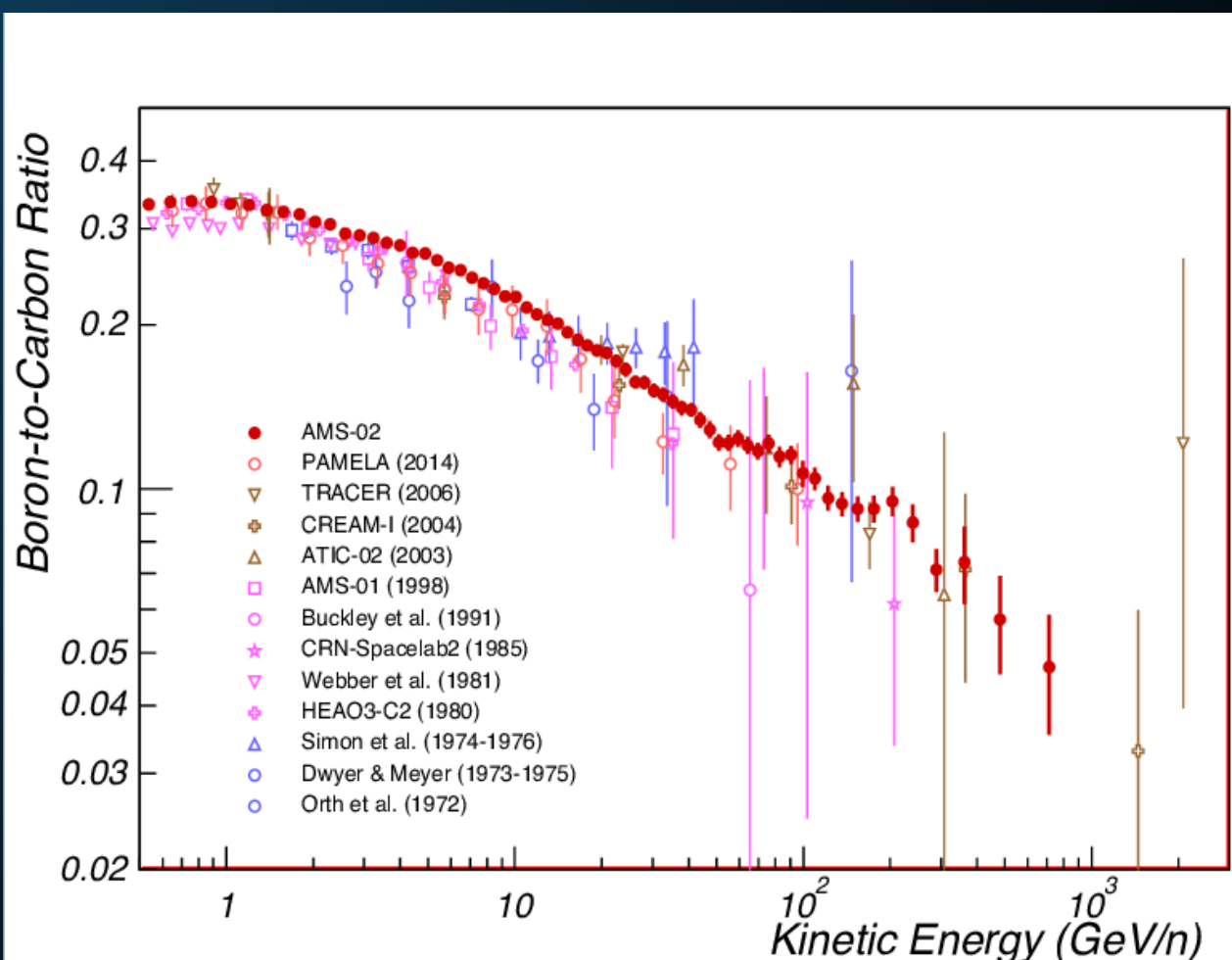
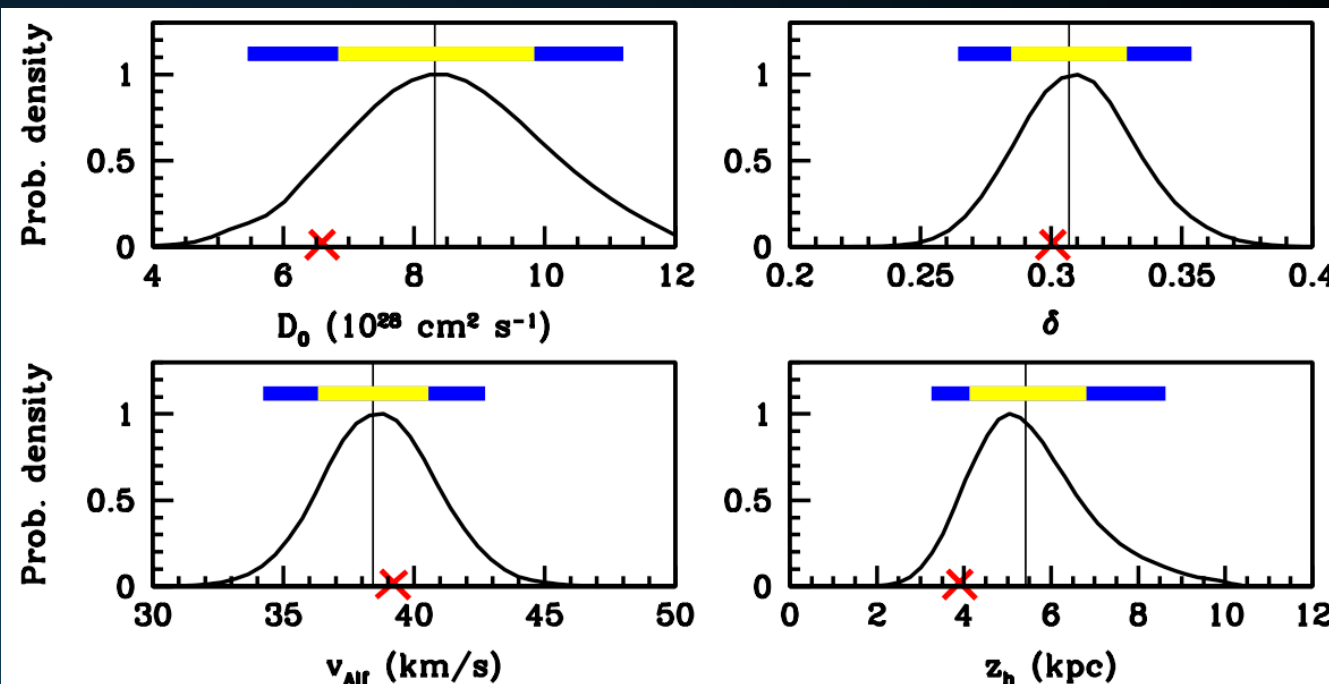
Geminga
Star 

Geminga is a neutron star approximately 250 parsecs from the Sun in the constellation Gemini. Its name, attributed by its discoverer Giovanni Bignami, is both a contraction of Gemini gamma-ray source, and a transcription of the words ghè minga, meaning "it's not there" in the Milanese dialect of Lombard. [Wikipedia](#)

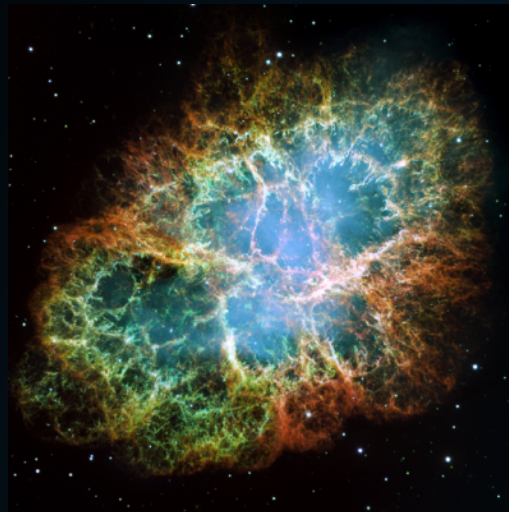
Distance to Earth: 815.4 light years
Magnitude: 25.5
Constellation: Gemini
Apparent magnitude (V): 25.5
Right ascension: 06^h 33^m 54.15^s
Declination: +17° 46' 12.9"

Feedback *Feedback*

- **Cosmic-Ray primary to secondary ratios tell us about:**
 - **The average grammage encountered by cosmic-rays before they escape the galaxy (e.g. B/C)**
 - **The average time cosmic-rays propagate before they escape (eg. $^{10}\text{Be}/^{9}\text{Be}$).**

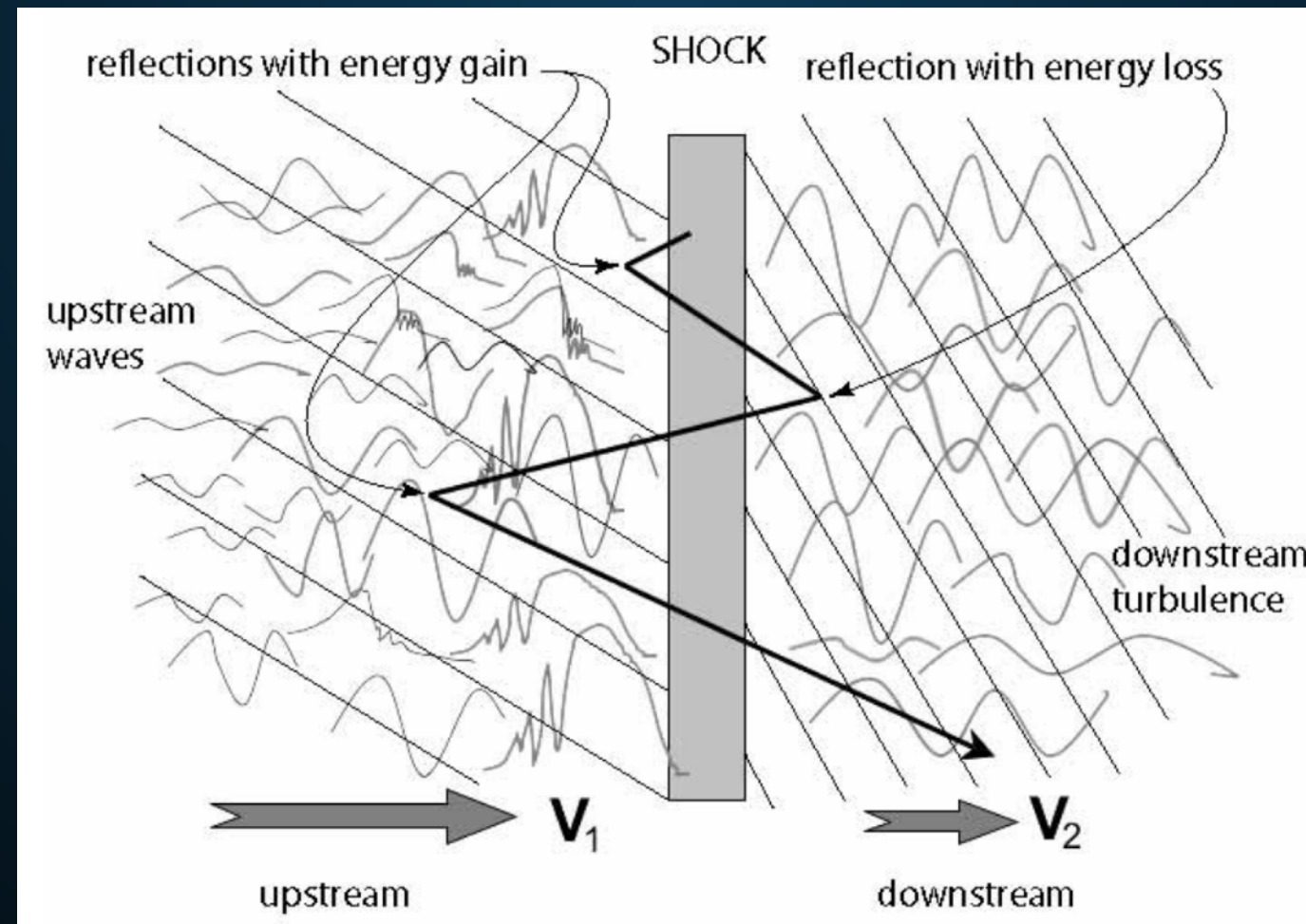


COSMIC-RAY ACCELERATION AND PROPAGATION



Start with a source of relativistic cosmic-rays

- Supernova Explosions
- Supernova Remnants
- Shocks/Mergers



COSMIC-RAY ACCELERATION AND PROPAGATION

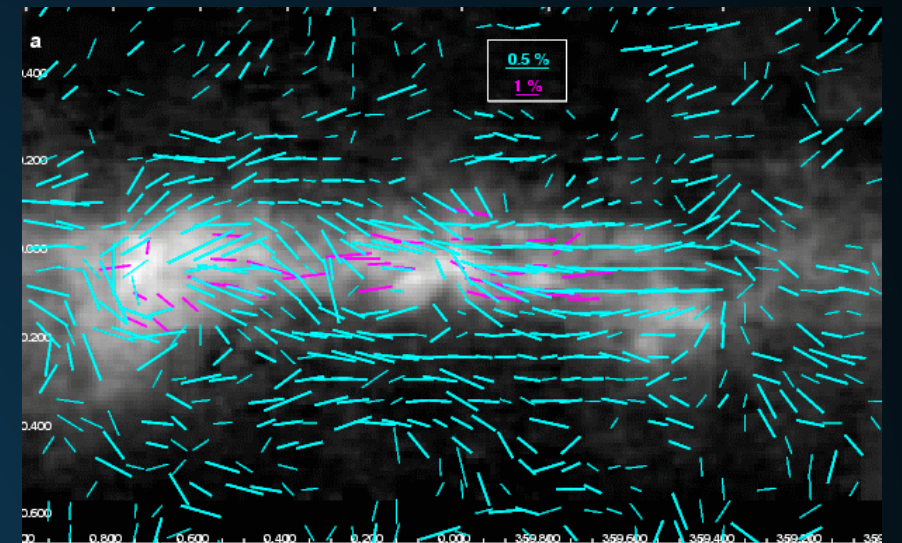


Start with a source of relativistic cosmic-rays

cosmic rays propagate

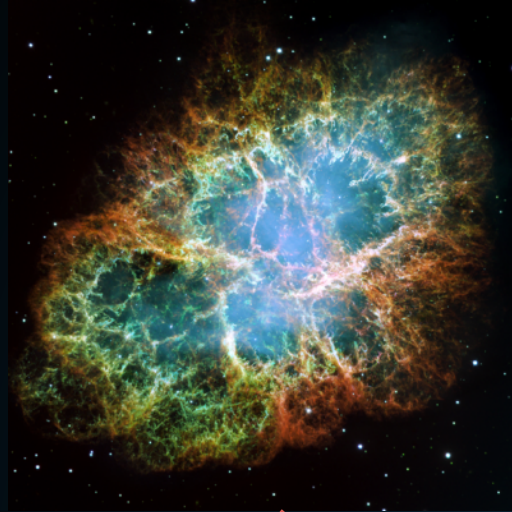
$$\frac{\partial \psi}{\partial t} = q(\vec{r}, p) + \vec{\nabla} \cdot (D_{xx} \vec{\nabla} \psi - \vec{V} \psi) + \frac{\partial}{\partial p} p^2 D_{pp} \frac{\partial}{\partial p} \frac{1}{p^2} \psi - \frac{\partial}{\partial p} \left[\dot{p} \psi - \frac{p}{3} (\vec{\nabla} \cdot \vec{V}) \psi \right] - \frac{1}{\tau_f} \psi - \frac{1}{\tau_r} \psi$$

Solved Numerically:
e.g. Galprop



- If they propagate to Earth, can be detected:
 - AMS-02/PAMELA
 - CREAM/HEAT/CAPRICE

COSMIC-RAY ACCELERATION AND PROPAGATION



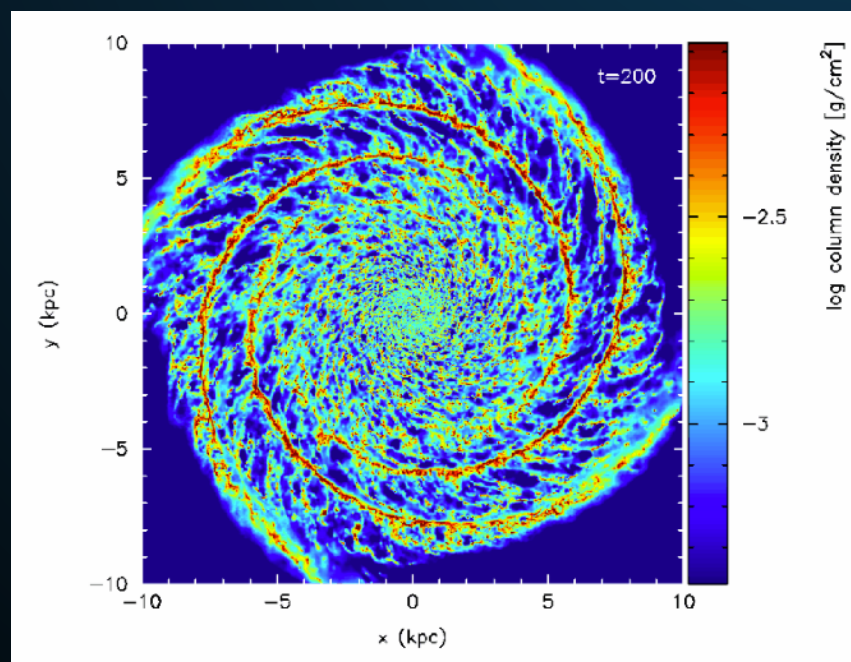
Start with a source of relativistic cosmic-rays

cosmic rays propagate

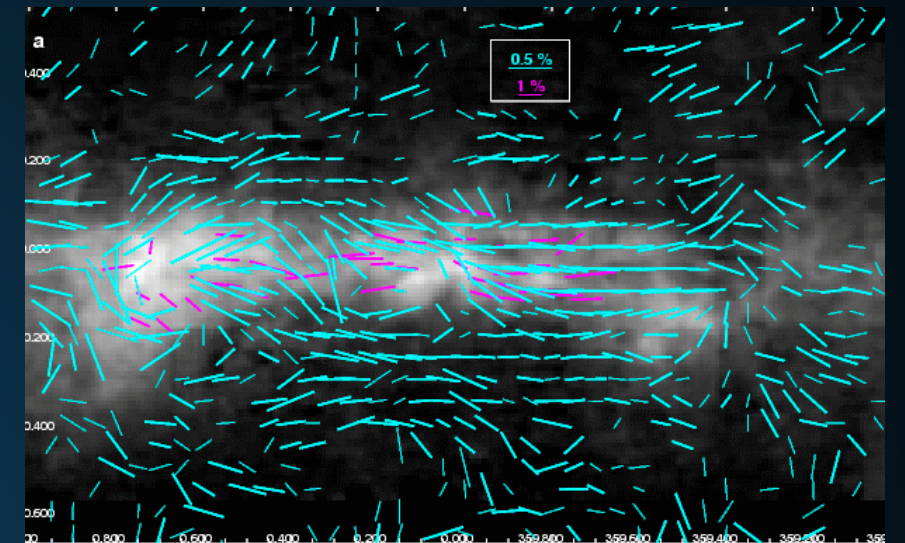
$$\frac{\partial \psi}{\partial t} = q(\vec{r}, p) + \vec{\nabla} \cdot (D_{xx} \vec{\nabla} \psi - \vec{V} \psi) + \frac{\partial}{\partial p} p^2 D_{pp} \frac{\partial}{\partial p} \frac{1}{p^2} \psi - \frac{\partial}{\partial p} \left[\dot{p} \psi - \frac{p}{3} (\vec{\nabla} \cdot \vec{V}) \psi \right] - \frac{1}{\tau_f} \psi - \frac{1}{\tau_r} \psi$$

Solved Numerically:
e.g. Galprop

Gas/ISRF



- Alternatively can collide with Galactic gas or the interstellar radiation field.



COSMIC-RAY ACCELERATION AND PROPAGATION



Start with a source of relativistic cosmic-rays

cosmic rays propagate

$$\frac{\partial \psi}{\partial t} = q(\vec{r}, p) + \vec{\nabla} \cdot (D_{xx} \vec{\nabla} \psi - \vec{V} \psi) + \frac{\partial}{\partial p} p^2 D_{pp} \frac{\partial}{\partial p} \frac{1}{p^2} \psi - \frac{\partial}{\partial p} \left[\dot{p} \psi - \frac{p}{3} (\vec{\nabla} \cdot \vec{V}) \psi \right] - \frac{1}{\tau_f} \psi - \frac{1}{\tau_r} \psi$$

Solved Numerically:
e.g. Galprop

Gas/ISRF

